JPhys Photonics





ROADMAP • OPEN ACCESS

Roadmap on specialty optical fibers

To cite this article: Mário F S Ferreira et al 2025 J. Phys. Photonics 7 012501

View the article online for updates and enhancements.

You may also like

 1 GHz fundamental repetition rate thuliumdoped all-polarization maintaining modelocked fiber laser
 C Cuadrado-Laborde, H Muñoz-Marco, P Pérez-Millán et al.

 Quantitative differential phase contrast imaging system using FPGA for cellular imaging

Yen-Chih Yu, Sunil Vyas, J Andrew Yeh et al

 A review of label-free photonics-based techniques for cancer detection in the digestive and urinary systems
 G Castro-Olvera, E Baria, D Stoliarov et al.

Journal of Physics: Photonics



OPEN ACCESS

RECEIVED

10 May 2023

REVISED

16 February 2024

ACCEPTED FOR PUBLICATION 30 July 2024

--,--, ----

PUBLISHED

13 January 2025

Original content from this work may be used under the terms of the Creative Commons Attribution 4.0 licence.

Any further distribution of this work must maintain attribution to the author(s) and the title of the work, journal citation and DOI.



ROADMAP

Roadmap on specialty optical fibers

Mário F S Ferreira^{1,18,*}, Mohd Rehan², Vishwatosh Mishra³, Shailendra Kumar Varshney⁴, Francesco Poletti⁵, Nguyen Phuoc Trung Hoa⁶, Weichao Wang⁷, Qinyuan Zhang⁷, Wenyu Du⁸, Benli Yu⁸, Zhijia Hu⁸, Xian Feng⁹, Jindan Shi⁹, Anjali¹⁰, Sunil Kumar¹⁰, Michal Kamrádek¹¹, Mukul Chandra Paul¹², Kazi Abedin¹³, Bertrand Kibler¹⁴, Frédéric Smektala¹⁴, Xiushan Zhu¹⁵, Andrey Pryamikov¹⁶ and Stephan Reitzenstein¹⁷

- Institute of Nanostructures, Nanomodelling and Nanofabrication, University of Aveiro, Aveiro, Portugal
- Engg. Mat. & Nanotech. Department, Mackgraphe, Mackenzie Presbyterian University, Sao Paulo 01302907, Brazil
- ³ School of Science, National Institute of Technology Andhra Pradesh, Kolkata, India
- ⁴ FOQNP Group, Advance Photonics Lab, Department of E & ECE, Indian Institute of Technology Kharagpur, Kharagpur, India
- Optoelectronics Research Centre, University of Southampton, Southampton, United Kingdom
- ⁶ University of Science, Vietnam National University, Ho Chi Minh City, Vietnam
- State Key Laboratory of Luminescent Materials and Devices, Guangdong Provincial Key Laboratory of Fiber Laser Materials and Applied Techniques, School of Physics and Optoelectronics, South China University of Technology, Guangzhou, People's Republic of China
- Information Materials and Intelligent Sensing Laboratory of Anhui Province, Key Laboratory of Opto-Electronic Information Acquisition and Manipulation of Ministry of Education, School of Physics and Opto-electronics Engineering, Anhui University, Hefei, People's Republic of China
- 9 School of Physics and Electronic Engineering, Jiangsu Normal University, Xuzhou, Jiangsu, People's Republic of China
- Department of Physics, Indian Institute of Technology Delhi, Hauz Khas, New Delhi, India
- Institute of Photonics and Electronics, Czech Academy of Sciences, Chaberská, Kobylisy, Praha, Czech Republic
- $^{12}\,$ Fiber Optics and Photonics Division, Central Glass & Ceramic Research Institute, Kolkata, India
- 13 LGS Labs, CACI International, Florham Park, NJ, United States of America
- $^{14}\,$ Laboratoire Interdisciplinaire Carnot de Bourgogne UMR6303 CNRS-UBFC, Dijon, France
- Wyant Colleges of Optical Sciences, University of Arizona, Tucson, AZ, United States of America
- $^{16}\,$ Prokhorov General Physics Institute of the Russian Academy of Sciences, Moscow, Russia
- $^{17}\,$ Institute of Solid State Physics, Technische Universität Berlin, Berlin, Germany
- ¹⁸ Guest editor of the Roadmap.
- * Author to whom any correspondence should be addressed.

E-mail: mfernando@ua.pt

Keywords: hollow-core fibers, soft-glass fibers, multimode fibers, photonic crystal fibers, mid-infrared fibers, nonlinear fiber optics, chalcogenide optical fibers

Abstract

Optical fibers, long an enabling technology for telecommunications, are proving to play a central role in a growing number of modern applications, starting from high speed broad band internet to medical surgery and entering across the entire spectrum of scientific, military, industrial and commercial applications. Specialty optical fibers either special waveguide structure or novel material composition becomes heart of all fiber based advanced photonics devices and components. This rapidly evolving field calls on the expertise and skills of a broad set of different disciplines: materials science, ceramic engineering, optics, electrical engineering, physics, polymer chemistry, and several others. This roadmap on specialty optical fibers addresses different technologies and application areas. It is constituted by fourteen contributions authored by world-leading experts, providing insight into the current state-of-the-art and the challenges their respective fields face. Some articles address the area of multimode fibers, including the nonlinear effects occurring in them. Several other articles are dedicated to doped, plastic, and soft-glass fibers. Large mode area fibers, hollow-core fibers, and nanostructured fibers are also described in different sections. The use of some of such fibers for optical amplification and to realize several kinds of optical sources—including lasers, single photon sources and supercontinuum sources—is described in some other sections. Different approaches to satisfy applications at visible, infrared and terahertz spectra regions are also discussed. Throughout the roadmap there is an attempt to foresee and to suggest future directions in this particularly dynamic area of optical fiber technology.

Contents

1. Nonlinear optics in multimode fibers (MMFs)	3
Acknowledgments	5
2. Hollow core optical fibers (HCFs)	6
3. Chalcogenide photonic crystal fibers (PCFs)	9
Acknowledgments	10
4. Nanostructured soft-glass optical fibers	11
5. Plastic optical fibers (POFs)	14
6. LMA fibers	18
Acknowledgments	20
7. Terahertz (THz) optical fibers	21
8. Nanoparticles-doped silica fibers	24
Acknowledgments	25
9. Doped fibers for OA	26
10. MMF amplifiers (MMFAs)	29
11. MIR fibers for SCG	32
12. MIR fiber lasers	35
13. MIR gas-filled HCF lasers	39
14. Single-photon fiber sources	41
Data availability statement	42
References	42

1. Nonlinear optics in multimode fibers (MMFs)

Mohd Rehan¹, Vishwatosh Mishra² and Shailendra Kumar Varshney³

- ¹ Engg. Mat. & Nanotech. Department, Mackgraphe, Mackenzie Presbyterian University, Sao Paulo-01302907, Brazil
- ² School of Science, National Institute of Technology Andhra Pradesh, Kolkata, India
- ³ FOQNP Group, Advance Photonics Lab, Department of E & ECE, Indian Institute of Technology Kharagpur, Kharagpur, India

Status

The MMF-came in 1970s, surpassed by single-mode fiber (SMF), has drawn significant attention owing to space division multiplexing applications, and have took over the stage for a wide range of applications in the last few years [1]. MMFs are the excellent platform to implement the complex nonlinear phenomena due to the multiple ways in which modes interact with each other, the large intensity accommodation, and the ability to regulate the spectral, temporal, and spatial characteristics of ultra-short pulses. Among the three types of MMFs namely step-index (SI), graded-index (GRIN), and multicore (MC) fibers (shown in figure 1(A)), GRIN-MMF attracted much attention due to smaller intermodal dispersion [1]. The nonlinear effects in MMFs mainly intermodal four-wave mixing, cascaded Raman scattering, four-wave mixing, and cross-phase modulation are being exploited for applications like in supercontinuum generation (SCG), multimode soliton propagation, beam shaping, nonlinear optical imaging, and spatio-temporal dynamics [2–5]. Initially, SCG and nonlinear microscopy in MMFs were investigated, however, controlled spatiotemporal phenomena in MMF took over, where spatial degrees of freedom (DOFs) in MMFs offered rich applications like spatiotemporal mode-locking, femtosecond solitons, and Kerr beam self-cleaning [6, 7]. Major contribution in realizing nonlinearity in MMFs was put forward by Wright and co-workers in 2015 where femtosecond nonlinear optics in GRIN-MMF propelled curiosity among researchers and opened the new avenues [8]. Parallel to this, there has been advancement in MMF pulse propagation throughout time. In order to explain the propagation of pulses in MMFs with an intensity-dependent refractive index, Crosignani et al proposed a set of coupled-mode nonlinear Schrödinger equations (NLSEs) in 1982 [9]. Poletti and Horak described an enhanced variant of the multimode NLSEs (or MMGNLSEs) for MMFs in 2008 [10], which included wavelength-dependent mode coupling, nonlinear coefficients, higher-order dispersion, Kerr and Raman nonlinearities, and self-steepening effects. Following that, in 2012, Mafi provided a complete analysis of the modal properties, dispersive behavior, and nonlinear mode coupling in GRIN MMFs [11]. An improved version of the MM-GNLSEs was later created by Pedersen et al [12] that considers the dispersion of the transverse field distributions. Khakimov et al provided a numerical technique to solve the MM-GNLSEs in 2013 [13]. Wright et al have suggested a parallel numerical solution strategy for the MM-GNLSE system, which is freely accessible [14]. The well-known split-step Fourier technique may be used to solve the MMGNLSE either in time domain or the frequency domain, with the frequency domain solution being more effective and inexpensive in time [14, 15]. Few of the recently results are summarized to provide glimpses of different nonlinear applications in figures 1(B)–(E). The beam profiles and modal decompositions are displayed in figure 1(B) dictating beam-cleanup [2]. When the peak power exceeds 10 kW, the spatial profile transforms into a high-intensity bell-shaped lobe with low-intensity background which is about equal in size to the fundamental mode of the fiber. A typical example of SCG in GRIN MMFs utilizing femtosecond laser pulses with peak power 1 MW is illustrated in figure 1(C) [3]. In figure 1(D), the principle of spatiotemporal mode locking attractor in MMF lasers is shown using operators [4]. In figure 1(E), example of conical waves in a SI MMF is shown with full spatiotemporal power (over 3 decades), modal distribution of phase-matched frequencies (red squares), and evolution of a realistic ultrashort (80 fs) conical waves [5].

Current and future challenges

Precise measurements of all relevant parameters and physical phenomena, such as the space and time dependence of the refractive index distribution, supported modes, intermodal interactions, polarizations, and so on, present a challenge to the nonlinear dynamics in MMFs. A further experimental challenge in connection to beam self-cleaning effect is to characterize the modal contents of the light output from a highly multimode nonlinear fiber based upon the M^2 parameter is not suitable for MMFs. A natural extension of the experimental research in silica based GRIN MMFs, can be made to non-silica (e.g. tellurite and chalcogenide) fibers to design high-power supercontinuum (SC) and ultrashort-spatiotemporal soliton sources in mid-IR (MIR) (3–12 μ m) [4, 5] which is a crucial spectral region for multiple applications. However, these glasses are not compatible with traditional vapor deposition techniques, new fiber drawing techniques are highly desired. Another big challenge is the computational complexity of the mode-resolved coupled MMGNLSEs with cubic nonlinearity scales as M^4 [14], and the formulation becomes inefficient

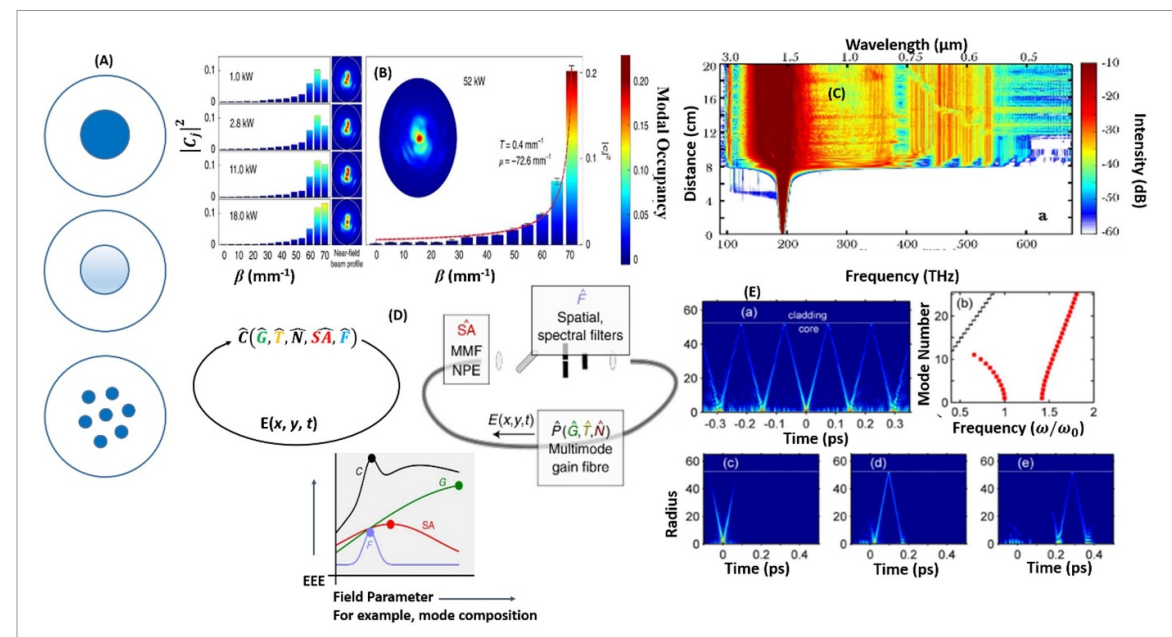


Figure 1. (A) Cross-sectional view of step-index (SI), graded-index (GRIN), and multicore (MC) fibers. Some recent results of realization nonlinearity in MMFs for the applications like (B) self-beam cleaning, (C) supercontinuum generation, (D) spatiotemporal mode-locking, and (E) canonical wave emission in MMFs [2–5]. (A) Reproduced from [2], with permission from Springer Nature. (B) Reproduced from [3]. CC BY 4.0. (C) Reproduced from [4], with permission from Springer Nature. (D) Reprinted figure with permission from [5], Copyright (2021) by the American Physical Society. We allow at most two figures (or 1 figure and 1 table) that are roughly the size of this box.

beyond $M \sim 30$ [16], even after utilizing the current computational efficiencies of GPUs; beyond this value of M, a full (3+1)-D spatiotemporal GNLSE must be solved. Spatiotemporally localized higher-dimensional solitons (also known as light bullets) are equally interesting objects that have piqued the curiosity of researchers in recent years. The (3+1)-D GNLSE, on the other hand, is famously difficult to solve analytically, and functional analytic techniques must be used to show the existence and uniqueness of light bullets [16]. Another challenge is the existing inability to tailor the dispersion profiles of distinct modes independently of one another. We highlight that if this is accomplished, we will have a great deal of freedom in shaping the SC and four-wave mixing spectra of MMFs.

Advances in science and technology to meet challenges

To enhance single-mode (SM) light applications and to enable qualitatively new capabilities and uses, systems that use richer, multimode coherent light are now becoming more popular. To characterize the individual modal contributions to the output Kerr self-cleaned beam, a mode-decomposition technique relying upon spatial-light-modulators has been recently experimentally established [17], further advancement will be useful. As pointed out in the previous section, the conventional fiber-drawing techniques impose big challenge to draw non-silica GRIN MMFs and we could find only one experimental work in this direction which can lead to further development [18]. Well-controlled multimode photonics necessitates photonic designs and control systems with many DOFs, such as high-resolution optoelectronics or other reconfigurable substrates, which are now being met the requirements by the increasing accessibility of computing power and high-resolution, high-performance optoelectronic interfaces, such as cameras, displays, and spatial light modulators. In the ensuing decades, this pattern is most likely to persist. Although it will take years for these multimode photonic technologies to become commercially viable, there is now a strong economic incentive to create reconfigurable multimode photonics that are low-cost and high-performing. There is experimental evidence of individual mode dispersion engineering to increase the bandwidth of intermodal parametric nonlinearities in MMFs [19]. However, there is still a significant issue in having independent control over the dispersion patterns of the distinct modes. Recent advances have been made in understanding the theoretical foundation behind spatiotemporal solitons, the process of spatiotemporal mode-locking [4], and beam cleaning effects.

Concluding remarks

MMFs are still a hot and promising active research area. Highly multimode nonlinear optical systems involve significant technical and conceptual obstacles for understanding and design. But there is a solid foundation for dealing with these problems thanks to developments in the knowledge of multimode linear systems, the

creation of optical components with several DOFs, and improved processing power. We anticipate that future photonics engineers will be able to develop nonlinear multimode instruments and devices in ways that are currently difficult or unattainable with the use of these technologies. We believe that once the ultimate aim of being able to independently modify the different modal characteristics is reached, innovative nonlinear theoretical concepts and practical technologies will arise. MMF endoscope-based deployment, for example, may benefit from laser-driven particle accelerators. Spatial-temporal mode locking may result in on-demand ultrashort pulses with multi-gigawatt peak power levels. These pulses are useful in a variety of scientific fields, including physics, chemistry, and biology because they offer novel techniques for spectroscopy, metrology, and imaging. We anticipate that this new class of complicated nonlinear optical devices will have a significant influence on optical research and will enable a wide variety of new applications, considering the pace of technological and resource improvements.

Acknowledgments

Author SKV would like to thank funding agency DST, Govt. of India for their kind support through vide sanction DST/NM/NT/2018/9(G) and INT/KOREA/P-56.

2. Hollow core optical fibers (HCFs)

Francesco Poletti

Optoelectronics Research Centre, University of Southampton, Southampton, United Kingdom

Status

Since the first experimental demonstration in 1999 of a flexible silica fiber capable of transmitting light in an air-core [20], HCFs have made a very substantial progress and are now competing with more conventional glass-core versions in many areas. In the last 20 years the attenuation coefficient of these air or vacuum guiding fibers has been reduced by six orders of magnitude, from dB cm⁻¹ [20] to fractions of a dB km⁻¹ [21], very close to fundamental limits of silica fibers at telecommunications wavelengths. Outside telecoms wavelengths and throughout most of the near-IR spectrum, HCFs can now be produced with a lower loss than it is fundamentally achievable in glass-core optical fibers [22]. The operational bandwidth where air-guidance occurs can exceed one octave within a single antiresonant window, or considerably more in fibers supporting multiple transmission windows, and the modal quality in HCFs (uncontrollably few-moded at first) has also improved to the point that purely single mode fibers can now be produced [21]. All this progress has been captured in and fuelled by more than 5500 peer-reviewed publications to date (source: Web of science, January 2023), covering design, fabrication and application aspects of HCFs. A total of 500 of these have been published in 2022 alone. The total h-index of the field is well in excess of 100, fuelled by the numerous high-impact publications that were made possible by the unusual and revolutionary properties of these fibers. These include, amongst others: a lower loss than silica in the near infrared [22], ultraviolet (UV) [23] and far infrared [24], the ability to maintain ultrahigh polarization purity [25], a very low backscattering [26], the capability to support novel nonlinear effects in gases filling the core [27], an ultra-high damage threshold [28], low nonlinearity [29], the possibility to guide particles [30] and a reduced sensitivity to thermal variations [31]. Besides an ever-increasing interest from the scientific community, the technology is also reaching a sufficient level of maturity to support commercial products in areas where the fiber properties enable novel applications. These include the laser delivery of ultrashort laser pulses, the efficient generation of UV light, the laser transmission at far infrared wavelengths and, very recently, also the transmission of data with the lowest possible latency. From many points of view, the HCF technology has the potential to become the go-to solution of choice for most applications requiring the waveguiding of light. For this to happen though, in the next decade several challenges will need to be addressed (figure 2).

Current and future challenges

The first challenge will be to find innovative ways to keep extracting ever increasing performance from the fibers. Differently from SM solid-core fiber versions that have reached performances close to fundamental limits, in HCFs there appears to be still a considerable margin for further improvement. In the first decade of the century, HCFs were predominantly exploiting photonic bandgap guidance (PBG) and had a very reduced number of possible cladding topologies around the central core. In the last ten years though, the design space has opened up with the advent of fibers that guided light exploiting antiresonances in the glass membranes surrounding the core. Whilst some designs have emerged as superior to others, the search for 'the ultimate' design is still on. Any new design will need to be compatible with the constraints introduced by fluiddynamics during the fabrication process, e.g. the presence of surface tension and the need to counterbalance it with active pressure. While this will somehow limit the available options, many new directions are still possible. The next decade of research will indicate whether a single design dominating all application spaces will emerge, or whether multiple 'specialized' designs will be tailored to different applications. In the search for the optimum performance, a special role might be played by the material of choice. Thanks to a very small fraction of light overlapping with the solid core boundary (a few tens of parts per million), HCFs do not strictly need to be surrounded by an ultra-transparent medium. This allows, for example, guidance at wavelengths where the glass absorption is high, but it might also enable opportunities to explore alternative glasses or materials, not necessarily the most transparent but offering other advantages.

Another challenge will be that of improving interconnection to solid fibers or to the same type of HCF, and to engineer the integration between HCFs and active/passive optical components such as laser diodes or optical integrated circuits. In both cases, the processes will need to evolve from hero demonstrations to volume-scalable techniques.

As the fiber performance improves and the demand for fibers consequently increases, there will also be a strong push to ramp-up production volumes to reduce the production cost and satisfy the market. HCFs are currently mostly drawn in lengths from a few hundred meters to a few kilometers per preform on short (5–10 m tall) draw towers. While this is sufficient to satisfy the current market, in which a short HCF tailored for a niche application only supported by an air-cored waveguide can be sold at a thousand US dollars per

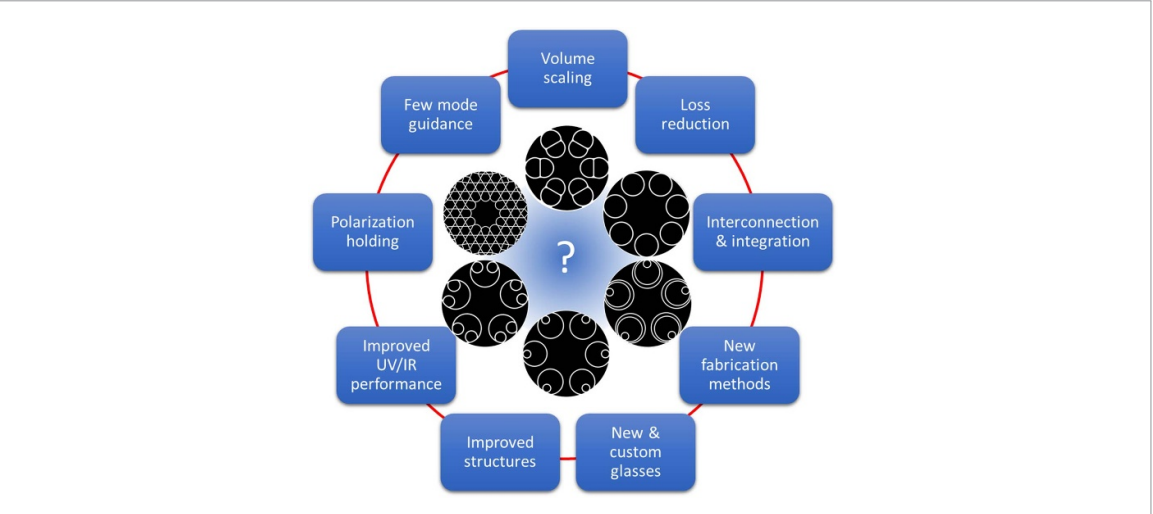


Figure 2. Some of the most successful HCF designs experimentally studied to date, and the main research challenges that will need to be tackled by the research community in the next decade for HCFs to truly become the best possible scientific and commercial waveguide.

meter, for future uses requiring much longer lengths such as for data transmission, distributed sensing, oil well laser drilling, the production cost will need to be reduced by several orders of magnitude. This will require considerable resources and inventive steps and drive innovation for the years to come.

Advances in science and technology to meet challenges

After more than a decade of supremacy, photonic bandgap guiding HCFs have now been surpassed in almost every performance metrics by the easier to fabricate antiresonance guiding fibers (see example cross sections in figure 2). Antiresonant hollow core fibers offer, amongst other benefits, lower loss at all wavelengths, improved suppression of high order modes and lower overlap of the optical field with the glass. Amongst the many tens of antiresonant HCF designs, those based on nested or double-nested nodeless types have emerged as those offering arguably the best all-round optical performance [21, 32]. It is however not clear what the future of this technology will look like. Active research is currently being performed worldwide in search of the next generation of HCFs, and tens of designs are proposed ever year. Only time will tell whether new designs with improved performance will be identified, what their ultimate loss will be, and whether these will be discovered by a human inventor or by machine learning assisted design approaches, of which an increasing number is being proposed.

Besides the fiber design, there is a need to explore alternative ways to produce HCFs, and in particular the primary preform from which these are drawn. Additive or subtractive manufacturing techniques might offer enhanced flexibility in the achievable structure and topology over what is currently possible with the stacking of cylindrical tubes.

The material of choice for HCFs nowadays tends to be chlorinated synthetic fused silica (most typically F300 from Heraeus). This is an outstanding glass developed for the telecoms industry and adopted by the microstructured/hollow core fiber community due to its broad availability. It is not however necessarily the optimum glass for HCFs. For example, chlorine out diffusion causes ammonium chloride formation that contaminates open-ended HCFs. As the industry grows, future work will be needed to develop custom glasses optimized for the HCF needs.

MIR laser delivery and gas sensing beyond wavelengths of \sim 4.5 μ m will also benefit from the use of alternative glasses, with lower phonon energy than silica. Although there have been some demonstrations of non-silica based HCFs already [33], a considerable amount of research is still needed to finesse the MIR-guiding fibers further and fulfill the potential of the technology in this application-rich spectral band.

At the other end of the spectrum, an increasing number of applications driven by quantum computer and biomedical research would require fibers guiding in the UV and visible range. Here, HCFs have already proved advantageous over solid-core versions (for example in terms of loss and immunity from solarization/photodarkening [23]), but more work will be needed to consolidate the technology, as well as to establish and reach its fundamental limits. New or adapted fabrication approaches might also be required for the required thin membrane/small core fibers.

Another area in need of focused research is that of polarization maintaining/single polarization fibers. HCFs have already shown the capability to maintain exceptional polarization purity when the fibers are stationary, way beyond what standard fibers can offer [25]. Achieving true polarization maintaining

capability is however more challenging. Interesting designs have already emerged [34] but further improvements seem possible.

Interesting opportunities in laser delivery, sensing and datacoms will also stimulate further research in the relatively little-explored field of HCFs that guide (controllably) more modes than just the fundamental one. Here, a handful of initial studies suggest the potential for breakthroughs [35], but a lot more work is certainly needed.

Fiber post-processing, either by changing the differential gas pressures inside the fibers [36] or by spinning them during the draw [37] can offer ways to improve the HCF performance beyond that of the conventional design. Other postprocessing methods might emerge in the next few years.

Finally, although most HCF properties have been studied in depth and now well understood [38], a few relatively unexplored areas still exist, like for example the acoustic pickup of HCFs or the impact of guided acoustic-wave Brillouin scattering, where focused/additional studies are needed.

Concluding remarks

Visionary works at the beginning of the century had forecasted a luminous future for the HCF technology. It has taken the international research community over two decades to solve various technological issues in the way of such a vision, but twenty-five years after the first demonstrated HCF, the future looks brighter than ever for the technology. Modeling indicates that with further improvements HCFs have the potential to outperform solid core fibers in almost every performance metrics. For this vision to realize, and for a significant market adoption and impact on society, the research community will need to tackle and solve the numerous research challenges discussed in this section.

3. Chalcogenide photonic crystal fibers (PCFs)

Nguyen Phuoc Trung Hoa University of Science, Vietnam National University, Ho Chi Minh City, Vietnam

Status

Chalcogenide PCFs have gained significant attention in recent years due to their unique properties, i.e. broad optical transparency, high nonlinearity, and versatility in fiber structure design. These properties make chalcogenide PCFs ideal for a wide range of applications, including optical sensing, spectroscopy, telecommunications, biomedical imaging, and laser systems. The chalcogenide glasses are usually composed of the chalcogen elements Se, S, Te with the elements As, Ge, Sb and without the element O. These glasses exhibit a wide transmission in the MIR, high refractive indices and large nonlinear coefficients which make them highly suitable for nonlinear applications.

Recent advances in chalcogenide PCF research include the optimization of the transverse fiber structures to tune their properties such as chromatic dispersion, nonlinearity and optical loss. Besides, the investigation of new applications for these fibers is also of great interest.

SCG, especially MIR SCG, is one important application of the chalcogenide PCFs. The MIR region $(2–20~\mu m)$ is unique in its ability to provide molecular fingerprints for various organic and inorganic compounds. Researchers use chalcogenide PCFs for generating ultra-broadband and coherent SC in the MIR for applications such as optical sensing, medical diagnostics and spectroscopy. For broadband SCG, the PCFs are commonly tailored such that the zero dispersion wavelengths of the fibers are close to the pump wavelengths [39, 40]. For coherent SCG, the all-normal dispersion PCFs are usually employed [41].

Another area of active research is the fabrication of chalcogenide PCFs with large birefringence. Large birefringent optical fibers are required in polarization-dependent applications, especially when the chalcogenide PCFs are combined with integrated optical devices. By breaking the symmetry in PCFs structures, a birefringence as large as 10^{-3} has been reported [42, 43].

Because of their immense potential, chalcogenide PCF research is very active. The development of new fiber designs and exploration of new applications are the driving force for this research area.

Current and future challenges

One of the major challenges in chalcogenide PCF research is the development of reliable fabrication methods for commercialization of chalcogenide PCFs. Although fabrication of special structure chalcogenide PCFs has been successfully carried out with traditional methods such as stack-and-draw [44, 45], or molding method [42], those processes are time-consuming and not well-suited for large-scale production. Such drawbacks limit the commercialization of chalcogenide PCFs. Future research would focus on the realization of more efficient and cost-effective fabrication methods.

Moreover, the low damage threshold power of most chalcogenide glasses has limited their applications from handling high optical power transmission. Using large mode area (LMA) PCFs or hollow core PCFs could be a solution for this problem [45, 46]. Besides, ongoing research would also engineer the compositions of chalcogenide glasses to obtain better optical properties.

Another challenge is to integrate chalcogenide PCFs into devices for practical applications. It is always tricky to couple the light into and out of an optical fiber. Even coupling the light between two different optical fibers is not an easy task without significant power loss. There has been suggestion of some techniques for splicing fluorotellurite and chalcogenide fibers [47] or silica and chalcogenide fibers [48] and has shown significant improvement in transmission efficiency. However, the techniques themself are not suitable for large-scale usage. Moreover, in practical devices, connecting the fiber to other optical components whose optical mode areas are quite different from that of the fiber is much more challenging. Future directions could include the development of new and more efficient coupling methods, as well as the integration of chalcogenide PCFs into micro- and nanoscale photonic devices.

Advances in science and technology to meet challenges

Recent advance in material research has put a step forward in realization of all-fiber laser system employing chalcogenide PCFs. Rare earth ions such as Dr^{3+} or Pr^{3+} have been doped into chalcogenide glasses and the glasses have shown strong emission around the wavelengths of 4–6 μ m [49, 50]. Together with its versatility in controlling the fiber chromatic dispersion, PCFs employing such materials will be potential as lasing or amplifying media in MIR laser systems. This is especially precious as MIR lasers are quite immature compared to their counterparts in the near-infrared region.

All-solid chalcogenide PCFs are good alternatives to air-hole PCFs [46]. Controlling the preform and rod sizes with all-solid PCFs is much more straightforward than controlling the air pressure with air-hole PCFs

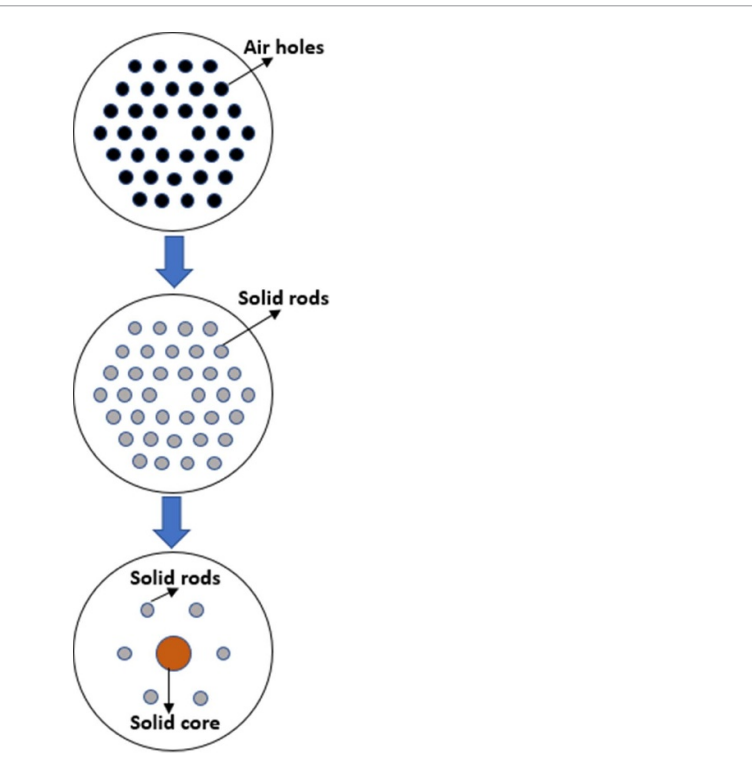


Figure 3. Cross-sections of alternatives to air-hole chalcogenide PCFs: air-hole chalcogenide PCF (top), all-solid chalcogenide PCF (middle) and all-solid hybrid microstructure chalcogenide fiber (bottom).

during fiber drawing. Moreover, the suggestion of all-solid hybrid microstructured chalcogenide fibers has brought a new family of fibers with great controllability of chromatic dispersion and feasibility in fabrication [51, 52]. The all-solid hybrid microstructured fiber consists of a central core with a high refractive index and surrounding rods with a low refractive index embedded in a cladding (figure 3). Thus, three chalcogenide glasses with enough contrast in refractive indices and a good compatibility in thermal properties are employed. Flattened chromatic dispersion with small values of 0 ± 0.4 ps km⁻¹ nm⁻¹ over a wavelength range from 6.0 to 13.2 μ m could be obtained with this family of fibers [51]. Furthermore, by breaking the symmetry of the surrounding rods around the core, high birefringence of 4.5×10^{-4} could also be obtained [52]. Such fibers have been applied in MIR SCG with broad bandwidth and high coherence. The use of all-solid chalcogenide PCFs not only eases the fabrication process but also brings more applicability if we need to connect the fibers with other optical components. Cleaving and splicing all-solid fibers are much simpler than with air-hole fibers. Even when we need tapering for mode-matching, the all-solid fiber structure would not be collapsed.

To address the challenge of device integration, especially to increase the coupling efficiency, the advances of nanotechnology and fiber-to-chip technology can provide the solutions. By depositing a chalcogenide thin film of a few hundred nanometers inside the air holes of a PCF, the transmission property of the fiber can be tuned with the light intensity [53]. A modified fiber end of a chalcogenide PCF using nanoimprinting technique acts as an effective anti-reflection layer and helps to increase the transmission by 27.9% [54]. Direct laser writing has enabled a fiber-to-chip coupler with a wide transmission spectrum [55]. The coupler is contact-free and does not require near-adiabatic tapering of the fiber. These advances will help commercialization of chalcogenide PCFs in the near future.

Concluding remarks

Chalcogenide PCFs are potential for various applications from sensing to laser systems. However, there are some technical and commercial challenges needed to be overcome to realize their potentials. With the increasing demand for high-performance, high-sensitivity optical systems, the research of chalcogenide PCFs is expected to continue to develop.

Acknowledgments

This research is supported by the Science and Technology Development Fund, Vietnam National University—Ho Chi Minh City, Vietnam.

4. Nanostructured soft-glass optical fibers

Weichao Wang and Qinyuan Zhang

State Key Laboratory of Luminescent Materials and Devices, Guangdong Provincial Key Laboratory of Fiber Laser Materials and Applied Techniques, School of Physics and Optoelectronics, South China University of Technology, Guangzhou, People's Republic of China

Status

Nanostructured optical fibers (NOFs) with nanostructured core and cladding show the advantage of tailorable dispersion, high strength, efficient fabrication, and protective tube-shaped cladding [56, 57]. The nano-structurization of soft-glass optical fiber opens up plenty of avenues for functional optical components and devices owing to the outstanding properties of the nanostructures and the nanostructured materials [58–60]. Soft glass is defined as a class of glass with a lower working temperature than soda-lime-silica glass melts [61]. The distinctive features of soft-glass include the prolonged UV and MIR transmission window, low phonon energy, high nonlinear refractive indices, moderate processing temperature, high rare-earth (RE) solubility, and protection from UV-induced damage [62–64].

The fabrication of optical fiber can be classified by a one-step approach and a two-step approach based on the preparation procedure (figure 4). The one-step approach was often utilized to produce optical fiber preforms before the 1980s. However, the yield of the one-step approach is relatively low due to the limitations of the technology and equipment. After the 1980s, the two-step approach was most frequently adopted for the production of preform, that is, the core rod of the preform is manufactured first and then the outer cladding. Techniques for preform preparation include vapor deposition, plasma spraying, sol—gel, and rod-in-tube methods. The current optical fiber fabrication techniques and different optical fibers are summarized in table 1.

To date, soft-glass NOFs have shown tremendous promise as innovative waveguides for lasers, photochemistry, and nonlinear wavelength conversion applications [59, 60, 65]. Glass-ceramic (GC) fibers and quantum dot (QD) fibers are two typical NOFs, which show potential applications in tunable fiber lasers and broadband fiber amplifiers [65, 66]. GC fibers can be fabricated by the double-crucible method, rod-in-tube method, and melt-in-tube (MIT) method. QD fibers can be prepared by the hollow fiber filling method and MIT method. PCF allows light to be controlled in a periodic array of small air holes or solid cores, which can be fabricated by including but not limited to stack-and-draw, extrusion, pressure-assisted melt filling (PAMF), drilling, and 3D printing [67–70]. Further advances in the fabrication techniques of NOFs will accelerate the development of versatile devices in the fields of optoelectronics, quantum optics, biomedical science, etc.

Current and future challenges

The fabrication of soft-glass NOFs is facing two major challenges: (1) the rapid variations in viscosity with temperature, possible devitrification, and distortion during multiple reheating steps; (2) GC fibers and QD fibers face inherent difficulties such as core/cladding mismatch, irregular interface, and element diffusion. Glass formation is an anti-crystallization kinetic process. It requires a sufficiently high viscosity at crystallization temperature to prevent nucleation and crystal growth. At a constant temperature, melt viscosity is determined by structural chemistry (e.g. single-band energy, field strength, electronegativity, and space occupancy) [71]. The relationship between critical cooling rate and melt viscosity at the melting point is inversely functional during the glass formation. The softening temperatures of GC fibers and QD fibers are usually higher than the peak crystallization temperature. Crystals in the fiber core grow fast because the crystallization barrier of glass components is low enough at the softening temperature. As a result, the sizes of the crystals in the fiber core are big enough so that high-transmission and low-loss optical fibers are difficult to achieve. Although GC has the advantages of enhanced luminescence and efficiency in bulk glass, the net gain, laser output power, and slope efficiency of GC fibers are still lower than those of state-of-the-art fiber lasers [72]. Similarly, QD fibers have advantages in terms of tunable emission and optical amplification (OA) characteristics, but their gain is still much smaller than that of RE-doped fiber [73]. The limiting issues of the stack-and-draw method for preparing PCF preforms are relatively high fiber loss, time-consuming, labor-intensive, and mostly limited to circular holes placed in a hexagonal lattice [74]. Moreover, the fabrication of PCFs containing nano-inclusions is more challenging than that of micron-scale devices due to the small tolerance of temperature and pressure variations during the fiber drawing and the higher probability of formation of defects caused by the non-uniformity of the preform [75].

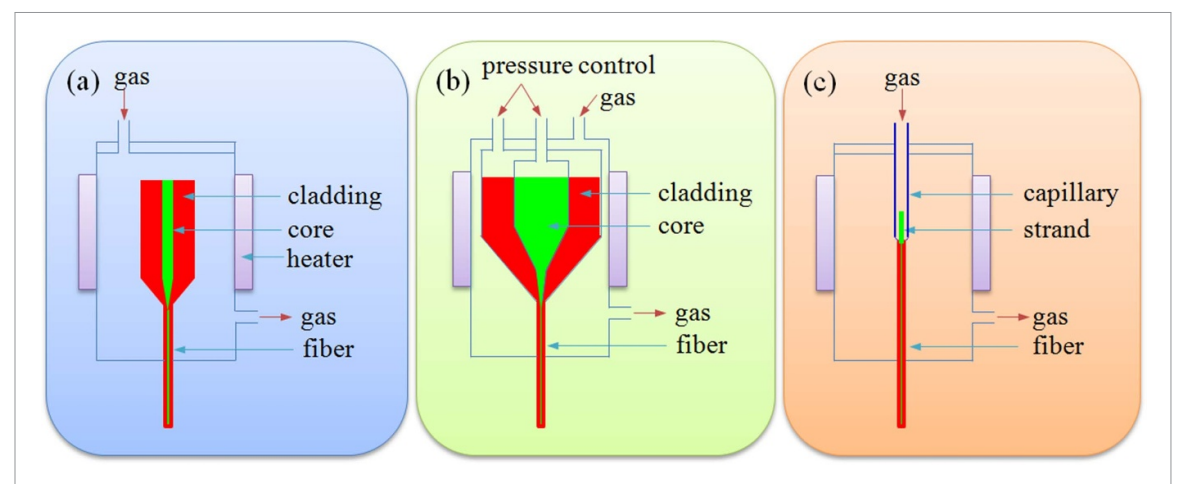


Figure 4. Preparation of optical fiber by the two-step and one-step approaches. (a) Rod-in-tube method. (b) Double-crucible method. (c) Filling method.

Table 1. Comparison of various fiber preparation technologies.

Step	Chemical theory	Preparation methods	Advantages	Disadvantages	Typical applications
One-step approach	Melting	Double-crucible	High-efficient, low-loss, avoid the drilling process, one-step heating	High requirement of the fiber drawing tower, difficulty in stirring the melt and removing the impurity	Fluoride fiber, chalcogenide fiber, silicate fiber, GC fiber
Two-step approach	Vapor deposition	MCVD	Low-loss, simplicity, multifunction, mass production	Only suitable for glass with a simple composition	Silica fiber
	Non-vapor	Rod-in-tube	Easy operation, wide applicability	High fiber loss, time-consuming, difficult for mass production	Most glass fibers
		Suction/Build-in casting/ Extrusion	Efficient, save materials, easy to design the fiber structure	Only suitable for glass with low melting temperature, difficult to determine the preparation	Soft optical glass with lower viscosity
		Stack-and-draw	Easy to design the fiber structure	High fiber loss	Microstructural fiber
		Pressure-assisted melt-filling	High-efficient, save the materials	Limited fiber length, mainly for the core with low melting temperature	Hybrid fiber, the fiber core is toxic
		Melt-in-tube	Avoid crystallization	High fiber loss, requires a unique glass composition	GC fiber, QD fiber, Bi-doped fiber

Advances in science and technology to meet challenges

The selection of soft-glass for the fabrication of NOFs is based on the consideration of both thermal stability and high infrared transparency. To improve the performance of NOFs, one should take the structural chemistry of glass melt, and the relationship of the viscosity-cooling rate during the fiber preparation and post-process treatment into account may open doors to significant advances [59, 71]. From the viscosity-temperature curve, the operating temperature range can be found, which helps to determine whether the preform can easily be drawn into a transparent fiber. As shown in figure 5(a), the desired viscosity ranges of the preform extrusion and fiber drawing are between 4–6 Pa·s and 7–9 Pa·s, respectively. Considering that glass viscosity and cooling rate are closely related, we proposed a viscosity/cooling rate approach to understanding the structural characteristics and physical properties of glass, glass formation,

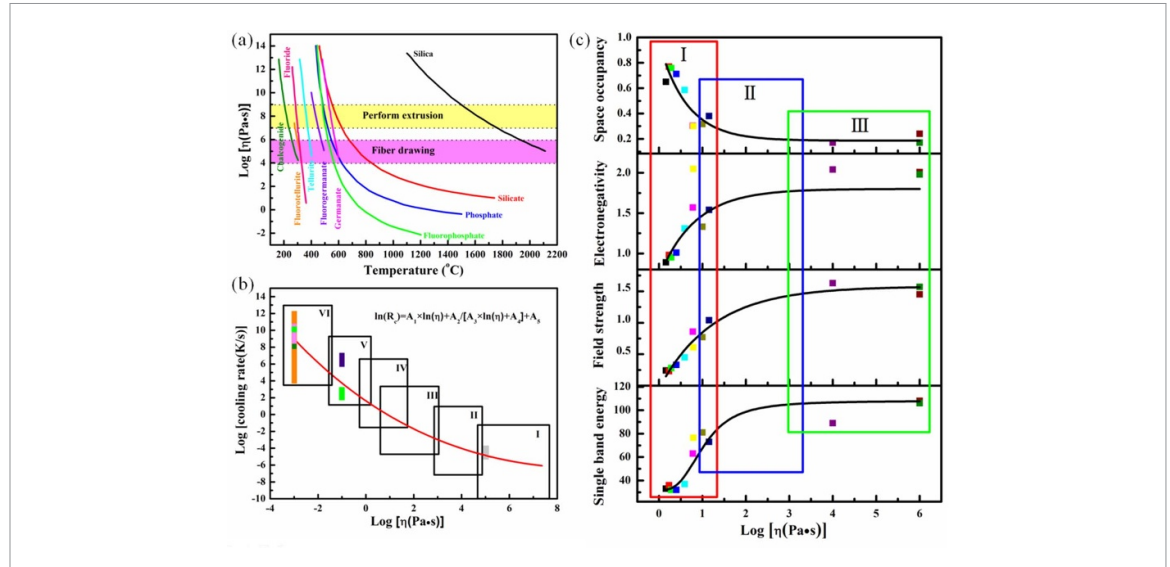


Figure 5. (a) Relationship of viscosity-temperature for several typical glasses. (b) Glass formation concerning the viscosity and cooling rate. (c) Schematic diagram of glass formation based on the viscosity and the single-band energy, field strength, electronegativity, and space occupancy.

and glass transition (see figure 5(b)). The factors that predominantly determine the viscosity are plotted in figure 5(c), including the chemical bonds, structure, and eutectic point in the glass.

Another way to address the future development challenges of soft-glass NOFs is to precisely match the compositions of the core and cladding and to strictly control the sizes and distribution of nanocrystals during the fabrication of GC fibers and QD fibers. The preparation techniques need to be further optimized to reduce the defect state and the loss of the optical fiber. For instance, the interior surface of the cladding glass can be coated to minimize reactions between the cladding glass and the molten core during the molten core fiber formation [76]. Femtosecond laser processing is a promising technique to write on-demand nanocrystals and QDs inside the core of the fiber for the preparation of GC fibers and QD fibers, respectively [77]. The advanced methods developed for multi-material fibers can also be used as a reference to meet the demand for the preparation of NOFs in the future. The availability of better prominence, low loss in the MIR region, and high-strength soft-glass NOF fibers will undoubtedly empower innovative applications in amplifiers, lasers, sensors, and photonics devices.

Further application improvements of the NOFs can be done by providing higher bandwidth, transmission capacities for longer distances, and introducing devices with a lower cost. The combination of two-dimensional materials with specialized NOFs enables wide applications in the fields of nonlinear photonics, medical instruments, and quantum technology that require low power consumption, device miniaturization, and broadband operating range [78]. Modern techniques such as layer-by-layer deposition used for the modification of the fiber structure may produce an enhanced detection sensitivity, as well as the surface functionalization processes used for selective adsorption of target molecules [79]. The combination of microfluidics and the self-assembled monolayer method enables precise control of the spectral characteristics of the functionalized NOFs [80].

Concluding remarks

This roadmap aims to elucidate the challenges and opportunities of the soft-glass NOFs in their fabrication and application. The fabrication of soft-glass NOFs remains challenging due to the rapid variations in viscosity with temperature, possible devitrification, and distortion during multiple reheating steps. Various techniques have been developed for the fabrication of soft-glass NOFs, including but not limited to the MIT approach for the GC and QD fibers, the modified stack-and-draw and extrusion techniques for soft-glass PCFs with solid-core and hollow-core, and the PAMF method for hybrid fibers with soft-glass core and silica cladding. Advancements in functionalized NOF-based devices will greatly expand and increase their potential applications in sensing, biomedicine, and nonlinear optics.

Acknowledgments

The authors acknowledge financial support from the National Science Foundation of China (52172003 and 52130201).

5. Plastic optical fibers (POFs)

Wenyu Du, Benli Yu and Zhijia Hu

Information Materials and Intelligent Sensing Laboratory of Anhui Province, Key Laboratory of Opto-Electronic Information Acquisition and Manipulation of Ministry of Education, School of Physics and Opto-Electronics Engineering, Anhui University, Hefei, People's Republic of China

Status

POF is a type of plastic fiber comprising a polymer light-guiding core layer and an outer cladding layer [81]. The initial development of step index (SI) POF with polymethyl methacrylate (PMMA) as the core material by DuPont in the 1960s resulted in a transmission loss of up to 1000 dB km⁻¹. However, Mitsubishi Corporation's utilization of a high-purity MMA monomer in 1980 reduced the transmission loss to 200 dB km⁻¹. The predominant loss mechanism for POFs is Rayleigh scattering, which is influenced by the molecular size of the fiber material to the power of 6. Consequently, POFs inherently exhibit higher transmission losses than silicon fibers. A critical criterion for selecting POF core materials is their low transmission loss.

POFs can be classified into SM and multi-mode POFs, graded index and SI POFs [82], passive and gain material [83, 84] doped POFs, and microstructured POFs [85] based on different standards. The fabrication process for SI POFs generally involves preform stretching, coating, and co-extrusion methods [86], with the commercial production process predominantly favoring co-extrusion. While the preform stretching method is commonly employed in laboratory settings for pulling POF [87], these light-guiding plastics are characterized by their low cost, flexibility, ease of processing, and excellent biocompatibility. SM POFs, for instance, have found applications in the biomedical industry for ultrasound detection and investigating the mechanical properties of bone cement. Moreover, mPOFs enable selective or localized detection of antibodies, as the sensor layer of the biomolecule can be immobilized in the air pores of the mPOF [88].

The successful development of PMMA POF, along with the rapid progress made in polystyrene POF and polycarbonate POF, has been facilitated by the maturity of PMMA synthesis technology. Additionally, the use of fluorinated polymer materials has enhanced the mechanical and chemical properties of POFs while effectively reducing transmission loss. Furthermore, novel polymer materials tailored for specific scenarios have broadened the application potential of POFs, particularly in areas such as optical communication and data transmissions in automobiles, including audio control, road sign indication, and driving system control.

Undoubtedly, the most significant growth area for POF lies in short-haul, high-speed data transmission. The demand for increased bandwidth is evident in the automotive industry, consumer electronics, and various applications like fiber-to-the-home (FTTH), fiber-to-the-room, and fiber-to-the-desk (FTTD). The adoption of FTTD technology, where optical fiber replaces traditional copper wires to connect computer terminals, represents the realization of a true 'all-optical network'. In these applications, fiber connectivity and ease of installation are crucial and cost-effective considerations. POFs are also utilized as data lines in office and residential networks within local area networks (LANs).

Current and future challenges

Compared to silica, which exhibits a loss of 0.15 dB km⁻¹ at 1550 nm, the main drawback of polymer optical fibers (POFs) is their significantly higher transmission loss, ranging from 100 to 1000 times that of silica. Efforts have been made to mitigate this issue, such as the use of deuterated polymers like PMMA-d8, which can reduce attenuation to approximately 10 dB km⁻¹. However, the production cost of deuterated monomers is prohibitively expensive, and they also tend to increase water absorption. Consequently, POFs are generally unsuitable for long-distance optical signal transmission, but are commonly employed in short-distance optical communication over distances of up to a hundred meters. Therefore, extensive research in POFs focuses on reducing transmission losses and increasing transmission bandwidth.

FTTH networks represent the optimal solution for broadband access. However, telecom operators recognize that meeting the substantial demand for data output necessitates fast data transfer rates across the network. Hence, it is crucial to minimize transmission losses in polymer fibers. The introduction of fluorine atoms in PMMA can decrease the inherent loss of POF by reducing the content of C–H bonds in the polymer.

Another limitation of POFs pertains to their poor heat resistance. In applications with high ambient temperatures, such as aerospace or manufacturing industries, the use of POFs can lead to significant issues, including accelerated signal degradation and extensive aging. The glass transition temperatures (Tg) of the POF core and cladding materials serve as critical indicators of the heat resistance of POFs. When the environmental temperature exceeds the glass transition temperature, the inherent and non-inherent losses in POF transmission increase. Therefore, the development of a polymer material with a higher Tg is essential to construct heat-resistant POFs [89]. Furthermore, this material must meet the same standards as POF

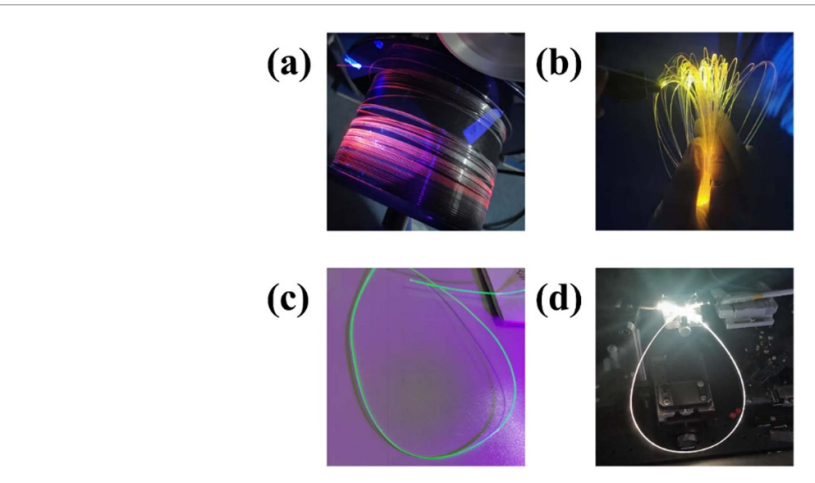


Figure 6. Special POFs. (a) Scintillating POF. (b) Gain material doped POF. (c) Liquid core POF filled with perovskite material. (d) Nonlinear material doped POF.

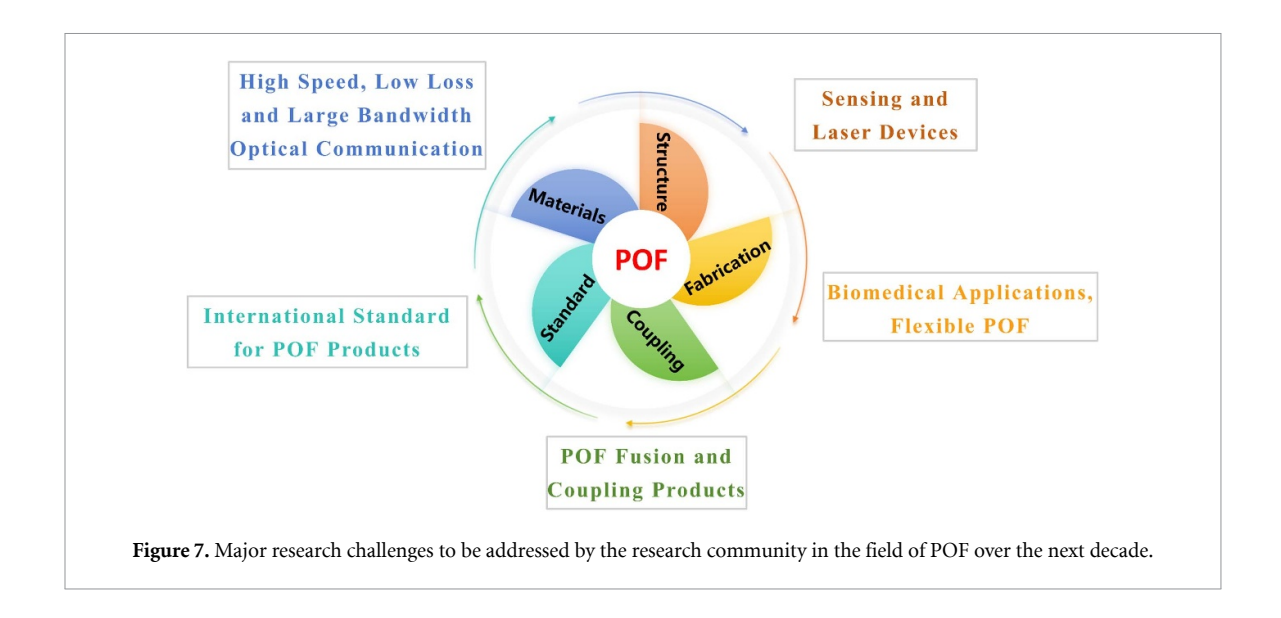
materials, including high transparency, a higher glass transition temperature, and preferably amorphous characteristics.

A third noteworthy limitation is the POFs' tendency to absorb water. Water absorption not only affects the expansion and contraction of POFs but also leads to significant performance degradation. The absorption of photon energy by the polymer is greatly influenced by the vibrations of absorbed water molecules. A substantial portion of the photon energy is converted into molecular vibrations. The resonance wavelength of the O–H bond in water molecules is even closer to the visible wavelength range. To minimize attenuation, it is crucial to operate at wavelengths far from these resonances. The effect of water molecule vibrations can be controlled by material selection or the replacement of specific elements with different weights. Waterproofing measures are employed throughout the fabrication of POFs. Proper drying procedures must be implemented to remove water present in the polymer particles used to fabricate the preform. Failure to do so may result in the release of trapped water as bubbles during fiber stretching, leading to significant transmission losses and quality defects. Certain polymers, such as TOPAS, exhibit high tolerance against humidity. This class of cyclic olefin copolymer (COC) comprises amorphous, transparent, and thermoplastic polymers, with properties varying depending on the substituents. Additionally, specific materials like N-aryl-substituted methylacrylamide demonstrate good water resistance, and the softening point temperature of a 10% n-phenyl methylacrylamide and MMA copolymer can reach 154 °C [88, 90].

Advances in science and technology to meet challenges

Scintillation POF (SPF) was developed in the early 1980s. The SPF is a functional component with both ray detection and optical signal transmission functions. Figure 6 shows some special POFs fabricated by our team. Figure 6(a) shows a SPF doped with RE material Eu(TTA)3(TPPO)2, emitting pink light under UV light. Scintillation fibers have a wide range of applications in the detection of high-energy particles such as long-range scintillation detection and high-resolution imaging. However, current commercial scintillation fibers are based on organic scintillators (mainly organic dyes such as 2,5-diphenoxazole) as the core material to achieve scintillation detection, which generally has the disadvantages of low light yield and poor detection sensitivity, so there is an urgent need to explore the fabrication of new types of scintillation fibers. We introduced the europium complex into the fiber core and produced europium complex-based PSF (Eu-PSF) with excellent scintillation detection performance. Eu-PSF has excellent performances in high luminescence, low-dose-rate x-ray detection, high radiation stability, and long-range and high-resolution x-ray imaging. At the same time, Eu-PSF has good light transmission and can realize long-distance detection.

And figure 6(c) shows a liquid core SPF filled with perovskite material CsPbBr₃, which emits green light under a UV lamp. Because the fiber absorbs short-wave energy (such as UV or gamma rays) and emits at longer wavelengths, it is sometimes referred to as a wavelength shifter. Perovskite scintillators have attracted extensive attention because of their demonstrated exciting performance and significant applications in high-energy particle detection. Such perovskite POFs also exhibit excellent flexibility: they can be easily recovered after 90° bending and their x-ray imaging properties are almost unaffected by bending. POFs based on halide perovskite has many obvious advantages, such as high optical absorption coefficient, large carrier mobility, and simple synthesis method, which can be used as a high-resolution detector for medical imaging, or low bit error rate fiber communication.



Another novel type of POF is the nonlinear POF. Dipolar materials are doped into the core of nonlinear POF, including nitroamine, aniline, styrene, etc [91]. These materials contain non-deterministic π -electron conjugation structures, which have strong nonlinear optical effects. Figure 6(d) shows the nonlinear POF doped with Au nanoclusters, which can be used to study the second and third order nonlinear effects. This kind of nonlinear POF can make electro-optical and nonlinear optical devices.

In addition, POFs doped with gain material PM597 as shown in figure 6(b) have unique advantages in random laser (RL) [92–98]. Compared with conventional lasers requiring a cavity formed by stationary mirrors, RLs only rely on an active medium and a scattering medium, in which an optical feedback is realized by multiple scattering. High threshold and non-directionality are its main disadvantages. On the one hand, to overcome those drawbacks, optical fibers are applied to obtain fiber RLs (FRLs). The two-dimensional confinement of such waveguide geometry allows the combination of multiple scattering and total reflection, which leads to a low threshold RL, certain directionality, and integration simplicity. On the other hand, among all the realized RLs systems, polymers bring together various kinds of gain materials and scattering structures. There are many different types of materials that can be doped into polymers, which provide abundant methods for the regulation of RLs. Accordingly, polymer optical FRLs (PFRLs) were first proposed by us in the last 10 years. Considering the excellent elasticity and transparency of POFS, PFRLs property will be of great significance to biomedical applications.

Concluding remarks

The future demand for POFs in industry and academia is influenced by several crucial factors. Firstly, the rapid development of digitalization and information technology has created a growing need for high-speed communications. POFs exhibit low loss and high bandwidth in the visible light band, making them suitable for data center interconnects, LANs, and metropolitan area networks. Secondly, their exceptional biocompatibility and flexibility make them highly suitable for medical devices used in optical imaging and laser therapy. Lastly, there is an increasing demand for POFs in optical sensing applications such as temperature, pressure, strain measurement, and environmental monitoring.

Several technical challenges hinder the development of POF applications. Firstly, the performance of these fibers, including their loss and dispersion characteristics, needs improvement to meet communication demands. Secondly, the complex manufacturing process results in high production costs, requiring the development of more efficient techniques. Additionally, ongoing standardization and formalization play a critical role in facilitating widespread adoption. Lastly, integrating POFs with other devices requires addressing compatibility and stability issues. Overcoming technical challenges in materials, processes, standardization, and device integration is the key to realizing their extensive applications across various fields, as depicted in figure 7.

Acknowledgments

National Natural Science Foundation of China (12174002, 11874012, 6220032001); Excellent Research and Innovation Team of Anhui Province (2022AH010003), Key Research and Development Plan of Anhui Province (202104a05020059); University Synergy Innovation Program of Anhui Province (GXXT-2020-052); Innovation Project for the Returned Overseas Scholars of Anhui Province (2021LCX011), Anhui Project (Grant No. Z010118167).

6. LMA fibers

Xian Feng and Jindan Shi

School of Physics and Electronic Engineering, Jiangsu Normal University, Xuzhou, Jiangsu, People's Republic of China

Status

The development of LMA fiber technology has been driven by the highly demanded applications of generating or delivering multi-kW continuous wave (CW) laser or mJ-level pulsed laser with high beam quality. Figure 8 summarizes the maximum resistable peak power density of silica, fluoride, tellurite, and chalcogenide glasses, under irradiation of pulsed laser with various pulse durations [99–106]. To avoid (i) fiber failure under high power density (e.g. damage threshold of >1.5 GW cm⁻² for silica under CW laser irradiation [99]) and (ii) laser degradation in spatial, frequency, or time domain due to nonlinear effects. Specifically, the dominant nonlinear optical limitations in high-power fiber laser include stimulated Raman scattering (SRS), stimulated Brillouin scattering, and transverse mode instability, etc, which degrade the beam quality and limit laser output power [107]. LMA fiber technology is straightforward to solve these issues arising from the power density in the power scaling. The strategy of LMA fiber technology requires precisely controlling the index difference between core and cladding at an extremely low level for suppressing higher-order modes. For example, when the MFD of LP₀₁ mode increases from 10 μ m to 100 μ m, the required fiber numerical aperture (NA) decreases from 0.15 down to 0.015, to ensure single mode operation. Correspondingly, the core/cladding index differential ($\Delta n = n_{\rm core} - n_{\rm clad}$) should be below 10^{-4} .

The state-of-the-art vapor deposition techniques for fabricating silica preforms can precisely control the core/cladding index differential within the range of 10^{-3} – 10^{-4} . Therefore, such methods can provide single mode fiber with controllable core diameter $\leq 45~\mu m$ (i.e. NA of 0.04 ± 0.01) for $1~\mu m$ fiber lasers. To obtain a SM ultra-large-mode-area (ULMA) fiber with MFD $> 50~\mu m$, it requires a core/clad index difference $< 10^{-4}$ and ULMA PCF technology [108] is required. ULMA PCF technology has been successful in developing high-power/high-energy silica fiber lasers with near-diffraction-limited beam quality. So-far, the recorded largest MFD is 135 μm in active silica PCFs and 205 μm in passive silica PCFs, respectively [109, 110]. In the former case, ns laser with 26 mJ pulse energy [109] and fs laser with 3.8 GW peak power [111] have been demonstrated, respectively.

In addition, novel active all-solid bandgap ULMA fiber laser has been also demonstrated [112]. In a traditional index-guided PCF, air or low-index-glass is filled in the holey microstructured cladding composed of high-index background material. In an all-solid bandgap fiber, instead, high-index glass is filled inside the periodically arranged microstructured holes and photonic bandgaps is therefore built at the desired wavelengths. By carefully designing the microstructure arrangement, higher-order modes can be effectively suppressed and SM laser can be realized. In addition, ASE and SRS can also be highly suppressed under high power level with the assistance of the designed photonic bandgaps. Near 1 kW CW laser has been demonstrated in an Yb-doped silica all-solid bandgap fiber with a core diameter of 60 μ m, with a near-diffraction-limited-beam quality M^2 of \sim 1.3. It is the so-far recorded highest SM CW laser power from active ULMA PCFs.

Current and future challenges

The challenges of ULMA fiber technique include two aspects: (i) the limitation of material homogeneity (i.e. refractive index fluctuation) and (ii) the issues in practical usage. Both originate from the requirement on ultralow index difference of $<10^{-4}$ between fiber core and cladding.

Figure 9(a) plots the cross section of an index-guided PCF with the triangle-lattice-arranged cladding, where Λ is the hole spacing, d the hole diameter, λ the operation wavelength, and core diameter $D_{\rm core} = 2 \Lambda - d$, respectively. Following references [108, 113, 114], our simulation shows that, an ULMA PCF with 3–5 rings of holes exhibits two zones for SM and dual-mode (DM) operation within wide ranges of $D_{\rm core}$ and λ (see figure 9(b)). Because index-guided PCFs only support leaky modes, the confinement loss (CL) of a certain transverse mode is the function of the geometry and dimension of mode field and the gap between neighboring holes. Therefore, the two operation zones plotted in figure 9(b) are mainly determined by PCF geometric parameters (i.e. d and Δ), and not very sensitive to the refractive indices of the background material and the filling material inside the holes.

When the MFD of LP₀₁ mode is between 100 and 200 μ m, the difference of the effective indices of LP₀₁ mode and the cladding is within 1–5 \times 10⁻⁵. The index fluctuation of the fiber glass is required to be \leq 10⁻⁶, i.e. \leq 10% of the index difference between LP₀₁ mode and the cladding. Otherwise, it causes the mode deformation and CL deterioration of LP₀₁, and additional scattering loss. Figure 9(c) plots the deformation of the simulated LP₀₁ mode when a point defect with diameter of d' and index fluctuation Δn is introduced

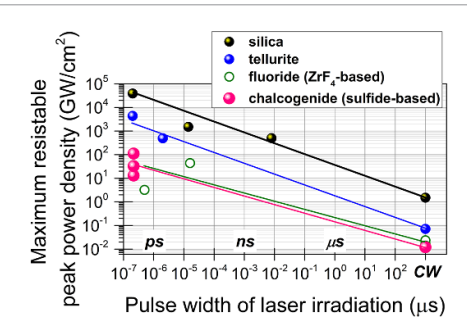


Figure 8. Comparison of maximum resistable peak power density of silica, fluoride, tellurite, and chalcogenide glasses, under laser irradiation with various pulse durations [99–106].

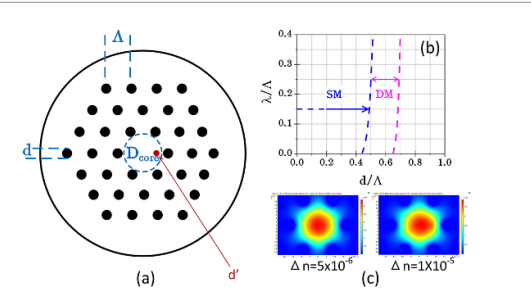


Figure 9. (a) Cross-section of ULMA PCF with triangle lattice. (b) Calculated single-mode (SM) and dual-mode (DM) operation zones. (c) Deformation of LP₀₁ mode when point defect with diameter d' (given $D_{core}/d' = 4$ and $D_{core}/\lambda = 40$) and index fluctuation Δn (left: 5×10^{-6} and right: 1×10^{-5}) is introduced in core area.

in core area (see figure 9(a)), given that the index of the background material n = 1.5. Mind that the best index fluctuation (peak to valley) inside high-quality Schott optical glasses is $0.5-1.0 \times 10^{-6}$ [115], while in the high-quality silica optical glasses used for PCF drawing, such a value is comparable, $\leq 2 \times 10^{-6}$ [116].

Secondly, the extremely low NA of an ULMA fiber makes realizing all-fiber devices challenging, because it is difficult to achieve low-loss splicing between fibers with very different MFDs and NAs. In addition, an extremely low-NA ULMA fiber need to be kept nearly straight for usage because such fibers suffers from high bending loss even at relatively large bending radius.

Advances in science and technology to meet challenges

The solutions to meet such challenges are nothing more than manipulating either the fiber materials or the fiber micro-/nano-structures, as the researchers have done historically in developing optical fibers.

The optical homogeneity of optical glass is the outcome of glass fabrication process and thermal history. The state-of-the-art optical homogeneity of optical glasses means that the largest MFD of a SM ULMA PCF should be \sim 200 μ m, in good agreement with the reported largest MFD of 205 μ m in silica ULMA PCFs [110].

To deal with glass homogeneity issues in ULMA fibers, approaches of tailoring fiber micro-/nano-structures have been demonstrated. For example, the recently developed nanostructured core fiber technology [117] have indicated that the controllable index uniformity 10^{-4} – 10^{-5} can be achieved by nanostructuring the core materials.

A remaining problem of the practical usage of the above SM ULMA fibers is the high bending sensitivity due to the ultralow NA of ULMA fibers. Large bending radius is required in the operation. Few-moded ULMA PCF could be a tradeoff solution. A few-moded (particularly a dual-moded) ULMA fiber can possess both ultra-large MFD and relatively high NA for light collection. Figure 9(b) shows that stable DM operation zone exists in an ULMA PCF design with a d/Λ ranging between 0.5-ish and 0.6-ish. Recently, effective single modeness with an MFD of 115 μ m at 2 μ m has been realized in a DM chalcogenide glass ULMA PCF, by carefully bending the fiber [46], because the higher-order modes suffer from high bending loss than the lower-order modes (e.g. LP01).

Concluding remarks

The rapid development of high-power/high energy fiber lasers presents active and passive ULMA fibers with great opportunities and challenges. A comprehensive solution for realizing practical ULMA fibers is to combine multidisciplinary technologies, including glass material science and engineering, fiber design and

fabrication, optical engineering, and so on, for fulfilling the task of generating or delivering multi-kW power/multi-mJ pulse energy laser output with near-diffraction-limited beam quality. Ultimately, we can expect ULMA fiber technology for high power laser generation and delivering would move from the laboratory into industry usage, after further improvement of fiber design and fabrication and commercialization of auxiliary fiber optic components matching the ultra-large mode field.

Acknowledgments

This work is supported by the National Natural Science Foundation of China (NSFC, 62175096, 62275111), Jiangsu innovation and entrepreneurship Team, Priority Academic Program Development of Jiangsu Higher Education Institutions, and Jiangsu Collaborative Innovation Centre of Advanced Laser Technology and Emerging Industry.

M F S Ferreira et al

7. Terahertz (THz) optical fibers

Anjali and Sunil Kumar

Department of Physics, Indian Institute of Technology Delhi, Hauz Khas, New Delhi, India

Status

The latest developments in the THz science and technology and the growing interest in related applications demand creation of novel sources, detectors, waveguides, and other components at THz frequencies. One of the key technologies is the development of low-loss and low-dispersion waveguides. The recent availability of viable sources and detectors has boosted attention on THz band, closing the so-called 'THz gap' that was previously caused by a dearth of efficient sources and detectors, and other affordable and suitable components. Exciting applications in this new frontier include non-invasive medical imaging [118], pharmaceutical non-destructive drug testing [119], characterization of dielectric materials [120], label-free and non-invasive molecular detection [121], sensing [122], detection of DNA hybridization [123], astronomy and broadband optical communication [124], to name a few. Despite all these potential uses, THz science and technology is still in the developing stage because the majority of the current THz devices are limited to and frequently rely on free-space transmission. Therefore, it is required to construct low-loss waveguides for enhancing the functionalities of the THz devices. Several types of waveguides, including those consisting of metallic two-wires [125], dielectric tubes with metal coatings [126], parallel plates [127], microstructured-fibers [128], Bragg fibers [129], hollow-core fibers [130], porous-core fibers [131], and anti-resonant THz fibers [132], have been proposed as a solution in some earlier studies, while the practical realization of many of them is still in the primitive stage. THz fibers with tunable transmission and guiding properties under certain external stimuli, such as changes in temperature, pressure, or electric/magnetic fields are also proposed [133, 134], thus enhancing the application functionality in sensing, communication, imaging and so on. One of the main limiting factors in producing low-loss waveguides is the choice of the background material. Polymers exhibit better THz characteristics, including the low-loss and nearly dispersion-less transmission in a wide THz frequency range than glasses or the other materials for the said purpose. Hence, the THz waveguides are mostly made of different types of polymers [125-132, 135] due to the fabrication feasibility, high tolerance in the properties against externally induced structural deformations, design versatility, reduced weight, cost-effectiveness, and good environmental stability.

Current and future challenges

Some of the popular materials or dielectrics, such as, silicon, silica, or chalcogenides cannot be widely employed for THz device applications due to significant loss and high dispersion at moderate and high THz frequencies (>0.5 THz) [135–137]. Compared to glasses, polymers have lower absorption losses at THz [135]. Also, to attain desired characteristics of the THz waveguides with substantially low absorption loss, it necessitates to have specific designs, either in the core or cladding or both. Majority of the polymers have modest dispersion over a wide THz frequency range. Although, polyethylene (PE) based PCFs with clad consisting of a pattern of air holes to achieve PBG became quite popular early on, for THz waveguiding and group velocity dispersion management [138], those cannot aid in dispersion tunability in the desired broadband range. PE could be used as the host material for suspended core fibers to produce a sizeably large THz transparency; however, the struts limit its application to only a constrained frequency range (~0.2–0.5 THz) and render it fragile [131]. Other PCF designs that were attempted to achieve either minimal bending loss [130] or birefringence [132], are proven to be challenging to manufacture.

Advances in science and technology to meet challenges

The standard fabrication techniques used for optical fibers in visible and IR range cannot be adapted in the THz range because of the differences in the dimensions and the materials required in the later. Among the polymeric materials, which are transparent to THz radiation, such as polystyrene, PMMA, polytetrafluoroethylene or Teflon (PTFE), COC (commercially known as Topas), cyclo-olefin polymer (commercially known as Zeonex), Vero White Plus (photopolymer), acrylonitrile butadiene styrene, high-density PE (HDPE), Silica (SiO₂), are some of the suitable ones [135–137]. HDPE, Teflon, cyclo olefin polymer, and cyclic olefin co-polymer, all exhibit comparable optical properties at THz frequencies [135]. Zeonex and Topas, however, exhibit smaller losses than Teflon and HDPE at higher THz frequencies [135]. Teflon, Picarin, TPX, and Polypropylene have higher absorption coefficients than COC [136]. Polycarbonate, PMMA and HDPE exhibit lesser absorption than polystyrene [137]. Table 2 lists out some of the representative experimentally realized THz fiber designs, the materials and fabrication techniques used, and the main applications demonstrated.

THz fiber category	Characteristics and application	Material; fabrication method	Fiber design	References
Solid core fiber	High absorption loss and high bending loss, high group velocity dispersion, single and multimode guidance	PMMA core; stack and draw technique		Reproduced from [139]. CC BY 4.0.
Porous core fiber	Low absorption loss, high bending loss, high group velocity dispersion,	PMMA core; Extrusion technique		Reproduced from [140]. CC BY 4.0.
	multimode guidance	PE core. Micro-structured molding technique		Reproduced from [131]. CC BY 4.0.
		Teflon (PTFE) core; sacrificial polymer technique		Reproduced from [141]. © IOP Publishing Ltd. All rights reserved.
Photonic crystal fiber	High absorption and high bending loss, single and multimode guidance.	Topas (COC) core; Drill and draw technique		Reproduced from [142]. CC BY 4.0.
Suspended core fiber	Low absorption loss, single-mode guidance	PE core; combination of drilling and stacking techniques	lum lum	Reproduced from [143]. CC BY 4.0.
PBG and Kagome hollow-core fiber	Low absorption and low bending loss, low group velocity dispersion, multimode bandgap guidance	Vero white core; 3D printing technique		Reproduced from [144]. CC BY 4.0.
Anti-resonant fiber	Low absorption loss, multimode guidance	Resin core; 3D printing technique	0	Reprinted from Yang et al Copyright (2019), with permission from
		PLA core; 3D printing technique	**	Elsevier. [132] Reprinted from [145] Copyright (2019), with permission from Elsevier.
Bragg fiber	Low absorption loss, isolated fiber core, multimode guidance	PMMA core; 3D printing technique		Reproduced from [129]. CC BY 4.0.

When designing a polymer-based THz optical fiber, fabrication restrictions are essential to be considered. Due to their ability to exhibit flat dispersion and low loss characteristics in the THz realm, polymers are the natural choice for THz guiding. In some cases, THz polymer fibers can be fabricated using techniques that were developed for microstructured optical fibers. Drilling/stacking & drawing, extrusion, solvent deposition, casting/molding, and 3D printing are all common fabrication techniques for microstructured optical fibers. Technology such as 3D printing could make it much easier to create THz fibers based devices while maintaining the desired performance. Thanks to 3D printing, rapid prototyping, which is incredibly practical, accurate, mass-producible and flexible, is becoming one of way to go. There is a certain limitation with the 3D printing technology, i.e. the choice of material is compromised for improved surface roughness, nevertheless, it could be made versatile with further improvements in the technology.

Concluding remark

According to the latest microstructured fiber designs available in the literature, low-loss transmission and guidance can be achieved by steering the THz beam mostly through air inclusions in the fibers. Due to their geometrical simplicity, fabrication feasibility, and resistance to fabrication tolerances, anti-resonant fibers distinguish themselves from other hollow-core fibers. For the majority applications, the key goal is to combine simplicity in the design, fabrication feasibility, low attenuation and dispersion at large bandwidths, and SM guidance in a large spectral range. One of the most promising areas of current and upcoming research includes studies on fibers with composite cladding including the metamaterial inclusions in either core of the cladding region. In addition, controlling THz signals propagating through helically twisted fibers shall be investigated that can help incorporate and tune an orbital angular momentum in the THz beam during the guidance itself.

8. Nanoparticles-doped silica fibers

Michal Kamrádek

Institute of Photonics and Electronics, Czech Academy of Sciences, Chaberská, Kobylisy, Praha, Czech Republic

Status

Silica glass, although being one of the first materials intended for telecommunications since 1960s, is still the keystone of today's fiber optics. Without the world-famous erbium-doped fiber amplifier, the current form of the internet would not be imaginable. In comparison with other glasses, silica offers high optical transparency from UV to near-IR region, thermal durability, chemical stability or mechanical strength. But, shifting beyond telecommunication windows and increasing power of fiber lasers, silica drawbacks, at first high phonon energy and low miscibility with RE ions, are starting to dominate and limit the usability of silica glass. In order to mitigate such weaknesses, doping of silica glass with nanoparticles have been proposed [146–148].

Incorporation of RE ions into nanoparticles, of course compatible with SiO_2 matrix, enables modification of the RE³⁺ close vicinity, prevents clustering and tailors their fluorescence and laser properties [149, 150]. It was Podrazký *et al* [147] who, for the first time, used Al_2O_3 nanoparticles in the modified chemical vapor deposition (MCVD) technology and proposed also future utilization of mixed Al-RE oxide nanoparticles. Since this time, the nanoparticle doping has been extensively developed and nanoparticles of numerous oxides (e.g. La_2O_3 , $Y_3Al_5O_{12}$, ZrO_2 , CaO) and fluorides (e.g. LaF_3 , CaF_2 , BaF_2) have been used for preparation of various fibers [151, 152], see scheme in figure 10. For lasers and amplifiers, the nanoparticles should be able to minimize clustering (through non-bridging oxygens) and have phonon energy lower than silica to suppress non-radiative processes. Nanoparticles should also be stable enough to withstand the conditions during preform and fiber preparation.

Nanoparticles-doped optical fibers (DOFs) can be prepared within two basic methods—(1) direct doping with prepared nanoparticles where the nanoparticles are incorporated into a preform [147, 151, 152] and (2) post heat-treatment during which nanoparticles are formed in a preform from appropriate precursors [153–155]. The advantage of direct doping lies in preparation of defined particles and their good characterization; on the other hand, there is a risk of their decomposition during preform processing and drawing. The benefit of nanoparticles formation in a preform can be seen in their controllable formation and growth. Nevertheless, in certain cases, there are still issues with increased losses due to Rayleigh scattering of phase-separated nanoparticles. For a use in high-power lasers, in which high concentration of RE³⁺ is necessary, further research of nanoparticle-doped fibers is needed in order to minimalize the scattering.

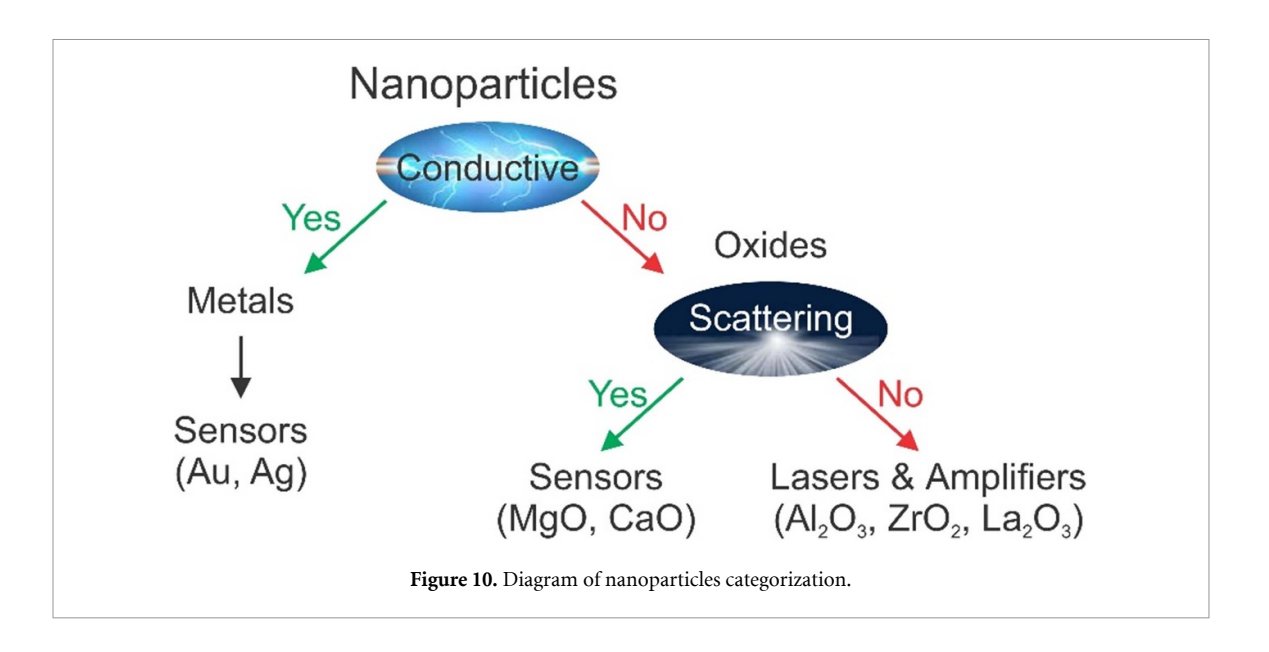
On the other hand, the scattering can be exploited for distributed sensing applications [156, 157]. The nanoparticles play a role of scattering sites along the entire length of an optical fiber and thus enable a continuous real-time detection. Sensing applications such as thermal, radiation, shape or biosensing have recently been reported. Regarding materials, fibers for distributed sensing are based predominantly on silica doped with magnesium or calcium oxide.

Another kind of nanoparticle-doped fibers are those containing metal nanoparticles. Such fibers doped mainly with gold and silver are predominantly used as sensors based on local surface plasmon resonance (LSPR) [158]. The applications of these sensors of high sensitivity and compact structure can be found in monitoring of physical, environmental and biochemical parameters. Compared to plasmonic devices and fiber sensors, those based on LSPR offer fast response time, low fabrication cost and flexible design.

Current and future challenges

One of the limiting issues of nanoparticle-doped fibers for fiber lasers are optical losses due to the Rayleigh scattering [159, 160]. The scattering is a function of the nanoparticle refractive index and its size. For specific nanoparticles, the refractive index is given, and only their size can be controlled. Since the size is closely related to nanoparticle concentration (particle density) in fibers, only fibers with low content of nanoparticles can meet the acceptable losses. Unfortunately, such lowly-doped fibers are not suitable for high-power fiber lasers, which are today the most-needed for practical applications [161]. For high-power fiber lasers, RE³⁺ concentration need to be reasonably high; the RE-doped nanoparticles need to be investigated more deeply and structured more precisely to increase their concentration in fibers while keep the losses low. Moreover, the risk of nanoparticles decomposition, break up or their reaction with the SiO₂ matrix during the thermal processing of a preform [157, 162] need to be taken into account.

The main challenges are associated with chemical and phase analysis of the nanoparticles and their close vicinity in the glass matrix. Due to low nanoparticles concentration and abundance of amorphous matrix around, the analysis is considerably complicated. A detailed compositional study of nanoparticles doped



with magnesium and phosphorus oxides was published by Blanc *et al* [163]. The authors have used 3D atom probe tomography and observed compositional changes depending on the nanoparticles size.

In the field of fibers for distributed sensing applications, the key for up-to-date practical exploitation is scattering-level multiplexing which enables a simultaneous detection of multiple fibers [156]. Simultaneous measurements of different parameters or concentrations is a challenge also for sensors based on LSPR. Their extension from laboratory probes to practical monitoring of civil infrastructure, such as bridges or dams, are limited due to poor production repeatability, unstable long-term work and short service life [158]. The design and precise preparation of advanced metal nanostructures will form research directions for development of relevant LSPR sensors.

Advances in science and technology to meet challenges

Although, the use of nanoparticles in active optical fibers has gained growing attention in the last 15 years, not so much effort have been devoted to the study of the nanoparticle-doped glass structure. If at all, the local RE³⁺ environment has been studied indirectly [162, 164]. The involvement of advanced analytical methods, such as FIB/SEM or atom probe tomography [163, 165] may bring better insight to the chemical and phase composition of nanoparticles and the local vicinity of active RE ions. A detailed analysis of the fiber core structure may set new research directions to enhance the performance of fiber lasers.

A special attention should be given also to structural changes which the nanoparticles undergo during preform preparation and fiber drawing [165, 166]. It seems, Al_2O_3 nanoparticles used for doping are dissolved during thermal treatment [162, 164], while different oxides are phase-separated and nanoparticles are, on the contrary, formed during the fiber preparation or targeted thermal annealing [155]. Detailed analysis and precise structuring are the cornerstones also for both types of nanoparticle-doped fibers used for sensing applications.

Concluding remarks

Nanoparticles in silica-based optical fibers have their irreplaceable role in various types of applications. Oxide nanoparticles in active fibers for fiber lasers bring certain advantages by preventing clustering of RE ions and decreasing phonon energy in their close vicinity, but they can by also detrimental. The harmful effects lie in increased losses due to Rayleigh scattering when exceeded certain concentration level of nanoparticles. However, what is detrimental for fiber lasers can be utilized in fiber sensors based on distributed sensing. In such applications, scattered light is used for detection of various physical and chemical parameters. For sensing applications, also metal nanoparticles in silica fibers can be used. Such sensors are based on enhanced light field obtained on the surface of nano-scaled metal particles. Both types of sensors can be used for real-time monitoring of various physical, chemical and environmental parameters.

Acknowledgments

The author thanks the Czech Science Foundation for financial support (Project No. 21–45431L).

9. Doped fibers for OA

Mukul Chandra Paul

Fiber Optics and Photonics Division, Central Glass & Ceramic Research Institute, Kolkata, India

Status

DOF with incorporation of suitable REs and other co-dopants serve as an important component for OA in doped fiber amplifier which become a key element of long-haul optical transmission systems with the success of development of low loss transmission fibers, pump laser diodes, and high-speed photo diodes. The first DOF with incorporation of neodymium (Nd) in a SM fiber was demonstrated in 1960 [167]. The real revolution of OA started in late 1980 using erbium doped fiber (EDF). Prof. D. Payne and E. Desurvire have done significant research in this area [168, 169]. The first Er³⁺-doped fiber amplifier (EDFA) was demonstrated in 1989. The most important of all rare earth elements for telecommunication fiber network is erbium because it can amplify signals in the most important frequency spectrum in silica fiber: now-a-days the technology about the EDF for amplification is fully maturated from view point of optical gain as well as noise figure. On the other hand, erbium or Er/Yb co-doped fiber for OA within 1530–1625 nm region covering both C and L band is not fully matured. Besides the REs another important DOF known as bismuth DOFs having different host materials such as aluminosilicate, phosphosilicate, and germanosilicate glass shows broad band amplification under suitable pumping wavelength within 1150–1600 nm wavelength [170, 171].

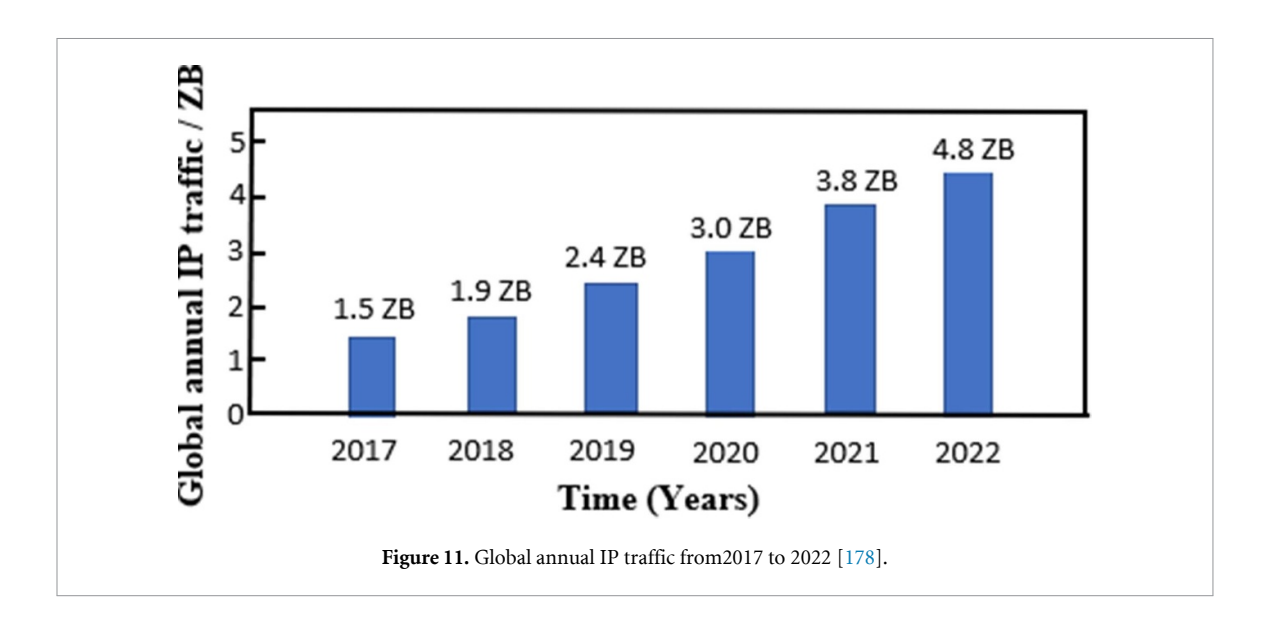
DOF with incorporation of various REs or bismuth serve as a heart of optical fiber amplifier where the amplification of incoming electromagnetic radiation happened through a stimulated emission in the amplifier's gain media. Such kind of DOF for OA into wider spectral region covering 1260–1650 nm wavelength region is very much important into ultra-wide broad-band optical communication system (OCS) due to increase of data traffic, requirement of ultra-definition video as well as upgradation of the fifth-generation (5G) communication system where require the enhancement of gain bandwidth for OA covering all the bands of optical window.

If the optical fiber doped with suitable co-dopants into silica or non-silica glass matrix is being able for OA having an average optical gain greater than 30 dB with NF of less than 4.5 dB covering S, C and L band, it will change the whole scenario of our modern OCS considering the increased global demand of internet connection. The recent report shows that more than five billion users are internet connection worldwide till April, 2022 which becomes 63.1% of global population [172].

Current and future challenges

The current gain bandwidth of the OA of EDF limits the enhancement of the transmission capacity in optical fiber communication systems. Recently Chen *et al* [173] reported an erbium—ytterbium co-doped phosphosilicate fiber to increase the transmission capacity by extending the L-band gain bandwidth to 1623 nm having average gain of 20 dB and NF of 6.01 dB at 1623 nm with 23 dBm saturated output power under the signal power of 3.7 dBm and pump power of 720 mW at 1480 nm. Qiu *et al* [174] demonstrated the OA using a few mode Er/Yb co-doped cladding pump fiber for extended L-band 1570–1620 nm operation achieving average gain of 20 dB. Bi-DOFs will have great potentials to expand the gain bandwidth of the optical amplifier to multiple bands covering O, E, S, C, L and U for the SMF transmission [175, 176]. The doped fiber amplifier of high-gain and large-bandwidth (O to U band) are desirable for future high-capacity OCS in order to satisfy the requirements of high-performance multi-band optical communication networks. To develop such kind of doped fiber amplifier require new and more advanced materials based optical fibers with incorporation of multiple REs with bismuth into suitable compositional glass-based material and need to proper waveguide design.

The research on doped fiber based optical amplifier is facing two major challenges: One: limitation of bandwidth of doped fibers for OAs in O, E, and S telecom bands, second: Most of doped fibers suffer from the strong excited-state absorption noticeably spectrally narrowing the net gain and suppressing its magnitude. With the development of various emerging technologies such as the internet of things, big data, virtual reality, artificial intelligence (AI), and 5G mobile communication, society demands increasingly more information exchange and transmissions [177]. According to the research data released by Cisco in 2019, shown in figure 11, global annual internet (IP) traffic will grow from 1.5 zettabytes (ZB) in 2017 to 4.8 ZB in 2022, with a compound annual growth rate of 26% [178]. The lack of suitable doped fibers for OA covering O, E, S, C, L and U which used in OCS serving as the backbone of communication networks will be faced stronger challenges with respect to such kind high-traffic growth trend. The doped fiber for broad band OA in high-speed and high-capacity optical fiber communications systems and networks will be the main development direction in this area [178].



Advances in science and technology to meet challenges

The main challenge in our present OCS is the high demand of data communication with the development of global mobile internet, cloud computing, 5G communication system which showing an explosive growth. So, the suitable technology should be adopted to increase the transmission capacity of optical fiber communication systems through development of suitable DOF for OA achieving reasonable optical gain covering both C + L band along with O and E bands. In this direction, one of the most prominent approach is the adjustment of the ratio of phosphorus to aluminum in the silica glass for extending the bandwidth in the L-band [179, 180] of EDFA. In the past decades, researchers are not succeeded to develop other doped fiber based commercial optical amplifier module due to its low efficiency which stimulated the search of novel optical materials for broad-band amplification.

As a result of it, the latest status of Bi doped fiber shows the maximum gain of 31 dB, a minimum noise figure of 4.75 dB [181]. The depressed cladding bismuth-doped phosphosilicate fiber [182, 183] shows a record gain coefficient of 0.18 dB mW $^{-1}$ at 1.3 μ . Bi/Er-codoped glass optical fiber [182, 183] shows ultra-broadband luminescence between 1000 and 1570 nm wavelength which typically cover O, E, S, C and L bands of optical window. The efficient fiber amplifier serving as key component of high-speed ultra-broadband optical fiber communication, for the spectral ranges 1300–1520 nm and 1610–1700 nm are still unavailable. Some recent results have been demonstrated potential possibility to achieve ultra-broadband gain which can possibly cover entire optical ranges from 1000 to 1700 nm [184].

The research on combination of two different doped active fibers serving as hybrid fiber based optical amplifier may address the challenges of attaining C + L band OA under suitable pumping scheme. In this direction, a modern wideband and flat gain erbium-doped fiber amplifier which consists of hafnia-bismuth-EDF (HB-EDF) and zirconia-EDF as a hybrid active fiber under backward pumping attained a gain flatness of 23.8 dB with the maximum gain variation of ± 1.3 dB, throughout a wide bandwidth of 70 nm, that is from 1530 nm to 1600 nm [185] shown in figure 12.

Therese archon dual-stage EDF amplifier based on a combination of bismuth EDF and HB-EDF provide amplification in C– and L–band region, respectively showing a flat gain of about 14 dB with gain fluctuation less than 1 dB over the wavelengths from 1535 nm to 1605 nm at input signal power of -10 dB [186].

Concluding remarks

Research on development of suitable material composition based doped fibers for ultra-broad-band OA will be one of the important aspects to meet the future demand of high data- OCS. We believe that Bi-DOFs will have great potentials to expand the gain bandwidth of the optical amplifier to multiple bands for the SMF transmission. The doped fiber amplifier of high-gain and large-bandwidth (O to U band) are desirable for future high-capacity-OCS in order to satisfy the requirements of high-performance multi-band optical communication networks. To develop such kind of doped fiber amplifier require new and more advanced materials based optical fibers with incorporation of multiple REs with bismuth into suitable compositional silica glass-based material and needs to proper waveguide design. In the future, it is hoped that the research and development related to doped fiber for OA needs a new optical fiber which can be designed to reduce the transmission loss and form very efficient optical amplifier of large gain and a low noise figure promoting the

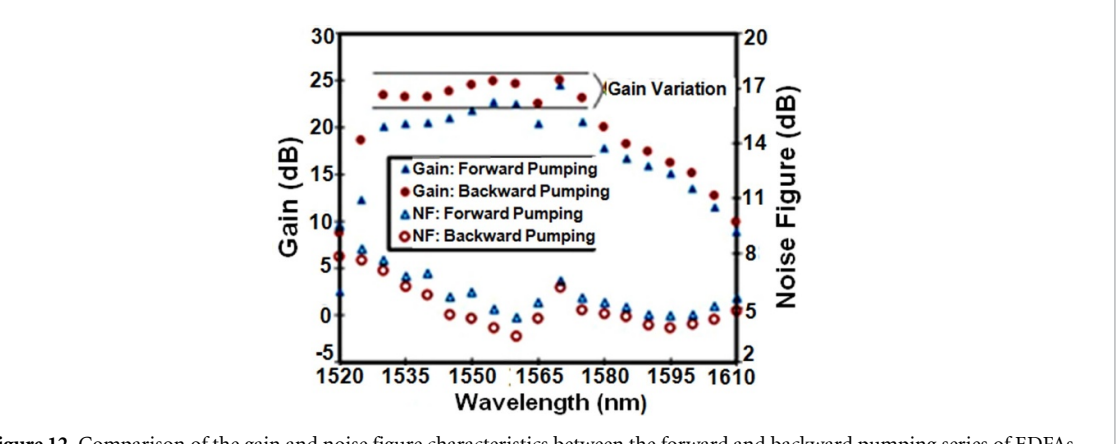


Figure 12. Comparison of the gain and noise figure characteristics between the forward and backward pumping series of EDFAs at input power of -30 dBm. Reprinted from [185], Copyright (2019), with permission from Elsevier.

progress of optical fiber communication technology. The advance research in the field of doped fiber for OA can have a very beneficial impact on power consumption efficiency as well as data transport cost.

Acknowledgments

The author is grateful to his colleague's Dr Anirban Dhar and Dr Shyamal Das for their contributions. The author also thanks to Council of Scientific and Industrial Research (CSIR), New Delhi for providing suitable funding related to development of fiber optic based broad-band source at NIR region.

10. MMF amplifiers (MMFAs)

Kazi Abedin

LGS Labs, CACI International, Florham Park, NJ, United States of America

Status

Optical fiber amplifier exhibits multimodal behavior when the *V*-number (defined as $V = 2\pi a (NA)/\lambda = 2\pi a \sqrt{n_1^2 - n_2^2}/\lambda$, where, *a* is the core radius, *NA* is the core NA, n_1 , n_2 are the core and cladding refractive index) of the gain fiber exceeds 2.405. Operation of a MMFA was first experimentally demonstrated in 1991 using an EDF with a core diameter of 13 μ m and NA of 0.32, supporting ~22 modes [187]. Such amplifiers were intended for amplifying multimoded signals in optical systems, including LANs and fiber sensors, which demanded low cost and robust optical paths.

The initial purpose of developing MMFA was to amplify multimoded light by guiding over the entirety of modes without considering any individual ones. However, in recent years there have been growing interests in developing MMFAs that provided access to each individual modes for the purpose of amplifying multiple signal channels. Amplifiers were built using fibers that supported 2-, 4-, and 6-fiber modes for application in space division multiplexed optical communication systems. To realize such few-mode fiber amplifiers, gain fibers with different core size/shape, refractive-index distribution, such as step, graded, ring, as well as different RE dopant distributions, e.g. confined, extended, annular, multi-step have been proposed [188–193].

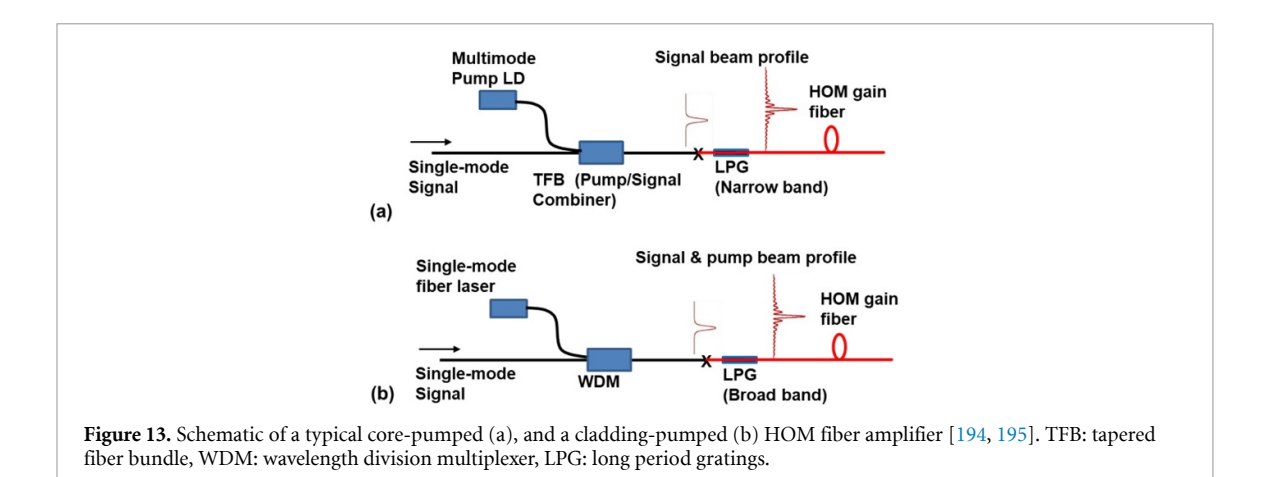
Apart from optical communication, MMFAs have also been used for generating spectrally and spatially coherent high power laser beam. It has been found that the linearly-polarized (symmetric) higher order modes (HOMs), LP_{0,N}, of MMF is less bend-sensitive compared with the fundamental mode LP_{0,1} and they can be propagated with remarkable robustness when N is sufficiently high. The number of symmetric modes in a MMF is given by V/π . For operation in the 1.55 and 1 μ m wavelength region, erbium and ytterbium-doped MMFs with core size larger than 100 μ m were developed, which could support LP_{0,N} with N as large as 10. Such HOMs exhibited effective mode areas of several thousand μ m² [194, 195] making them particularly suited for high-power pulse amplification.

To excite such large core gain fiber, pump sources with relatively high power are needed. Core-pumped erbium-doped HOM fiber amplifiers, usually employ SM CW 1480 nm cascaded Raman fiber laser as a source for pump, where the pump wave is co-propagated with signal as the same $LP_{0,N}$ mode [194]. Propagating the signal and the pump in the same mode number results in better overlap between excited region of the gain fiber and the signal and thus efficient energy transfer from the pump to the signal. On the other hand, in Yb-based HOM amplifiers the gain fiber is pumped efficiently through the cladding using 976 nm multimode pump diodes [195]. The schematics of a typical core- and cladding-pumped HOM fiber amplifiers are shown in figure 13. It is important to note that, prior to launching into the gain fiber, mode conversion of signal from $LP_{0,1}$ to $LP_{0,N}$ is essential for both cases, which can be achieved by several devices, such as, fiber long period gratings (LPGs), spatial light modulators, axicon, or phase plate.

Current and future challenges

Due to the involvement of multiple modes in MMFA, designing and implementing an efficient MMFA could be quite challenging. There are several factors that need to be considered in this connection.

- Minimization of intermodal coupling: In MMFAs where multiple signal channels are propagated as different modes of the multimode gain fiber, it is crucial to suppress the coupling between the modes to avoid crosstalk. The coupling between neighboring modes depends strongly on the separation between the effective refractive indices of the Eigen modes of the fiber.
- Minimization of differential modal gain (DMG): It is often observed that in MMFAs, the gain associated with different modes are not the same because of the difference in overlap of the modes with the inverted region of the RE doped core [188, 189]. DMG could pose serious problem for application related to communication, where different signal channels are sent using multiple spatial modes.
- Suppression of amplified spontaneous emission (ASE) noise: In HOM amplifier, cladding-pumping of the large doped-core (over $100~\mu m$ in diameter) tends to produce large amount of ASE noise due to the coexistence of hundreds of modes supported by the core. This could result in a severely reduced slope efficiency of the amplifier and degradation of mode purity particularly when the input signal power is low. Hybrid amplifier design has also been proposed to overcome this problem [195].
- Realization of the amplifier with small form factor: For efficient launching of signal(s) and pump into the multimode gain fiber low-loss all-fiber combiner is desired. It is important that each spatial mode is launched with proper amplitude and phase distribution to ensure a high overlap integral with the



corresponding guided mode of the gain fiber. Any mismatch that a mode experience at the input not only lowers the net gain, but also results in increased noise figure. In HOM amplifier that are core-pumped, both signal and pump are required to be launched as the same $LP_{0,N}$ mode, which is typically achieved using a LPG with bandwidth wide enough to cover both the signal and the pump wavelengths [194, 195]. Moreover, an additional high-index core-structure is added at the center of the core to guide fundamental mode light that will be subsequently converted to $LP_{0,N}$ mode by an LPG inscribed on it.

Advances in science and technology to meet challenges

During the last decade, there have been research and development efforts across the globe towards realization of efficient and compact MMFAs for use in various applications, overcoming much of the challenges outlined above.

Gain fibers with different core diameters and refractive index profiles have been studied to reduce the intermodal coupling by increasing the effective index differences of the various modes. In the case of SI MMF, the average separation between the effective indices of the neighboring modes is proportional to λ^2/a^2 , while it remains independent of Δn . Here λ is the wavelength, a is the core radius, Δn is core-cladding index difference. This suggests that to increase the number of fiber modes supported by the fiber, it is beneficial to increase the refractive index difference instead of the core size. Moreover, fiber could be made to have elliptical core to break the azimuthal symmetry and reduce the coupling between the asymmetric modes of two different orientations [193], e.g. LP_{11a} and LP_{11b}.

To reduce DMG, different techniques have also been developed, which includes, using a tailored pump intensity distribution for core-pumped amplifiers [194], and optimized the RE dopant distribution in the case of cladding-pumped amplifiers [195, 196]. Genetic algorithm-based optimization technique has also been applied for achieving the optimal dopant distribution that offered lowest DMG in a gain fiber. One remaining problem is that despite implementing all these measures DMG is still difficult to completely avoid in dynamic situation, when the signal power in different modes varies with time.

As fan-in and fan-out, few-mode fused fiber coupler [197] as well as photonic lanterns have been developed [198], which has led to small size of the amplifier. These novel and unique approaches are found to be highly effective in providing one-to-one correspondence between the signal channel and a specific mode of the multimode gain fiber.

Besides step and parabolic index, MMF has been made lately using a core with more intricate structure to guide structured light [199]; beams that manifest abrupt changes in amplitude, phase and/or polarization within the beam envelope. Gain fiber with ring shaped core have been developed to amplify ring-shaped beam possessing orbital angular momentum [192]. Recently, in [200], a MMF capable of guiding Airy beam as LP_{0,4} mode has been designed using inverse waveguide problem technique from the electric field profile and was successfully fabricated by using modified plasma-assisted chemical vapor deposition and used to demonstrate Airy beam propagation. This powerful method can be used to design other fibers that have the potential to effectively generate modes with other field shapes. For example, the normalized index distribution required for a fiber to support sink and super-Gaussian shaped electric field distributions are shown in figures 14(b) and (c), respectively [201].

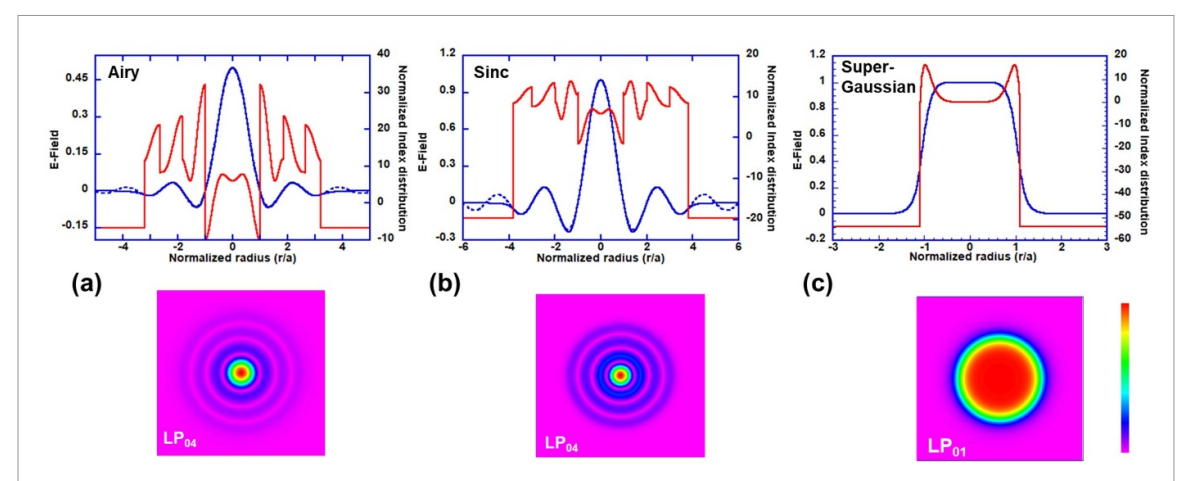


Figure 14. Fibers designed to guide optical field of various shapes. Blue lines show the field profile ψ and red lines is the corresponding normalized refractive index distribution ν , defined as ν (r/a) = $a^2k_0^2$ ($n^2-n_{\rm eff}^2$), here, k_0 is the propagation constant in free-space, n is the refractive index, $n_{\rm eff}$ is the effective index of the mode, (r/a) is the radius normalized to a length scale such as core radius as introduced in [200]. (a) LP_{0,4} mode guiding an Airy beam, $\psi = J_1$ (Cr/a) / (Cr/a), where J_1 is the Bessel function of the first kind of order 1, C=3.831 (the first zero), (b) LP_{0,4} mode guiding Sinc beam, $\psi = \sin(Cr/a)$ / (Cr/a), where $C=\pi$, and (c) fundamental mode LP_{0,1} guiding super-Gaussian beam $\psi = \exp[(-(r/a)^{2m})]$, m=4 (m is a parameter controlling the sharpness of Gaussian beam). Bottom row shows the transverse field distribution. Reproduced following figure 13 of [201].

Concluding remarks

There has been tremendous progress made in the area related to MMFA to meet their demand in different application. There are still ample opportunities to explore further in this area. It is expected that there will be further progress in developing technologies related to MMFA, including development of gain fiber of different dopants with precise distribution, that could be useful for creating structured light directly from the fiber output. It would be possible to develop RE-doped gain fiber that will guide and simultaneously amplify structured light for use in a myriad of applications including fiber-optic or free-space communications, high-resolution microscopy, quantum entanglement, machining and so on.

11. MIR fibers for SCG

Bertrand Kibler and Frédéric Smektala Laboratoire Interdisciplinaire Carnot de Bourgogne UMR6303 CNRS-UBFC, Dijon, France

Status

Fiber SC sources may combine high brightness and coherence of a laser with multi-octave frequency bandwidth of a lamp, as well as flexible delivery and compactness inherent to fiber-format systems. All this makes them unique tools capable of replacing most existing light sources ranging from blackbody radiations to synchrotron beamlines used today in numerous applications related to metrology, spectroscopy, imaging and remote sensing [202-205]. SCG in optical fibers has been a subject of intense investigation over the last 25 years, benefiting from the comprehensive understanding of nonlinear fiber optics and the continuous development of mature cutting-edge technologies such as ultrashort pulse lasers and optical fibers [205–208]. Significant efforts have been devoted to overcome inherent shortcomings of broadband nonlinear wavelength conversion during pulse propagation into an optical fiber, such as polarization state preservation, power spectral density optimization, damage threshold, coherence and stability issues. As a consequence, table-top fiber SC sources are nowadays robust and reliable, and build for non-experts in the field as turn-key and low-maintenance units. Commercial fiber SC sources are mostly based on silica- and fluoride-glass fibers, with watt-level output average power over their complete transmission windows, from 0.4 to $2.4 \mu m$ and up to $4.8 \mu m$ respectively, by using near-infrared pulsed pumping (see figures 15(a) and (b)). Nevertheless, emerging SC products extending up to the 10 μ m waveband can be found with a cascaded nonlinear MIR fiber system including a chalcogenide-glass fiber [205].

The field of research on fiber SC sources still remains very active worldwide in targeting such capabilities over the entire MIR range. This is driven by the current need for the next-generation sources in this 2–20 μ m waveband, for instance overcoming drawbacks of traditional thermal emitters [209, 210]. This broad spectral domain contains the main IR atmospheric windows and cover spectroscopic signatures of numerous molecules, also known as the molecular fingerprint region (see figure 15(c)). This makes the MIR region of considerable interest, with a myriad of applications related to environmental monitoring, spectroscopy and imaging, security and defense, energy conservation and material processing, and free-space communication. Specialty optical fibers for SCG have already started playing a key role in this high-demanding field [69, 211]. But, how far into the infrared can we expect them to operate in a near future?

Current and future challenges

Besides current challenges for bridging the gap between lab-scale and commercial dimensions (i.e., replace bulky MIR pump lasers, simplify complex cascaded fiber systems and fiber splicing, optimize power spectral density, pulse-to-pulse stability and degree of polarization) [205], the progress on extending the wavelength coverage to the full MIR remains difficult (in particular beyond 15 μ m). Just beyond the MIR, the far-IR region is also of considerable importance for spectroscopy to determine intermolecular interactions, and the low-frequency collective motions of complex molecules, including polymers, peptides, or proteins [212, 213] (see also figure 15(c)), thus imparting wide-ranging impact in the physical, chemical, biological, and medical sciences. Note that main issues in the far-IR usually come from the strong phonon absorption in the Reststrahlen bands of semiconductor crystals [214]. The major challenge for fiber SC sources today is to bridge the gap between the MIR and far-IR spectral regions (see figure 15(a)).

Harnessing broadband spectral broadening is a very challenging task when tackling new spectral regions, in particular when less technologically mature, because of the lack of practical laser sources, and the weakness of both thermal emitters and detectors. This becomes especially difficult when entering the long-wavelength infrared (8–14 μ m) and even more beyond 15 μ m when approaching the far-infrared. However, the way to success still depends on our end-to-end control of both materials chemistry and nonlinear fiber optics to optimize each of the crucial steps, such as glass synthesis and purification, fiber design and drawing, as well as engineering of SCG. Recent advances in MIR fiber SC sources can be attributed to the improving quality of specialty fibers made of non-silica soft glasses, but also to the development of compact and powerful MIR pulsed laser pumps. The latter now enable efficient pumping of SCG from the CW down to the femtosecond pulse regime, up to MHz repetition rate, and over the 2–10 μ m wavelength range [215].

Among the large variety of MIR fibers that have been developed and intensively tested for SCG, three relevant families of soft-glass compositions emerge, namely fluorides (mainly based on ZrF₄ or InF₃), tellurites (TeO₂-based), and chalcogenides (mainly composed of the following chalcogen elements: S or Se). With respectively increasing transmission windows into the MIR, and increasing nonlinearity as well, the research state-of-the-art for MIR SCG in such fibers has confirmed their potential usage over their entire intrinsic glass transmission (see figures 15(a) and (b)), as with silica glass for the near-IR region [216–218].

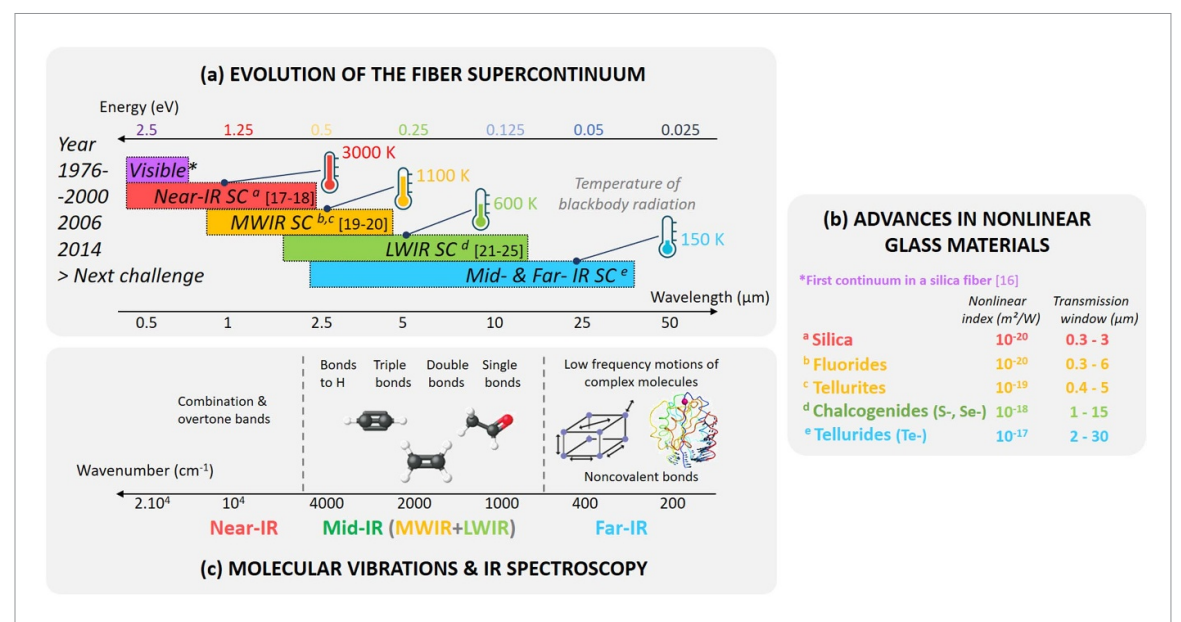


Figure 15. Supercontinuum generation and addressed absorption spectroscopy with specialty optical fibers and glasses. (a) Brief history of the evolution of fiber SC bandwidth towards the mid-IR. More references for the different spectral regions can be found in [205–208]. Corresponding temperature of blackbody radiation peak at some specific wavelengths is also indicated. (b) Main features of corresponding glass families used for fibers dedicated to SC generation. (c) Molecular vibrations and IR spectroscopy addressed by corresponding SC spectra shown in (a). In all subplots, note that key figures were chosen to provide a simple overview of the research topic and the vast literature.

Typically, fluoride- and tellurite-based fibers can be used for SCG up to about 4–5 μ m [219, 220], whereas selenide (Se-based) fibers can reach longer wavelengths, routinely 10–13 μ m [221, 222] and sometimes until 15–18 μ m [223–225]. To go further in the MIR and reach the far-IR, some pioneering works have already taken a new step forward in the development of tellurium-rich glass systems compatible with fiber processing [226–229]. In fact, the width of the transmission window is usually determined by the phonon energy spectrum of the glass used (i.e. controlled by the mass of the component elements). Among the numerous families of chalcogenide glasses, sulfur- and selenium-based chalcogenides have been predominantly studied, but the family based on tellurium (Te-rich glasses: tellurides) possesses the widest infrared window of all amorphous materials and the strongest nonlinearity [229, 230] (see figure 15(b)), and thus emerges as the unique potential solution for simultaneous MIR and far-IR SC applications.

Advances in science and technology to meet challenges

The potential of developing new telluride (Te-rich) glasses with higher nonlinearity and broader transmission window to generate efficient MIR SCG that could extend into the far-IR is very exciting, but a great care has to be paid on the selection of composition elements to form stable glasses without decreasing the IR transparency. Initial efforts to prepare such telluride glasses were already done to enable fiber drawing, but significant advances (novel compositions, purification techniques, fiber preform production) are still required to optimize them for nonlinear applications [228, 229]. The long-wavelength edge of SC sources also depends on the pumping configuration. Direct pumping around 5–8 μ m with high-power ultrashort pulses delivered by expensive laser chains based on optical parametric amplification and difference-frequency generation has shown to clearly favor the MIR extension until the intrinsic multi-phonon absorption edge of selenide glasses [223-225]. As a first step, one will need direct femtosecond pulse pumping in the MIR close to 10 μ m (near the zero-dispersion wavelength of telluride fibers [228]) to generate SC in very short fiber lengths (cm-long). In order to optimize SCG in optical fibers (bandwidth, power spectral density, coherence), this requires a detailed knowledge of the physics behind (dispersion vs nonlinearity, soliton dynamics, etc). We will not enter into these details (we refer the reader to review articles and books [205–208]), but simply, we remind that the closer the pump to the zero dispersion wavelength the better, and even the lower and flatter positive group-velocity dispersion the more suitable. As a function of available laser pump and soft-glass used for fiber drawing, one has then to design an optimized waveguide geometry (e.g. SI, double-clad, microstructured or tapered fibers) to enable an extreme confinement of the electromagnetic field and a high efficiency of wavelength conversion by means of nonlinear effects. Last but not least, an important task relies on the accurate characterization of SC light generated. Measurements of such mid- and far-IR spectra are far more difficult because of the weakness of available detectors, the thermal radiation background and strong environment absorptions.

Concluding remarks

In summary, we are reaching a turning point in the growing development of MIR fiber SC sources, can we overcome demanding limitations at the interface between materials chemistry and nonlinear optics to efficiently cover the 15– $20~\mu m$ waveband and go beyond? Being close to cover the full molecular fingerprint region by means of fiber technology, and to break the far-IR frontier, the last advances in fiber-based SC sources and the emerging telluride fibers offer a very promising and exciting route with successive key challenges. Filling current gaps in spectral coverage will facilitate the development of full IR optical technology (i.e., complete systems and diagnostics from the light source to the detector/sensor).

12. MIR fiber lasers

Xiushan Zhu

Wyant Colleges of Optical Sciences, University of Arizona, Tucson, AZ, United States of America

Status

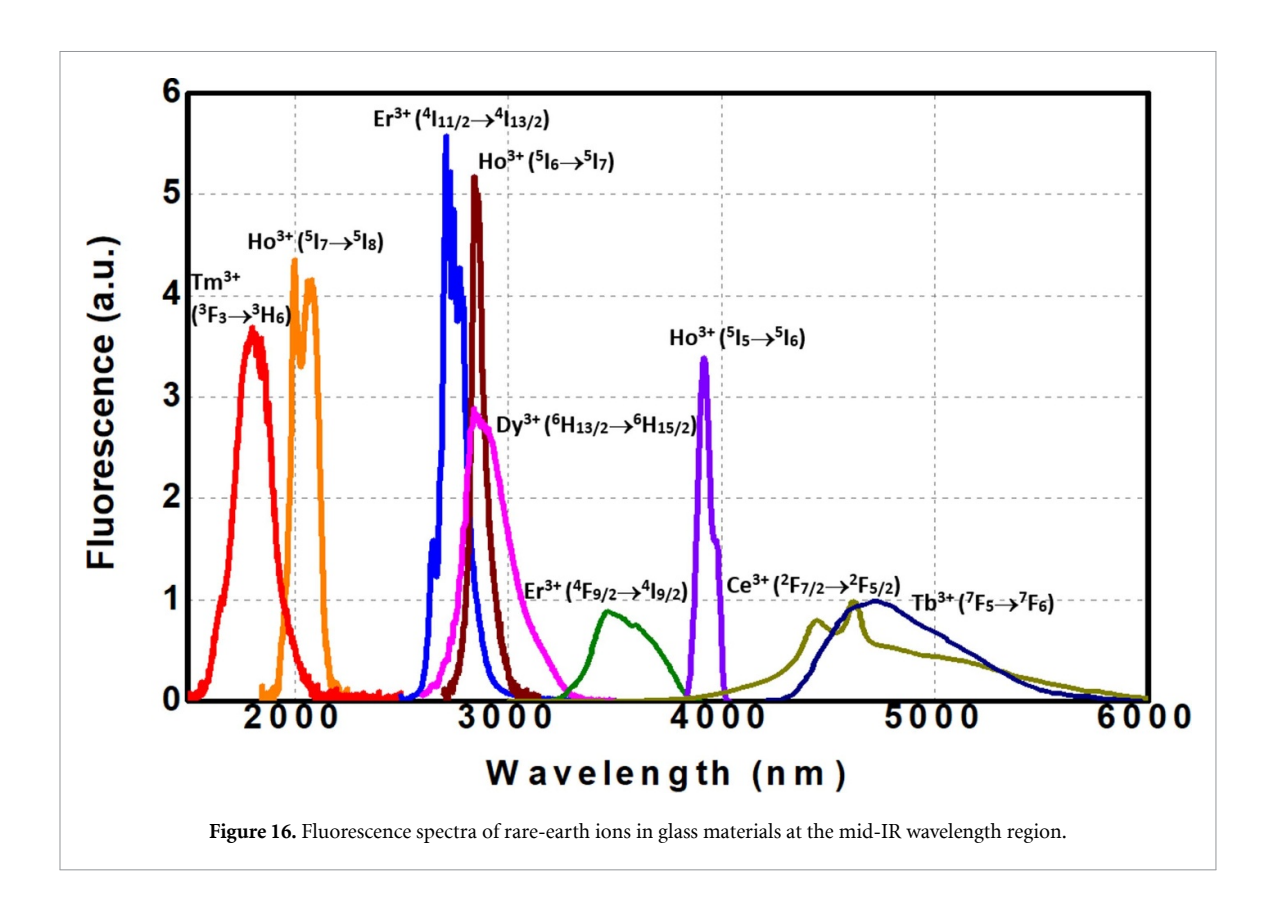
MIR lasers (generally in the 2–12 μ m wavelength region) have found a wide range of scientific and technological applications including spectroscopy, metrology, sensing, medicine, defense and security because the MIR spectrum convers several important atmospheric windows and the strong absorption fingerprints of many molecules. MIR lasers have been developed with most available laser technologies including fiber lasers, semiconductor lasers, solid-state lasers, and gas lasers. During the last two decades, semiconductors have experienced tremendous progress for MIR laser emission. Quantum cascade lasers (QCLs) and interband cascade lasers (ICLs) are now able to generate laser covering most MIR bands. However, they usually have poor beam quality and low power scalability. The solid-state lasers based on direct transitions of active ions or nonlinear wavelength conversions in low-phonon-energy glass and crystals, and the gas lasers have been extensively used for applications where high power or wavelength tunable MIR lasers are required. However, these lasers generally have a bulky and complex configuration requiring careful alignment and frequent maintenance. MIR fiber lasers have always attracted great interest because fiber lasers have shown great advantages for their compactness, inherent simplicity, outstanding heat-dissipating capability, excellent beam quality, high-power scalability, and very high single-pass gain.

As shown in figure 16, several RE ions including thulium (Tm³⁺), erbium (Er³⁺), holmium (Ho³⁺), dysprosium (Dy^{3+}) , cerium (Ce^{3+}) , and terbium (Tb^{3+}) have broad MIR emissions through direct transitions between their energy levels and these ions dope optical fibers have been successfully used to develop MIR lasers. The early research on MIR fiber laser was started with RE-doped fluoride fibers in late 1980s because fluoride glass has low phonon energy (<650 cm⁻¹) and extended multi-phonon IR absorption edge, which are two critical conditions for the MIR laser transitions of RE ions in optical fibers [231]. With advances in high-brightness pump sources, new pumping schemes, and novel fiber designs, RE-doped MIR fluoride fiber lasers have experienced rapid development during the last three decades [232-241]. Watt-level and 10 s-watt-level CW RE-doped fluoride fiber lasers have been demonstrated in the 3 μ m wavelength region. In current years, there has been increasing interest in extending the laser emission to longer wavelengths with RE-doped chalcogenide fibers because chalcogenide glass has much lower phonon energy and longer IR absorption edge [242, 243]. In addition to direct transitions of RE ions, nonlinear effects in passive MIR fibers, such as fluoride, tellurite, and chalcogenide fibers, have also been widely utilized to achieve MIR lasers that cannot be obtained with RE-doped fiber lasers [244, 245]. With the advances of novel HCFs that can guide both the near-IR pump light and MIR signal light in the hollow core, gas-filled HCF lasers based on the vibrational mode transitions or Raman scattering of several gases, such as C_2H_2 , HCN, CO, CO₂, N₂, and H₂, have emerged as a promising approach to powerful MIR lasers [246, 247]. In this section, we focus on the status of RE-doped MIR fiber lasers and their challenges.

Current and future challenges

Figure 17 presents the highest output power levels of RE-doped MIR fiber lasers that have been reported so far. Since silica fiber has much higher melting temperature and mechanical strength than fluoride fiber and is still transparent at 2 μ m, Tm³⁺- and Ho³⁺-doped silica fiber lasers have produced the highest output powers at this wavelength range [248, 249]. A 1 kW Tm³⁺-doped silica fiber laser was demonstrated with slope efficiency as high as 53.2%, which is higher than the Stokes efficiency due to the unique 1-to-2 conversion of the cross-relaxation process [248]. The efficiency of a Tm³⁺-doped silica fiber laser can be further improved by optimizing the Tm³⁺ concentration and fiber design to enhance the cross-relaxation process and sufficiently cooling the gain fiber to mitigate the thermal effect on the population distribution. Compared to ${\rm Tm^{3+}}$, ${\rm Ho^{3+}}$ can have a longer emission wavelength. A 407 W ${\rm Ho^{3+}}$ -doped silica fiber laser at 2.12 $\mu{\rm m}$ was achieved by in-band pumping with six Tm^{3+} -doped fiber lasers at 1.95 μ m [249]. However, due to the increased multi-phonon non-radiative decay rate and intrinsic loss of Ho³⁺-doped silica fiber at this wavelength, the efficiency of this fiber laser is less than <40% even though the Stokes efficiency is nearly 92%. Compared to silica, germanate glass has lower phonon energy (<900 cm⁻¹) and longer IR absorption edge ($>3 \mu m$). Therefore, Ho³⁺-doped germanate fiber is a promising gain medium for high-efficient laser at 2.1 μ m. However, commercial germanate fibers with low loss that can be used to develop high-efficiency and high-power Ho³⁺ lasers at 2.1 μ m are not currently available.

Fiber lasers beyond 2.1 μ m have been mainly demonstrated with the RE-doped fluoride fibers because fluoride glass has high solubility, allowing high concentration doping of RE ions without concentration quenching, and low phonon energy, enabling efficient radiative transitions in these RE ions. Laser emissions



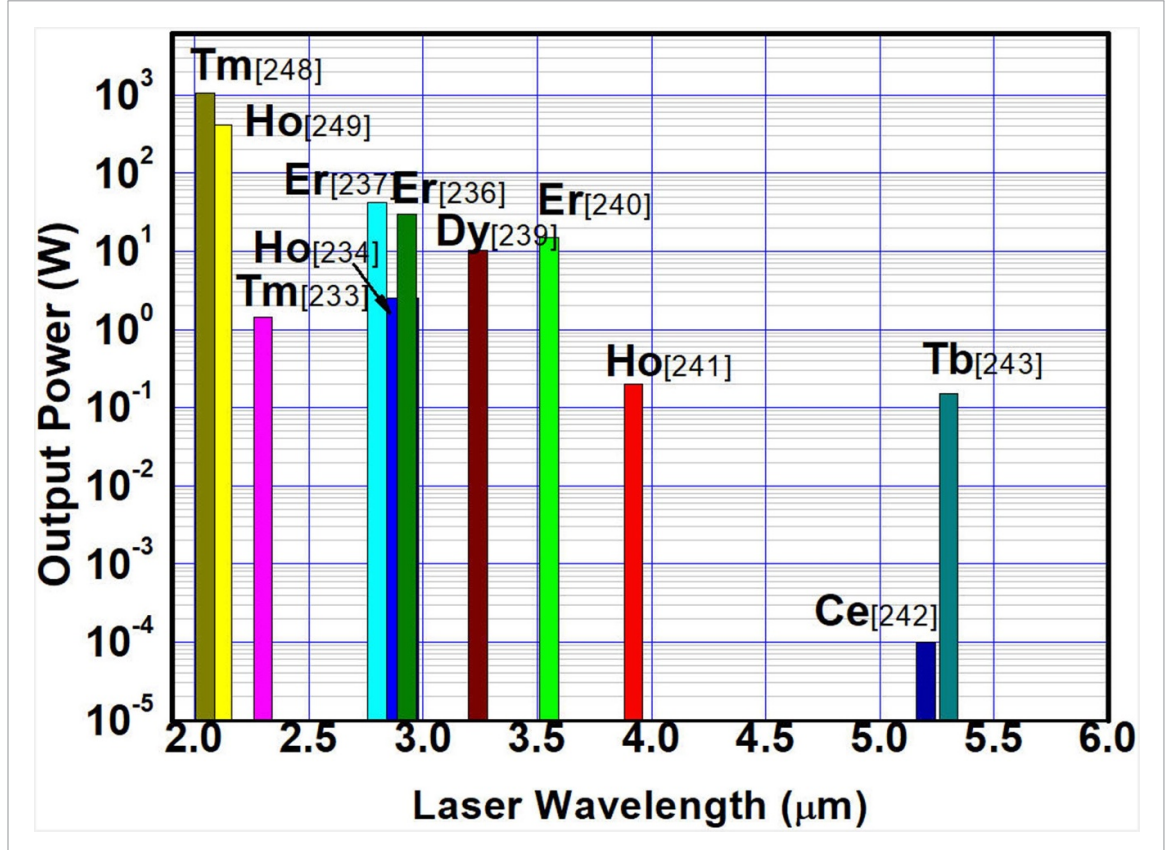


Figure 17. The highest continuous-wave output power levels at different mid-IR wavelengths obtained with the rare-earth-doped glass fiber lasers so far.

at 2.3 μ m have been obtained with Tm³+-doped fluoride fibers through the transition from energy level 3H_4 to 3H_5 [233]. However, the efficiency and power scalability of the 2.3 μ m fiber lasers are limited by the complicated energy level structure of Tm³+ and the competitive laser operation at 2 μ m. Since Er³+-doped

fluoride fiber laser can be pumped by readily available laser diodes at 980 nm and the laser efficiency can even be larger than the Stokes efficiency due to the 1-to-2 conversion of the upconversion energy transfer process, significant efforts have been conducted to improve the output power and other performance of this type of fiber laser [235–238]. An Er³⁺-doped fluoride fiber laser with CW output power as high as 41.6 W has been demonstrated with an all-fiber laser cavity by inscribing fiber Bragg gratings (FBGs) at both ends of the gain fiber [237, 250]. Because of the high hygroscopicity, low melting point, and low mechanical strength of fluoride fiber, the output power of this laser is limited by the catastrophic optical damage and the thermal issues of the gain fiber. By purging nitrogen to mitigate catastrophic damage and optimizing the pump wavelength to improve the laser efficiency and mitigate the heat load, a quasi-CW output of 70 W at 2.8 μ m was recently obtained, indicating that 100 W-level Er³⁺-doped fiber laser can be achieved as the optical damage and thermal issues are further mitigated [238]. Ho³⁺- and Dy³⁺-doped fluoride fiber lasers in the $3 \mu m$ wavelength region can emit longer wavelengths than Er^{3+} -doped fiber lasers. However, their output power levels have always been limited by the unavailability of high-power low-cost diode pumps at their absorption bands. In-band pumping with Er^{3+} -doped fluoride fiber lasers at 2.8 μ m is an effective approach for their power scaling. A 10.1 W Dy³⁺-doped fiber laser at 3.24 μ m has been demonstrated with in-band pumping [239]. The 100 W-level Ho³⁺- and Dy³⁺-doped fiber lasers can be obtained as they can be cladding pumped through MIR fiber combiners by many 2.8 μ m Er³⁺-doped fiber lasers.

To extend the operating wavelength of RE-doped fiber laser, one approach is to utilize the transitions between two intermediate states of a RE ion with small gap. Lasers at 3.5 μ m and 3.9 μ m have been obtained with Er³+- and Ho³+-doped fluoride fibers, respectively [240, 241]. A 15 W Er³+-doped fluoride fiber laser at 3.55 μ m was demonstrated with dual-wavelength pumping technique [240]. Using a Ho³+-doped indium fluoride fiber, a 200 mW 3.92 μ m laser was obtained at room temperature [241]. It becomes more challenging to obtain MIR laser beyond 4 μ m with RE-doped fluoride fibers because the non-radiative decay rate become dominant in a transition between two intermediate states. The other approach is to utilize the transitions between the first excited state and the ground state of RE ions in chalcogenide fibers, which have phonon energy of <300 cm⁻¹ and thus enables the laser operation beyond 5 μ m [242, 243]. Most recently, a Tb³+-doped chalcogenide fiber laser with 150 mW output at 5.1–5.4 μ m was demonstrated, showing the possibility of producing MIR lasers with RE-doped chalcogenide fibers [243]. However, due to the low solubility and low melting point of chalcogenide glass, it is still very challenging to make highly RE-doped chalcogenide fibers that can be used to develop high power laser beyond 5 μ m.

Pulsed lasers with high energy or high peak power in the MIR are in great demand for many applications [232]. A lot of pulsed RE-doped fluoride fiber lasers have been demonstrated with various Q-switching and mode-locking techniques that have been widely used for near-IR fiber lasers. However, due to the lack of MIR fiber devices such as coupler, wavelength division multiplexer (WDM), combiner, fiber-coupled isolator, etc, current pulsed fluoride fiber lasers were built with free-space optical components, which bring many negative impacts on the reliability, compactness and robustness of fiber lasers.

Advances in science and technology to meet challenges

With the advances of silica fiber laser technology, kW-class even 10 kW-class fiber lasers have already been developed and used in a wide range of applications. The techniques, experiences, and innovations of silica fiber lasers can be directly adopted for the development of MIR fiber lasers. Nevertheless, the first but not the last challenge for MIR RE-doped fiber lasers is to develop the laser in all-fiber configuration especially at the 3 μ m wavelength region and beyond. Thanks to the femtosecond laser FBG fabrication technique, gratings can be easily written in MIR fibers to form all-fiber laser cavity [250]. This is a major driving force for the development and commercialization of high power MIR RE-doped fiber lasers. However, the unavailability of other fiber devices still makes it very challenging to develop MIR fiber lasers in all-fiber configuration. Because of the fragility and easy crystallization of MIR fibers, it is still hard to fabricate MIR fiber devices using the fused tapered-fiber technique, which has been widely used for the fabrication of silica fiber devices. Even MIR fiber coupled devices based on miniature optics still lag behind the MIR fiber laser development. Significant efforts on the MIR fiber device fabrication and new fabrication tools are needed to remove the obstacles for the development of MIR all-fiber lasers and consequently improve the performance of current MIR fiber lasers.

One factor for the remarkable progress on 2.8 μ m Er³⁺-doped fluoride fiber lasers is the readily available pump diodes at 980 nm, which have experienced tremendous development during the past decades driven by the great demands for pumping EDFAs for optical communications, high-power ytterbium-doped lasers at 1 μ m, and Er³⁺-doped lasers at 1.55 μ m. Therefore, advances of laser diode technology, especially the QCL and ICL technology that can be used to directly excite RE ions, will trigger rapid development of MIR fiber lasers at other longer wavelengths.

Non-radiative decay is a major factor impairing the efficiencies of MIR RE-doped fiber lasers. The phonon energy of the glass material needs to be smaller as the laser wavelength is longer. Therefore, RE-doped chalcogenide fibers have been fabricated for MIR laser beyond 5 μ m. However, conventional chalcogenide glass has low solubility and the propagation loss of current chalcogenide fibers (>1 dB m⁻¹) is still much higher than that of fluoride fibers (<0.1 dB m⁻¹). New highly RE-doped chalcogenide fibers with low loss are essential for high power RE-doped fiber laser at longer MIR wavelengths.

Concluding remarks

MIR RE-doped fiber lasers have experienced tremendous progress on either CW or pulse operation performance during the last two decades. The power and energy of MIR RE-doped fiber lasers can be further increased by several folds by improving the thermal management to mitigate the fiber degradation and damage, optimizing the pump scheme and fiber design to increase the laser efficiency and heat dissipation capability, and building the laser in all-fiber format. New MIR optical fibers with lower phonon energy and higher solubility are needed to achieve high-efficiency fiber lasers at long MIR wavelengths. Alternatively, MIR fiber lasers operating at longer wavelengths can be achieved by employing the Raman scattering in MIR solid-core fibers. As substantial investment and effort are placed in the field of MIR fiber lasers, breakthroughs in laser output power, emission spectrum, reliability, and integration can be predicted in the next 1–2 decades.

13. MIR gas-filled HCF lasers

Andrey Pryamikov

Prokhorov General Physics Institute of the Russian Academy of Sciences, Moscow, Russia

Status

MIR gas-filled hollow core—core fiber lasers (GFHCFLs) have a rather long history. It is currently accepted that the term MIR generally covers the spectral region from 2.5 to 25 μ m. The first hollow-core waveguide gas laser was reported by Smith [251]. The laser operated with He–Ne mixtures at 0.633 μ m. The laser light propagated through the hollow-core dielectric tube with 430 μ m inner diameter and a length of 20 cm. The tube also served to confine the discharge. The first He–Ne laser operating at a wavelength of 3.39 μ m with 510 μ m inner diameter was demonstrated in [252]. It is also worth noting the creation of CO₂ waveguide gas laser which had a discharge tube 23.7 cm length and 3.3 mm diameter [253]. The obtained output power was 2.5 W. The waveguides was located between the mirrors that form the optical resonator. The main reasons that such waveguide gas lasers are not widely used are due to the impossibility of reducing the inner air core diameter without a significant increase in losses.

Despite such a long history of the development of GFHCFLs in the MIR range, strong interest in their development does not weaken. This is primarily due to the large number of their possible applications in such areas as laser absorption spectroscopy, high-quality cutting and ablation, efficient laser pump sources for longer-wavelength oscillators and many others. It is also worth noting such advantages of mid IR gas-filled hollow-core lasers as a beam quality and compact system configuration. In addition, it is necessary to take into account the fact that MIR GFHCFLs are devoid of such disadvantages as the relatively weak heat handling capacity of fluoride and chalcogenide glass fiber lasers. The creation of hollow-core PCFs (HCPCFs) [254, 255] allowed to avoid disadvantages of the first hollow-core laser designs. The lowest losses achieved in silica glass hollow-core photonic band gap fiber with an air-core diameter of 40 μ m were 2.6 dB m⁻¹ at a wavelength of 3.15 μ m [256]. Further efforts to penetrate into the mid IR spectral range with help of hollow-core silica glass photonic band gap fibers did not give a successful result due to strong power overlap of the air-core modes with silica cladding.

Current and future challenges

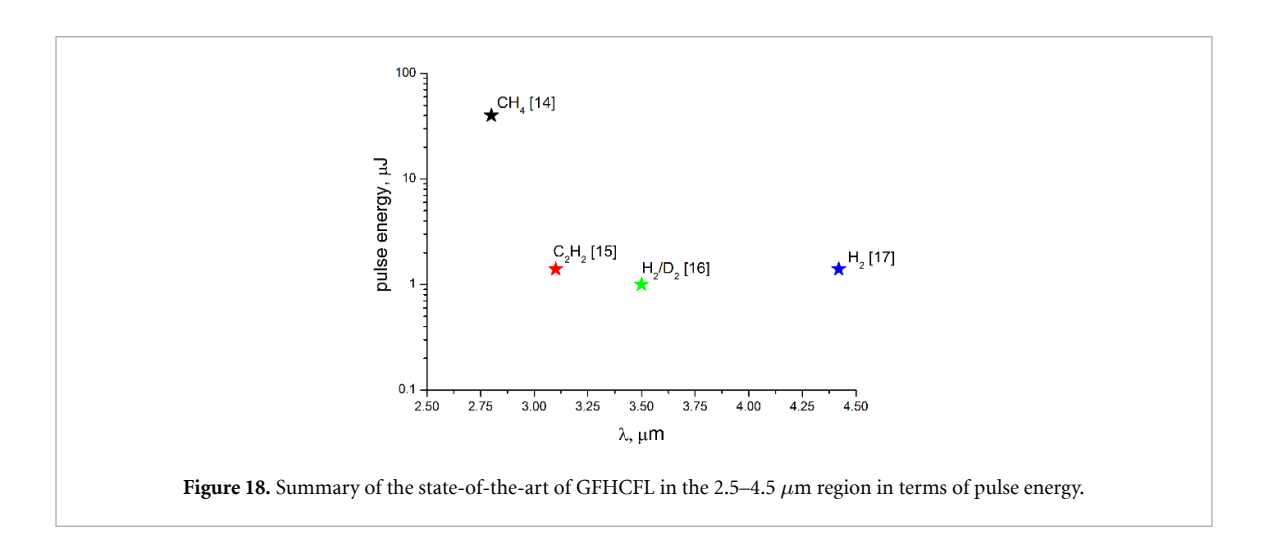
The first optically pumped GFHCFL based on HCPCFs operating in the MIR spectral range was demonstrated using Kagome lattice HCPCF [255]. This GFHCFL based on population inversion in $^{12}C_2H_2$ gas was pumped by 5 ns pulses at 1.52 μ m and lased at 3.12 μ m and 3.16 μ m. The diameter of the hollow-core was 45 μ m. The measured slope efficiencies of this gas fiber laser did not exceed a few percent due to high losses of the fiber at the laser wavelengths.

A breakthrough in the creation of new types of MIR GFHCFLs operating in both pulsed and CW mode was achieved thanks to the creation of new types of hollow-core micro-structured fibers [257–259]. This is also the main future challenge. A strong light localization in the negative curvature HCFs (NCHCFs) made it possible to avoid disadvantages of the first MIR GFHCFLs. This made it possible to expand the range of radiation transmission in the MIR spectral range in HCFs made of silica glass despite the high material losses [260].

MIR GFHCFLs can be divided into two types, namely, GFHCFLs based on population inversion and GFHCFLs based on Raman-active transitions. In the latter case, GFHCFLs implement SRS to transfer the pump power to longer wavelengths. Currently, the main active media used to fill the HCF of silica glass GFHCFLs based on population inversion are acetylene (C_2H_2), nitrous oxide (N_2O), carbon dioxide (CO_2) and HBr. Two last gases were used to create GFHCFLs operating in CW mode at wavelengths greater than 4 μ m. In the case of GFHCFL filled with CO_2 the authors obtained the output power of the laser up to 560 mW at 4.3 μ m and demonstrated a step-tunable laser behavior in the 4.27–4.43 μ m spectral range [261]. The output power of Hbr-based GFHCFL was scaled up to 3.1 W in CW mode at wavelength of 4.16 μ m [262]. Acetylene-filled lasers operate in both continuous and pulsed modes [263, 264]. Raman GFHCFLs filled with H_2 , D_2 or CH_4 (or their mixtures) work only in pulse mode due to high value pf threshold [264–267]. In order to demonstrate the capabilities of GFHCFLs for various gases in pulse mode, we have given data from recent studies in figure 18.

Advances in science and technology to meet challenges

Silica glass NCHCFs have a limit for transmitting radiation with losses that allow effective laser radiation in the mid IR spectral range. Usually these are wavelengths $>5 \mu m$. The solution to this problem can be carried out in two main ways, namely, either by creating hollow-core optical fibers from other glasses and materials with low material losses in the MIR spectral range, or by trying to propose new geometric structures of the



cross-section of the NCHCFs that allow for significantly greater localization of radiation even in silica glass HCFs. As for solving this problem in the first way, it can be solved by using tellurite [33] or chalcogenide glasses [268]. Progress especially noticeable in the development of HCFs made of chalcogenide glass [269]. In the case of the second way of solving the problem, it is necessary to achieve, as it seems to the author, a deeper and more accurate understanding of the mechanism of light localization in NCHCFs [270, 271], which will allow choosing the correct parameters of the fiber cladding (the shape of the core boundary, the number of the cladding elements, their thickness, etc) necessary to optimize its design and reduce losses. Perhaps in the future, optimization of the cladding design will become possible thanks to machine learning methods and the creation of complex cladding elements using 3D printing methods. And finally, in conclusion, it should be said that it may be possible to return to the idea of creating gas-discharge fiber lasers based on NCHCFs without using other fiber lasers based on solid-state optical fibers with their inherent limitations as pumping.

Concluding remarks

In conclusion, it must be said that the development of GFHCFLs is a dynamic and constantly changing process, depending on the success of research in fiber optics, laser physics and material science. There is no doubt that in the very near future there will be new GFHCFLs based on NCHCFs operating in the MIR spectral range.

14. Single-photon fiber sources

Stephan Reitzenstein Institute of Solid State Physics, Technische Universität Berlin, Berlin, Germany

Status

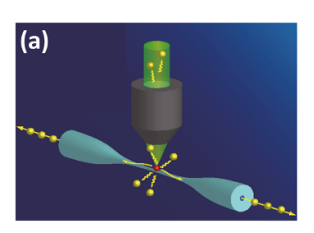
Fiber-coupled single-photon sources (SPSs) are important building blocks for many applications in photonic quantum technology [272]. On-demand SPSs can be realized by integrating quantum emitters such as single molecules, defect centers, and semiconductor QDs into photonic nanostructures with high photon extraction efficiency and near-ideal optical and quantum-optical properties [273]. Their emission wavelengths cover today the spectral range from UV to visible to near-infrared, including the O-band at 1.3 μ m and the C-band at 1.55 μ m [274]. Despite the tremendous advances in the development of the quantum emitters themselves, their direct fiber coupling is still in its infancy. The first concepts and numerical optimizations of practical fiber-coupled SPS date back to the early 2010s, when for example an optical-horn-based quantum emitter was coupled to a SM optical fiber [275]. Regarding experimental implementations of fiber-coupled SPSs one has to distinguish between approaches using micro- and nanofibers and ones using cleaved fibers. Here, micro- and nanofibers rely on evanescent field coupling to ensure an efficient transfer of photons from the emitter into the fiber-core (figure 19(a)). Cleaved-fiber based approaches use either near-field coupling or far-field coupling between the quantum emitter and the fiber core. Recently, deterministic emitter-fiber alignment technologies (figure 19(b)) have led to first stand-alone SPSs (figure 19(c) which deliver single photons directly into the core of multi- [276] and SM fibers [277]. We refer to Bremer et al [278] for a comprehensive overview of the underlying concepts.

Current and future challenges

In general, it is technically very challenging to couple single-photon emitters to optical fibers with high efficiency and in a robust manner. Firstly, high coupling efficiency requires high-NA optical fibers and good mode matching between the SPS and the fiber core, which is best optimized by numerical modeling of the entire system consisting of the single photon emitter, photonic nanostructure, mode-matching micro-optic, and optical fiber. For this, very efficient algorithms, such as Bayesian optimizers, are required to be able to handle the complex numerical problem consisting of subsystems with significantly different length scales from nanometers to millimeters. Moreover, fabrication and doping of optical fibers must be optimized to realize ultra-high-NA optical fibers with low optical losses. Secondly, the robust and sub- μ m exact alignment between the SPS and the optical fiber is challenging. In fact, many quantum emitters such as QDs are operated preferably at cryogenic temperatures, which makes active fiber alignment very difficult or, as a rule, impossible. Technical solutions must therefore be developed that allow optimal alignment and fixation of all components at room temperature and at the same time prevent maladjustment during repeated cooling to cryogenic temperatures. Ideally, appropriate concepts will allow fine adjustment of the emitter-fiber system during low-temperature operation. Thirdly, advanced applications in photonic quantum technologies require solutions that go beyond single-core systems. E.g. long-range quantum communication is based on entanglement, for which photon pair sources must emit entangled photons into branching fibers to send the two photons of a QD to different nodes of the network while maintaining the entanglement. Furthermore, multi-emitter-multi-core fiber systems can be very interesting to maximize the transmission bandwidth of QKD systems by spatial multiplexing, or to simultaneously transmit signals in quantum channels and classic ones via different cores of one and the same multi-core fiber.

Advances in science and technology to meet challenges

While current results already demonstrate the great potential of fiber-coupled SPSs (see [281], table 2 for an overview), there is an enormous need for technological optimization to open up real fields of application. For example, designs and technical solutions must be developed that increase the overall efficiency of robust and durable fiber-coupled SPSs from currently a few percent to values in excess of 90%. For example, 3D printed fiber holders and micro-optics in connection with quantum emitters in CBG cavities could be very suitable. Furthermore, excellent quantum properties in terms of single-photon purity, indistinguishability and entanglement fidelity must be guaranteed, and practical aspects such as electrical control and spectral fine-tuning, for example via piezo-induced strain-tuning, must be implemented. All of this places the highest demands on the production of the fiber-coupled SPS, which can possibly be met by using e.g. deterministic lithographic processes in combination with efficient fiber coupling technologies based on 3D microprinting an high-NA specialty fibers.





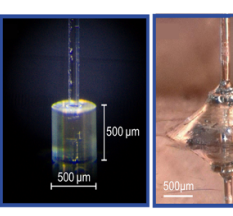




Figure 19. (a) Schematic view of a micro-fiber SPS. (b) Deterministic fiber-coupling of a QD-SPS using 3D microprinting of a lensed fiber (left) and a fiber-holder (center) aligned with sub- μ m accuracy to QD-micromesa. Finished device with glued fiber holder (right) (c) first stand-alone fiber-coupled QD-SPS with integrated Stirling cryo-cooler with a base temperature of 40 K. Reprinted with permission from [279]. Copyright (2011) American Chemical Society. Reproduced from [280]. CC BY 4.0. Reproduced from [276]. CC BY 4.0.

Concluding remarks

Single-photon fiber sources have high application potential in many fields of photonic quantum technologies. Their development and optimization require interdisciplinary collaboration between scientists in the areas of numerical optimization of nanophotonic structures, the manufacture of specialty optical fibers, the development of quantum light sources and experts in quantum engineering of advanced optoelectronic devices. In the future, these quantum devices can make an important contribution to the implementation of quantum networks.

Data availability statement

No new data were created or analyzed in this study.

Acknowledgments

This work was financial support by the Federal Ministry of Education and Research (BMBF) via Project QR.X, by the German Research Foundation (DFG) via Project Re2974-25/1.

ORCID iDs

Mário F S Ferreira https://orcid.org/0000-0001-8316-7022

Mohd Rehan https://orcid.org/0000-0002-7945-8254

Nguyen Phuoc Trung Hoa https://orcid.org/0000-0001-6908-807X

Anjali https://orcid.org/0000-0001-7864-8817

Mukul Chandra Paul https://orcid.org/0000-0001-8805-6129

Bertrand Kibler https://orcid.org/0000-0001-8838-0738

Frédéric Smektala https://orcid.org/0000-0002-6787-9289

Xiushan Zhu https://orcid.org/0000-0002-1265-8008

Stephan Reitzenstein https://orcid.org/0000-0002-1381-9838

References

- [1] Agrawal G P 2019 Nonlinear Fiber Optics 6th edn (Academic)
- [2] Pourbeyram H, Sidorenko P, Wu F O, Bender N, Wright L, Christodoulides D N and Wise F 2022 Direct observations of thermalization to a Rayleigh–Jeans distribution in multimode optical fibres *Nat. Phys.* 18 685–90
- [3] Eftekhar M A, Lopez-Aviles H, Wise F W, Amezcua-Correa R and Christodoulides D N 2021 General theory and observation of Cherenkov radiation induced by multimode solitons Commun. Phys. 4 137
- [4] Wright L G, Sidorenko P, Pourbeyram H, Ziegler Z M, Isichenko A, Malomed B A, Menyuk C R, Christodoulides N D and Wise F W 2020 Mechanisms of spatiotemporal mode-locking Nat. Phys. 16 565–70
- [5] Kibler B and Béjot P 2021 Discretized conical waves in multimode optical fibers Phys. Rev. Lett. 126 023902
- [6] Teğin U and Ortaç B 2018 Cascaded Raman scattering based high power octave-spanning supercontinuum generation in graded-index multimode fibers Sci. Rep. 8 1–7
- [7] Wright L G, Christodoulides D N and Wise F W 2022 Roadmap on spatiotemporal fields: spatiotemporal mode-locking J. Opt. 25 093001
- [8] Wright L G, Christodoulides D N and Wise F W 2015 Controllable spatiotemporal nonlinear effects in multimode fibres Nat. Photon. 9 306–10
- [9] Crosignani B, Cutolo A and Porto P D 1982 Coupled-mode theory of nonlinear propagation in multimode and single-mode fibers: envelope solitons and self-confinement *J. Opt. Soc. Am.* 72 1136–41
- [10] Poletti F and Horak P 2008 Description of ultrashort pulse propagation in multimode optical fibers J. Opt. Soc. Am. B 25 1645-54
- [11] Mafi A 2012 Pulse propagation in a short nonlinear graded-index multimode optical fiber J. Lightwave Technol. 30 2803–11

- [12] Pedersen M E V, Cheng J, Xu C and Rottwitt K 2013 Transverse field dispersion in the generalized nonlinear Schrödinger equation: four wave mixing in a higher-order mode fiber J. Lightwave Technol. 31 3425–31
- [13] Khakimov R, Shavrin I, Novotny S, Kaivola M and Ludvigsen H 2013 Numerical solver for supercontinuum generation in multimode optical fibers Opt. Exp. 21 14388–98
- [14] Wright L G, Ziegler Z M, Lushnikov P M, Zhu Z, Eftekhar M A, Christodoulides D N and Wise F W 2018 Multimode nonlinear fiber optics: massively parallel numerical solver, tutorial, and outlook *IEEE J. Sel. Top. Quantum Electron.* 24 1–16
- [15] Wright L G, Wu F O, Christodoulides D N and Wise F W 2022 Physics of highly multimode nonlinear optical systems Nat. Phys. 18 018–1030
- [16] Carles R and Sparber C 2021 Orbital stability vs. scattering in the cubic-quintic Schrödinger equation Rev. Math. Phys. 33 2150004
- [17] Gervaziev M D, Zhdanov I, Kharenko D S, Gonta V A, Volosi V M, Podivilov E V, Babin S A and Wabnitz S 2021 Mode decomposition of multimode optical fiber beams by phase-only spatial light modulator *Laser Phys. Lett.* 18 015101
- [18] Krutova E, Eslami Z, Karpate T, Klimczak M, Buczynski R and Genty G 2021 Octave-spanning infrared supercontinuum generation in a graded-index multimode tellurite fiber 2021 Conference on Lasers and Electro-Optics Europe & European Quantum Electronics Conference (CLEO/Europe-EQEC) (Munich, Germany) p 1
- [19] Tzang O, Caravaca-Aguirre A M, Wagner K and Piestun R 2018 Adaptive wavefront shaping for controlling nonlinear multimode interactions in optical fibres Nat. Photon. 12 368–74
- [20] Cregan R F, Mangan B J, Knight J C, Birks T A, Russell P S J, Roberts P J and Allan D C 1999 Single-mode photonic band gap guidance of light in air Science 285 1537–9
- [21] Jasion G T et al 0.174 dB/km hollow core double nested antiresonant nodeless fiber (DNANF) Optical Fiber Communication Conference (OFC) 2022 paper Th4C.7 (https://doi.org/10.1364/OFC.2022.TH4C.7)
- [22] Sakr H et al Hollow core NANFs with five nested tubes and record low loss at 850, 1060, 1300 and 1625nm Optical Fiber Communication Conference (OFC) 2021 paper F3A.4 (https://doi.org/10.1364/OFC.2021.F3A.4)
- [23] Yu F, Cann M, Brunton A, Wadsworth W and Knight J 2018 Single-mode solarization-free hollow-core fiber for ultraviolet pulse delivery Opt. Express 26 10879–87
- [24] Yu F, Song P, Wu D, Birks T, Bird D and Knight J 2019 Attenuation limit of silica-based hollow-core fiber at mid-IR wavelengths APL Photonics 4 080803
- [25] Taranta A, Numkam Fokoua E, Abokhamis Mousavi S, Hayes J R, Bradley T D, Jasion G T and Poletti F 2020 Exceptional polarization purity in antiresonant hollow-core optical fibres Nat. Photon. 14 504–10
- [26] Michaud-Belleau V, Numkam Fokoua E, Bradley T D, Hayes J R, Chen Y, Poletti F, Richardson D J, Genest J and Slavík R 2021 Backscattering in antiresonant hollow-core fibers: over 40 dB lower than in standard optical fibers *Optica* 8 216
- [27] St Russell P J, Hölzer P, Chang W, Abdolvand A and Travers J C 2014 Hollow-core photonic crystal fibres for gas-based nonlinear optics Nat. Photon. 8 278–86
- [28] Debord B, Alharbi M, Vincetti L, Husakou A, Fourcade-Dutin C, Hoenninger C, Mottay E, Gérôme F and Benabid F 2014 Multi-meter fiber-delivery and pulse self-compression of milli-Joule femtosecond laser and fiber-aided laser-micromachining Opt. Express 22 10735–46
- [29] Mulvad H C H et al 2022 Kilowatt-average-power single-mode laser light transmission over kilometre-scale hollow-core fibre Nat. Photon. 16 448–53
- [30] Romodina M N, Xie S, Tani F and Russell P S J 2022 Backward jet propulsion of particles by femtosecond pulses in hollow-core photonic crystal fiber Optica 9 268–72
- [31] Slavík R, Marra G, Fokoua E N, Baddela N, Wheeler N V, Petrovich M, Poletti F and Richardson D J 2015 Ultralow thermal sensitivity of phase and propagation delay in hollow core optical fibres Sci. Rep. 5 15447
- [32] Poletti F 2014 Nested antiresonant nodeless hollow core fiber Opt. Express 22 23807
- [33] Ventura A et al 2020 Extruded tellurite antiresonant hollow core fiber for mid-IR operation Opt. Express 28 16542
- [34] Hong Y, Jia A, Gao S, Sheng Y, Lu X, Liang Z, Zhang Z, Ding W and Wang Y 2023 Birefringent, low loss, and broadband semi-tube anti-resonant hollow-core fiber *Opt. Lett.* **48** 163–6
- [35] Shere W, Fokoua E N, Jasion G T and Poletti F 2022 Designing multi-mode anti-resonant hollow-core fibers for industrial laser power delivery Opt. Express 30 40425–40
- [36] Kelly T W, Horak P, Davidson I A, Partridge M, Jasion G T, Rikimi S, Taranta A, Richardson D J, Poletti F and Wheeler N V 2021 Gas-induced differential refractive index enhanced guidance in hollow-core optical fibers Optica 8 916–20
- [37] Edavalath N N, Günendi M C, Beravat R, Wong G K L, Frosz M H, Ménard J-M and Russell J P S 2017 Higher-order mode suppression in twisted single-ring hollow-core photonic crystal fibers Opt. Lett. 42 2074–7
- [38] Numkam Fokoua E, Seyed Abokhamis Mousavi M, Jasion G, Richardson D and Poletti F 2023 Loss in hollow core optical fibers: mechanisms, scaling rules and limits Adv. Opt. Photon. 15 1–85
- [39] Li J, Zhao F and Hui Z 2019 Mid-infrared supercontinuum generation in dispersion-engineered highly nonlinear chalcogenide photonic crystal fiber Mod. Phys. Lett. B 33 1950211
- [40] Petersen C R, Engelsholm R D, Markos C, Brilland L, Caillaud C, Trolès J and Bang O 2017 Increased mid-infrared supercontinuum bandwidth and average power by tapering large-mode-area chalcogenide photonic crystal fibers Opt. Express 25 15336
- [41] Chu Van L, Nguyen Thi T, Le Tran B T, Trong D H, Thi Minh N V, Van Le H and Hoang V T 2022 Multi-octave supercontinuum generation in As₂Se₃ chalcogenide photonic crystal fiber *Photon. Nanostruct.* 48 100986
- [42] Ghosh A N et al 2019 Chalcogenide-glass polarization-maintaining photonic crystal fiber for mid-infrared supercontinuum generation J. Phys. 1 044003
- [43] Hossain S, Shah S and Faisal M 2021 Ultra-high birefringent, highly nonlinear Ge₂₀Sb₁₅Se₆₅ chalcogenide glass photonic crystal fiber with zero dispersion wavelength for mid-infrared applications *Optik* 225 165753
- [44] Brilland L, Troles J, Houizot P, Désévédavy F, Coulombier Q, Renversez G, Chartier T, Nguyen T N, Adam J-L and Traynor N 2008 Interfaces impact on the transmission of chalcogenides photonic crystal fibres J. Ceram. Soc. Japan 116 1024–7
- [45] Désévédavy F, Renversez G, Troles J, Houizot P, Brilland L, Vasilief I, Coulombier Q, Traynor N, Smektala F and Adam J-L 2010 Chalcogenide glass hollow core photonic crystal fibers Opt. Mater. 32 1532–9
- [46] Feng X, Ren H, Xu F, Shi J, Qi S, Hu Y, Tang J, Han F, Shen D and Yang Z 2020 Few-moded ultralarge mode area chalcogenide photonic crystal fiber for mid-infrared high power applications Opt. Express 28 16658
- [47] Yang L, Wang Y, Jiao K, Dai S, Zhao R, Nie Q, wang X, Jia Z and Qin G 2022 High-coupling efficiency and robust fusion splicing between fluorotellurite and chalcogenide fibers *Infrared Phys. Technol.* 122 104075

- [48] Thapa R, Gattass R R, Nguyen V, Chin G, Gibson D, Kim W, Shaw L B and Sanghera J S 2015 Low-loss, robust fusion splicing of silica to chalcogenide fiber for integrated mid-infrared laser technology development *Opt. Lett.* 40 5074
- [49] Yang A, Sun M, Ren H, Lin H, Feng X and Yang Z 2021 Dy³⁺-doped Ga₂S₃-Sb₂S₃-La₂S₃ chalcogenide glass for mid-infrared fiber laser medium *J. Lumin.* 237 118169
- [50] Churbanov M F, Denker B I, Galagan B I, Koltashev V V, Plotnichenko V G, Snopatin G E, Sukhanov M V, Sverchkov S E and Velmuzhov A P 2021 Laser potential of Pr³⁺ doped chalcogenide glass in 5–6 μm spectral range *J. Non-Cryst. Solids* 559 120592
- [51] Nguyen H P T, Tuan T H, Xing L, Matsumoto M, Sakai G, Suzuki T and Ohishi Y 2020 Supercontinuum generation in a chalcogenide all-solid hybrid microstructured optical fiber *Opt. Express* 28 17539
- [52] Tong H T, Koumura A, Nakatani A, Nguyen H P T, Matsumoto M, Sakai G, Suzuki T and Ohishi Y 2022 Chalcogenide all-solid hybrid microstructured optical fiber with polarization maintaining properties and its mid-infrared supercontinuum generation Opt. Express 30 25433
- [53] Markos C, Kubat I and Bang O 2014 Hybrid polymer photonic crystal fiber with integrated chalcogenide glass nanofilms Sci. Rep. 4 6057
- [54] Petersen C R, Lotz M B, Woyessa G, Ghosh A N, Sylvestre T, Brilland L, Troles J, Jakobsen M H, Taboryski R and Bang O 2019 Nanoimprinting and tapering of chalcogenide photonic crystal fibers for cascaded supercontinuum generation Opt. Lett. 44 5505
- [55] Gehring H, Blaicher M, Hartmann W, Varytis P, Busch K, Wegener M and Pernice W H P 2019 Low-loss fiber-to-chip couplers with ultrawide optical bandwidth *APL Photonics* 4 010801
- [56] Liao M S, Yan X, Duan Z C, Suzuki T and Ohishi Y 2011 Tellurite photonic nanostructured fiber J. Lightwave Technol. 29 1018-25
- [57] Lee B, Roh S and Park J 2009 Current status of micro-and nano-structured optical fiber sensors Opt. Fiber Technol. 15 209-21
- [58] Canning J 2015 Optical fiber: structured Encyclopedia of Optical and Photonic Engineering (Taylor & Francis)
- [59] Wang W C, Zhou B, Xu S H, Yang Z M and Zhang Q Y 2019 Recent advances in soft optical glass fiber and fiber lasers *Prog. Mater.* Sci. 101 90–171
- [60] Bock M, Skibina J, Fischer D, Bretschneider M, Wedell R, Grunwald R, Burger S, Beloglazov V and Steinmeyer G 2013 Nanostructured fibers for sub-10 fs optical pulse delivery Laser Photon. Rev. 7 566–70
- [61] Shelby J E 2020 Introduction to Glass Science and Technology (Royal Society of Chemistry)
- [62] Wang W C, Yuan J, Liu X Y, Chen D D, Zhang Q Y and Jiang Z H 2014 An efficient 1.8 μm emission in Tm³⁺ and Yb³⁺/Tm³⁺ doped fluoride modified germanate glasses for a diode-pump mid-infrared laser J. Non-Cryst. Solids 404 19–25
- [63] Wang W C, Zhang W J, Li L X, Liu Y, Chen D D, Qian Q and Zhang Q Y 2016 Spectroscopic and structural characterization of barium tellurite glass fibers for mid-infrared ultra-broad tunable fiber lasers *Opt. Mater. Express* 6 2095–107
- [64] Wang W C, Mao L Y, Liu J L and Xu S H 2020 Glass-forming regions and enhanced 2.7 μ m emission by Er³⁺ heavily doping in TeO₂-Ga₂O₃-R₂O (or MO) glasses *J. Am. Ceram. Soc.* **103** 4999–5012
- [65] Kang S L, Dong G P, Qiu J R and Yang Z M 2020 Hybrid glass optical fibers-novel fiber materials for optoelectronic application Opt. Mater. X 6 100051
- [66] Cheng C, Hu N and Cheng X 2017 Experimental realization of a PbSe quantum dot doped fiber amplifier with ultra-bandwidth characteristic Opt. Commun. 382 470–6
- [67] Ballato J, Ebendorff-Heidepriem H, Zhao J B, Petit L and Troles J 2017 Glass and process development for the next generation of optical fibers: a review Fibers 5 11
- [68] Wang W C, Yang X, Wieduwilt T, Schmidt M A, Zhang Q Y and Wondraczek L 2019 Fluoride-sulfophosphate/silica hybrid fiber as a platform for optically active materials Front. Mater. 6 148
- [69] Tao G M, Ebendorff-Heidepriem H, Stolyarov A M, Danto S, Badding J V, Fink Y, Ballato J and Abouraddy A F 2015 Infrared fibers Adv. Opt. Photon. 7 379–458
- [70] Yan W, Page A, Nguyen-Dang T, Qu Y P, Sordo F, Wei L and Sorin F 2019 Advanced multimaterial electronic and optoelectronic fibers and textiles Adv. Mater. 31 1802348
- [71] Zhang Q Y and Jiang Z H 2015 The formation of glass: a quantitative perspective Sci. China Mater. 58 378–425
- [72] Pan Q W, Yang D D, Dong G P, Qiu J R and Yang Z M 2022 Nanocrystal-in-glass composite (NGC): a powerful pathway from nanocrystals to advanced optical materials *Prog. Mater. Sci.* 130 100998
- [73] Chen D Y et al 2022 Broadband optical amplification of PbS quantum-dot-doped glass fibers Adv. Photon. Res. 3 2200097
- [74] Knight J C 2003 Photonic crystal fibres Nature 424 847-51
- [75] Stefaniuk T, Pniewski J, Klimczak M, Pysz D, Stępień R and Buczyński R 2017 Nanostructured optical components: new opportunities and limitations 19th Int. Conf. on Transparent Optical Networks (ICTON) pp 1–5
- [76] Song S, Lønsethagen K, Laurell F, Hawkins T W, Ballato J, Fokine M and Gibson U J 2019 Laser restructuring and photoluminescence of glass-clad GaSb/Si-core optical fibres Nat. Commun. 10 1–7
- [77] Huang X J, Guo Q Y, Yang D D, Xiao X D, Liu X F, Xia Z G, Fan F J, Qiu J R and Dong G P 2020 Reversible 3D laser printing of perovskite quantum dots inside a transparent medium *Nat. Photon.* 14 82–88
- [78] Saini T S and Sinha R K 2021 Mid-infrared supercontinuum generation in soft-glass specialty optical fibers: a review Prog. Quantum Electron. 78 100342
- [79] Ermatov T, Skibina J S, Tuchin V V and Gorin D A 2020 Functionalized microstructured optical fibers: materials, methods, applications Materials 13 921
- [80] Csaki A et al 2010 Nanoparticle layer deposition for plasmonic tuning of microstructured optical fibers Small 6 2584–9
- [81] Hornak L A 1992 Polymers for Lightwave and Integrated Optics: Technology and Applications (Marcel Dekker Inc) ch 1
- [82] Bikandi I, Illarramendi M A, Durana G, Aldabaldetreku G and Zubia J 2014 Spectral dependence of scattered light in step-index polymer optical fibers by side-illumination technique *J. Lightwave Technol.* 32 3937–41
- [83] Kiesewetter D, Levin V and Baskakov G 2015 The application of side-illumination method for measurement of attenuation in fluorescent optical waveguides Conference on Advances in Wireless and Optical Communications (RTUWO) (Riga, LATVIA, 5–6 November 2015) (IEEE) pp 172–5
- [84] Pun C F J, Liu Z Y, Tse M L V, Cheng X, Tao M and Tam H Y 2012 Side-illumination fluorescence dye-doped-clad PMMA-core polymer optical fiber: potential intrinsic light source for biosensing *IEEE Photonics Technol. Lett.* 24 960–2
- [85] Argyros A 2009 Microstructured polymer optical fibers J. Lightwave Technol. 27 1571-9
- [86] Min R, Ortega B and Marques C 2019 Latest achievements in polymer optical fiber gratings: fabrication and applications Photonics 6 36
- [87] Beckers M, Schluter T, Vad T, Gries T and Bunge C A 2015 An overview on fabrication methods for polymer optical fibers Polym. Int. 64 25–36

- [88] Tam H Y, Pun C F J, Zhou G Y, Cheng X and Tse M L V 2010 Special structured polymer fibers for sensing applications *Opt. Fiber Technol.* 16 357–66
- [89] Mizuno Y, Theodosiou A, Kalli K, Liehr S, Lee H and Nakamura K 2021 Distributed polymer optical fiber sensors: a review and outlook Photon. Res. 9 1719–33
- [90] He R J, Teng C X, Kumar S, Marques C and Min R 2022 Polymer optical fiber liquid level sensor: a review IEEE Sens. J. 22 1081-91
- [91] Kim E S, Kinoshita T, Yu Y S and Jeong M Y 2007 Fabrication of nonlinear plastic optical fiber (POF) and application *Proc. SPIE* 6528 65280I
- [92] Gomes A S L, Moura A L, de Araujo C B and Raposo E P 2021 Recent advances and applications of random lasers and random fiber lasers Prog. Quantum Electron. 78 100343
- [93] Lu H B, Xing J, Wei C, Xia J, Sha J, Ding Y, Zhang G, Xie K, Qiu L and Hu Z 2018 Band-gap-tailored random laser *Photon. Res.* 6 390–5
- [94] Hu Z J, Liang Y Y, Qian X D, Gao P F, Xie K and Jiang H M 2016 Polarized random laser emission from an oriented disorder polymer optical fiber Opt. Lett. 41 2584–7
- [95] Hu Z J et al 2012 Coherent random fiber laser based on nanoparticles scattering in the extremely weakly scattering regime Phys. Rev. Lett. 109 253901
- [96] Hu Z J, Xia J, Liang Y, Wen J, Miao E, Chen J, Wu S, Qian X, Jiang H and Xie K 2017 Tunable random polymer fiber laser *Opt. Express* 25 18421–30
- [97] Hu Z J, Gao P F, Xie K, Liang Y Y and Jiang H M 2014 Wavelength control of random polymer fiber laser based on adaptive disorder Opt. Lett. 39 6911–4
- [98] Du W Y et al 2022 Thermal treatment effect on the random lasing polarization of polymer optical fiber Opt. Laser Technol. 149 107855
- [99] Lin H et al 2019 10.6 kW high-brightness cascade-end-pumped monolithic fiber lasers directly pumped by laser diodes in step-index large mode area double cladding fiber Results Phys. 14 102479
- [100] Smith A V and Do B T 2008 Bulk and surface laser damage of silica by picosecond and nanosecond pulses at 1064 nm Appl. Opt. 47 4812–32
- [101] Gaida C, Gebhardt M, Stutzki F, Jauregui C, Limpert J and Tünnermann A 2016 Thulium-doped fiber chirped-pulse amplification system with 2 GW of peak power Opt. Lett. 41 4130–3
- [102] Aydin Y O, Fortin V, Vallée R and Bernier M 2018 Towards power scaling of 2.8 µm fiber lasers Opt. Lett. 43 4542–5
- [103] Liu K, Liu J, Shi H, Tan F and Wang P 2014 High power mid-infrared supercontinuum generation in a single-mode ZBLAN fiber with up to 21.8 W average output power Opt. Express 22 24384–91
- [104] Hu T, Jackson S D and Hudson D D 2015 Ultrafast pulses from a mid-infrared fiber laser Opt. Lett. 40 4226-8
- [105] Jiao Y, Jia Z, Zhang C, Guo X, Meng F, Guo Q, Yu Y, Ohishi Y, Qin W and Qin G 2023 Over 50 W all-fiber mid-infrared supercontinuum laser *Opt. Express* 31 31082–91
- [106] Zhang M, Li T, Yang Y, Tao H, Zhang X, Yuan X and Yang Z 2019 Femtosecond laser induced damage on Ge-As-S chalcogenide glasses Opt. Mater. Express 9 555–61
- [107] Jauregui C, Stihler C and Limpert J 2020 Transverse mode instability Adv. Opt. Photon. 12 429-84
- [108] Russell P S J 2003 Photonic crystal fibers Science 299 358-62
- [109] Stutzki F, Jansen F, Liem A, Jauregui C, Limpert J and Tünnermann A 2012 26 mJ, 130 W Q-switched fiber-laser system with near-diffraction-limited beam quality Opt. Lett. 37 1073–5
- [110] Steinkopff A, Jauregui C, Stutzki F, Nold J, Hupel C, Haarlammert N, Bierlich J, Tünnermann A and Limpert J 2019 Transverse single-mode operation in a passive large pitch fiber with more than 200 μm mode-field diameter *Opt. Lett.* 44 650–3
- [111] Eidam T, Rothhardt J, Stutzki F, Jansen F, Hädrich S, Carstens H, Jauregui C, Limpert J and Tünnermann A 2011 Fiber chirped-pulse amplification system emitting 3.8 GW peak power *Opt. Express* 19 255–60
- [112] Dong L, Matniyaz T, Hawkins T W, Kalichevsky-Dong M T, Gafsi S and Li W 2020 All solid photonic bandgap fibers for high-power fiber lasers 2020 Opto-Electronics and Communications Conf. (OECC) (Taipei, Taiwan) pp 1–3
- [113] Jin W, Wang Z and Ju J 2005 Two-mode photonic crystal fibers Opt. Express 13 2082-8
- [114] Wong W S, Peng X, McLaughlin J M and Dong L 2005 Breaking the limit of maximum effective area for robust single-mode propagation in optical fibers Opt. Lett. 30 2855-7
- [115] TIE-26 homogeneity of optical glass (available at: www.schott.com/en-us/products/optical-glass-p1000267/downloads)
- [116] Data_and_Properties_Optics_fused_silica_EN (available at: www.heraeus.com)
- [117] Franczyk M, Pysz D, Pucko P, Michalik D, Biduś M, Dłubek M and Buczyński R 2019 Yb³⁺ doped silica nanostructured core fiber laser Opt. Express 27 35108–19
- [118] Siegel P H 2004 Terahertz technology in biology and medicine IEEE Trans. Microw. Theory Tech. 52 2438–47
- [119] Strachan C J, Taday P F, Newnham D A, Gordon K C, Zeitler J A, Pepper M and Rades T 2005 Using terahertz pulsed spectroscopy to quantify pharmaceutical polymorphism and crystallinity J. Pharm. Sci. 94 837–46
- [120] Balakrishnan J, Fischer B M and Abbott D 2009 Sensing the hygroscopicity of polymer and copolymer materials using terahertz time-domain spectroscopy *Appl. Opt.* 48 2262–6
- [121] Sharma P and Sharan P 2014 Design of photonic crystal-based biosensor for detection of glucose concentration in urine IEEE Sens. I. 15 1035–42
- [122] Rifat A A, Mahdiraji G A, Sua Y M, Shee Y G, Ahmed R, Chow D M and Adikan F M 2015 Surface plasmon resonance photonic crystal fiber biosensor: a practical sensing approach *IEEE Photonics Technol. Lett.* 27 1628–31
- [123] Nagel M, Haring Bolivar P, Brucherseifer M, Kurz H, Bosserhoff A and Büttner R 2002 Integrated THz technology for label-free genetic diagnostics Appl. Phys. Lett. 80 154–6
- [124] Ahmed F, Roy S, Paul B K, Ahmed K and Bahar A N 2020 Extremely low loss of photonic crystal fiber for terahertz wave propagation in optical communication applications *J. Opt. Commun.* 41 393–401
- [125] Mbonye M, Mendis R and Mittleman D M 2009 A terahertz two-wire waveguide with low bending loss Appl. Phys. Lett. 95 233506
- [126] Ma T, Guerboukha H, Girard M, Squires A D, Lewis R A and Skorobogatiy M 2016 3D printed hollow-core terahertz optical waveguides with hyperuniform disordered dielectric reflectors Adv. Opt. Mater. 4 2085–94
- [127] Atakaramians S, Afshar S, Monro T M and Abbott D 2013 Terahertz dielectric waveguides Adv. Opt. Photon. 5 169-215
- [128] Habib M A, Anower M S and Hasan M R 2018 Highly birefringent and low effective material loss microstructure fiber for THz wave guidance Opt. Commun. 423 140–4
- [129] Li J, Nallappan K, Guerboukha H and Skorobogatiy M 2017 3D printed hollow core terahertz Bragg waveguides with defect layers for surface sensing applications Opt. Express 25 4126–44

- [130] Sun B S, Tang X L, Zeng X and Shi Y W 2012 Characterization of cylindrical terahertz metallic hollow waveguide with multiple dielectric layers Appl. Opt. 51 7276–85
- [131] Dupuis A, Mazhorova A, Désévédavy F, Rozé M and Skorobogatiy M 2010 Spectral characterization of porous dielectric subwavelength THz fibers fabricated using a microstructured molding technique Opt. Express 18 13813–28
- [132] Yang S, Sheng X, Zhao G, Wang Y and Yu Y 2019 Novel pentagram THz hollow core anti-resonant fiber using a 3D printer *J. Infrared Millim. Terahertz Waves* 40 720–30
- [133] Wang D, Mu C, Li B and Yang J 2018 Electrically tunable propagation properties of the liquid crystal-filled terahertz fiber Appl. Sci. 8 2487
- [134] Wang S, Su M, Tang L, Li X, Li X, Bai H, Niu P, Shi J and Yao J 2023 Graphene-coated D-shaped terahertz fiber modulator *Front. Phys.* 11 1202839
- [135] Islam M S, Sultana J, Cordeiro C M, Cruz A L, Dinovitser A, Ng B H and Abbott D 2019 Broadband characterization of glass and polymer materials using THz-TDS 2019 44th Int. Conf. on Infrared, Millimeter, and Terahertz Waves (IRMMW-THz) (IEEE) pp 1–2
- [136] Fedulova E V, Nazarov M M, Angeluts A A, Kitai M S, Sokolov V I and Shkurinov A P 2012 Studying of dielectric properties of polymers in the terahertz frequency range *Proc. SPIE* 8337 144–52
- [137] Naftaly M and Miles R E 2007 Terahertz time-domain spectroscopy for material characterization Proc. IEEE 95 1658-65
- [138] Kumar V, Varshney R K and Kumar S 2020 Design of a compact and broadband terahertz polarization splitter based on gradient dual-core photonic crystal fiber Appl. Opt. 59 1974–9
- [139] Zhang Y, Li K, Wang L, Ren L, Zhao W, Miao R, Large M C and Van Eijkelenborg M A 2006 Casting preforms for microstructured polymer optical fibre fabrication Opt. Express 14 5541–7
- [140] Atakaramians S, Afshar S, Ebendorff-Heidepriem H, Nagel M, Fischer B M, Abbott D and Monro T M 2009 THz porous fibers: design, fabrication and experimental characterization Opt. Express 17 14053–62
- [141] Goto M, Quema A, Takahashi H, Ono S and Sarukura N 2004 Teflon photonic crystal fiber as terahertz waveguide *Jpn. J. Appl. Phys.* 43 L317
- [142] Nielsen K, Rasmussen H K, Adam A J, Planken P C, Bang O and Jepsen P U 2009 Bendable, low-loss Topas fibers for the terahertz frequency range Opt. Express 17 8592–601
- [143] Roze M, Ung B, Mazhorova A, Walther M and Skorobogatiy M 2011 Suspended core subwavelength fibers: towards practical designs for low-loss terahertz guidance Opt. Express 19 9127–38
- [144] Yang J, Zhao J, Gong C, Tian H, Sun L, Chen P, Lin L and Liu W 2016 3D printed low-loss THz waveguide based on Kagome photonic crystal structure *Opt. Express* 24 22454–60
- [145] Li S, Dai Z, Wang Z, Qi P, Su Q, Gao X, Gong C and Liu W 2019 A 0.1 THz low-loss 3D printed hollow waveguide Optik 176 611-6
- [146] Le Sauze A, Simonneau C, Pastouret A, Gicquel D, Bigot L and Choblet S 2003 Nanoparticle doping process: towards a better control of erbium incorporation in MCVD fibers for optical amplifiers Optical Amplifiers and Their Applications (OSA Technical Digest Series, paper WC5)
- [147] Podrazky O, Kasik I, Pospisilova M and Matejec V 2007 Use of alumina nanoparticles for preparation of erbium-doped fibers LEOS 2007-IEEE Lasers and Electro-Optics Society Annual Meeting Conf. Proc. vol 1 and 2 pp 246–7
- [148] Pastouret A, Gonnet C, Collet C, Cavani O, Burow E and Chaneac C 2009 Nanoparticle doping process for improved fibre amplifiers and lasers Fiber Lasers VI: Technology, Systems, and Applications vol 7195
- [149] Baker C C et al 2017 Nanoparticle doping for high power fiber lasers at eye-safer wavelengths Opt. Express 25 13903–15
- [150] Baker C C, Burdett A, Friebele E J, Rhonehouse D L, Kim W and Sanghera J 2019 Rare earth co-doping for increased efficiency of resonantly pumped Er-fiber lasers Opt. Mater. Express 9 1041–8
- [151] Kasik I, Peterka P, Mrazek J and Honzatko P 2016 Silica optical fibers doped with nanoparticles for fiber lasers and broadband sources Curr. Nanosci. 12 277–90
- [152] Vařák P, Kamrádek M, Mrázek J, Podrazký O, Aubrecht J, Peterka P, Nekvindová P and Kašík I 2022 Luminescence and laser properties of RE-doped silica optical fibers: the role of composition, fabrication processing, and inter-ionic energy transfers Opt. Mater. X 15 100177
- [153] Blanc W, Mauroy V, Nguyen L, Shivakiran Bhaktha B N, Sebbah P, Pal B P and Dussardier B 2011 Fabrication of rare earth-doped transparent glass ceramic optical fibers by modified chemical vapor deposition J. Am. Ceram. Soc. 94 2315–8
- [154] Paul M C et al 2012 Yb₂O₃ doped yttrium-alumino-silicate nano-particles based LMA optical fibers for high-power fiber lasers J. Lightwave Technol. 30 2062–8
- [155] Paul M C, Bysakh S, Das S, Dhar A, Pal M, Bhadra S K, Sahu J K, Kir'yanov A V and d'Acapito F 2016 Recent developments in rare-earths doped nano-engineered glass based optical fibers for high power fiber lasers *Trans. Indian Ceram. Soc.* 75 195–208
- [156] Tosi D, Molardi C, Sypabekova M and Blanc W 2021 Enhanced backscattering optical fiber distributed sensors: tutorial and review *IEEE Sens. J.* 21 12667–78
- [157] Blanc W, Lu Z, Robine T, Pigeonneau F, Molardi C and Tosi D 2022 Nanoparticles in optical fiber, issue and opportunity of light scattering Opt. Mater. Express 12 2635–52
- [158] Li J, Wang H, Li Z, Su Z and Zhu Y 2020 Preparation and application of metal nanoparticals elaborated fiber sensors Sensors 20 5155
- [159] Blanc W and Dussardier B 2016 Formation and applications of nanoparticles in silica optical fibers J. Opt. 45 247-54
- [160] Vařák P, Mrázek J, Blanc W, Aubrecht J, Kamrádek M and Podrazký O 2020 Preparation and properties of Tm-doped SiO₂-ZrO₂ phase separated optical fibers for use in fiber lasers Opt. Mater. Express 10 1383–91
- [161] Sincore A, Bradford J D, Cook J, Shah L and Richardson M C 2018 High average power thulium-doped silica fiber lasers: review of systems and concepts *IEEE J. Sel. Top. Quantum Electron.* 24 1–8
- [162] Vařák P, Mrázek J, Jasim A A, Bysakh S, Dhar A, Kamrádek M, Podrazký O, Kašík I, Bartoň I and Nekvindová P 2021 Thermal stability and photoluminescence properties of RE-doped (RE = Ho, Er, Tm) alumina nanoparticles in bulk and fiber-optic silica glass *Opt. Mater.* 118 111239
- [163] Blanc W et al 2019 Compositional changes at the early stages of nanoparticles growth in glasses J. Phys. Chem. C 123 29008–14
- [164] Kamrádek M, Kašík I, Aubrecht J, Mrázek J, Podrazký O and Cajzl J 2019 Nanoparticle and solution doping for efficient holmium fiber lasers *IEEE Photon. J.* 11 1–10
- [165] Cabié M, Neisius T and Blanc W 2021 Combined FIB/SEM tomography and TEM analysis to characterize high aspect ratio Mg-silicate particles inside silica-based optical fibres Mater. Charact. 178 111261
- [166] Vařák P *et al* 2022 Heat treatment and fiber drawing effect on the luminescence properties of RE-doped optical fibers (RE = Yb, Tm, Ho) *Opt. Express* 30 10050–62

- [167] James B A 1991 A review of the fabrication and properties of erbium doped fibers for optical amplifiers J. Lightwave Technol. 9 220–7
- [168] Mears R J, Reekie L, Jauncey I M and Payne D N 1987 Low-noise erbium-doped fibre amplifier operating at 1.54 μm J. Electron. Lett. 23 1026–8
- [169] Desurvire E, Simpson J R and Becker P C 1987 High-gain erbium-doped traveling-wave fiber amplifier J. Opt. Lett. 12 888–90
- [170] Dvoyrin V, Mashinsky V, Dianov E, Umnikov A, Yashkov M and Guryanov A 2005 Absorption, fluorescence and optical amplification in MCVD bismuth-doped silica glass optical fibres 2005 31st European Conf. on Optical Communication, ECOC 2005 vol 4 (IET) pp 949–50
- [171] Khegai A M, Alyshev S V, Vakhrushev A S, Riumkin K E, Umnikov A A and Firstov S V 2022 Recent advances in Bi-doped silica-based optical fibers: a short review J. Non-Cryst. Solids X 16 100126
- [172] Worldwide digital population July 2022 2022 Statista research department (Accessed 20 September 2022)
- [173] Chen Y et al 2021 Extending the L-band amplification to 1623 nm using Er/Yb/P co-doped phosphosilicate fiber J. Opt. Lett. 46 5834–7
- [174] Qiu Q et al 2022 Extended L-band few-mode Er/Yb Co-doped fiber amplifier with a cladding-pumped pseudo-two-stage configuration J. Opt. Lett. 47 2963
- [175] Wang Y, Thipparapu N K, Richardson D J and Sahu J 2020 Broadband bismuth-doped fiber amplifier with a record 115-nm bandwidth in the O and E bands *Optical Fiber Communication Conference, (Optical Society of America* Paper Th4B–1
- [176] Dianov E M 2012 Bismuth-doped optical fibers: a challenging active medium for near-IR lasers and optical amplifiers *Light Sci. Appl.* 1 e12
- [177] Liu X and Zhang X 2020 NOMA-based resource allocation for cluster-based cognitive industrial internet of things IEEE Trans. Ind. Inform. 16 5379–88
- [178] Cisco 2019 Cisco visual networking index: forecast and trends, 2017–2022 [R/OL] (available at: https://cyrekdigital.com/pl/blog/content-marketing-trendy-na-rok-2019/white-paper-c11-741490.pdf) (Accessed 12 June 2019)
- [179] Kakui M and Ishikawa S 2000 Long-wavelength-band optical amplifiers employing silica-based erbium doped fibers designed for wavelength division multiplexing systems and networks IEICE Trans. Electron. 83 799–815
- [180] Tanaka S, Imai K and Yazaki T 2002 Ultra-wideband L-band EDFA using phosphorus co-doped silica-fiber OFC (San Diego, California, United States) paper ThJ3
- [181] Donodin A, Dvoyrin V, Manuylovich E, Krzczanowicz L, Forysiak W, Melkumov M, Mashinsky V and Turitsyn S 2021 Bismuth doped fibre amplifier operating in E- and S- optical bands J. Opt. Mater. Express 11 127–35
- [182] Firstov S V et al 2020 Compact and efficient O-band bismuth-doped phosphosilicatefiber amplifier for fiber-optic communications Sci. Rep. 10 11347
- [183] Luo Y, Yan B, Zhang J, Wen J, He J and Peng G-D 2018 Development of Bi/Er co-doped optical fibers for ultra-broadband photonic applications *Front. Optoelectron.* 11 37–52
- [184] Lesniak M et al 2021 Structure and luminescence properties of transparent germanate glass-ceramics co-doped with Ni²⁺/Er³⁺ for near-infrared optical fiber application Nanomaterials 11 2115
- [185] Al-Azzawi A, lmukhtar A A, Hamid B A, Das S, Dhar A, Paul M C, Ahmad H and Harun S W 2019 Wideband and flat gain series erbium doped fiber amplifier using hybrid active fiber with backward pumping distribution technique *Results Phys.* 13 102186
- [186] Almukhtar A A et al 2019 Flat-gain optical amplification within 70 nm wavelength band using 199 cm long hybrid erbium fibers Optoelectron. Adv. Mater. Rapid Commun. 13 391–5
- [187] Nykolak G, Kramer S A, Simpson J R, DiGiovanni D J, Giles C R and Presby H M 1991 An erbium-doped multimode optical fiber amplifier IEEE Photonics Technol. Lett. 3 1079–81
- [188] Jung Y, Alam S, Richardson D J, Ramachandran S and Abedin K S 2020 Multicore and multimode optical amplifiers for space division multiplexing Optical Fiber Telecommunications VII ed A E Willner (Academic) ch 7, pp 301–33
- [189] Bigot L, Le Cocq G and Quiquempois Y 2015 Few-mode erbium-doped fiber amplifiers: a review J. Lightwave Technol. 33 588-96
- [190] Jin C, Ung B, Messaddeq Y and LaRochelle S 2013 Tailored modal gain in a multi-mode erbium-doped fiber amplifier based on engineered ring doping profiles *Proc. SPIE* 8915 89150A
- [191] Jung Y et al 2017 Few mode ring-core fibre amplifier for low differential modal gain 2017 European Conf. on Optical Communication (ECOC) pp 1–3
- [192] Jung Y, Kang Q, Sidharthan R, Ho D, Yoo S, Gregg P, Ramachandran S, Alam S and Richardson D 2017 Optical orbital angular momentum amplifier based on an air-hole erbium-doped fiber J. Lightwave Technol. 35 430–6
- [193] Trinel J-B, Quiquempois Y, Le Rouge A, Le Cocq G, Garcia L, Morizur J-F, Labroille G and Bigot L 2016 Amplification sharing of non-degenerate modes in an elliptical-core few-mode erbium-doped fiber Opt. Express 24 4654–61
- [194] Nicholson J W et al 2012 Nanosecond pulse amplification in a 6000 μ m² effective area higher-order mode erbium-doped fiber amplifier 2012 Conf. on Lasers and Electro-Optics (CLEO) pp 1–2
- [195] Abedin K, Ahmad R, DeSantolo A, Nicholson J, Westbrook P, Headley C and DiGiovanni D 2018 Cladding pumped Yb-doped HOM power amplifier with high gain *Proc. SPIE* 10512 10512–49
- [196] Abedin K, Ahmad R, DeSantolo A and DiGiovanni D 2019 Reconversion of higher-order-mode (HOM) output from cladding-pumped hybrid Yb:HOM fiber amplifier *Opt. Express* 27 8585–95
- [197] Li A, Chen X, Amin A A and Shieh W 2012 Fused fiber mode couplers for few-mode transmission *IEEE Photonics Technol. Lett.* 24 1953–6
- [198] Leon-Saval S G, Fontaine N K, Salazar-Gil J R, Ercan B, Ryf R and Bland-Hawthorn J 2014 Mode-selective photonic lanterns for space-division multiplexing Opt. Express 22 1036–44
- [199] Forbes A 2019 Structured light from lasers Laser Photon. Rev. 13 1900140
- [200] Gris-Sánchez I, Van Ras D and Birks T A 2016 The Airy fiber: an optical fiber that guides light diffracted by a circular aperture Optica 3 270–6
- [201] Abedin K 2022 Amplification of structured light in optical fibers 2022 Optical Fiber Communications Conf. and Exhibition (OFC) pp 1–2
- [202] Petersen C R, Moselund P M, Huot L, Hooper L and Bang O 2018 Towards a table-top synchrotron based on supercontinuum generation *Infrared Phys. Technol.* **91** 182–6
- [203] Zorin I, Gattinger P, Ebner A and Brandstetter M 2022 Advances in mid-infrared spectroscopy enabled by supercontinuum laser sources Opt. Express 30 5222–54
- [204] Israelsen N M, Petersen C R, Barh A, Jain D, Jensen M, Hannesschläger G, Tidemand-Lichtenberg P, Pedersen C, Podoleanu A and Bang O 2019 Real-time high-resolution mid-infrared optical coherence tomography Light Sci. Appl. 8 11

- [205] Sylvestre T et al 2021 Recent advances in supercontinuum generation in specialty optical fibers J. Opt. Soc. Am. B 38 F90-F103
- [206] Dudley J M, Genty G and Coen S 2006 Supercontinuum generation in photonic crystal fiber Rev. Mod. Phys. 78 1135–84
- [207] Dudley J M and Taylor J R (eds) 2010 Supercontinuum Generation in Optical Fiber (Cambridge University Press)
- [208] Alfano R R (ed) 2023 The Supercontinuum Laser Source: The Ultimate White Light 4th edn (Springer Nature)
- [209] Jung D, Bank S, Lee M L and Wasserman D 2017 Next-generation mid-infrared sources J. Opt. 19 123001
- [210] Hoffman A and Gmachl C 2012 Extending opportunities Nat. Photon. 6 407
- [211] Ohishi Y 2022 Supercontinuum generation and IR image transportation using soft glass optical fibers: a review *Opt. Mater. Express* 12 3990–4046
- [212] McKellar A R W 2010 High-resolution infrared spectroscopy with synchrotron sources J. Mol. Spectrosc. 262 1-10
- [213] El Khoury Y and Hellwig P 2017 Far infrared spectroscopy of hydrogen bonding collective motions in complex molecular systems Chem. Commun. 53 8389–99
- [214] Feng K, Streyer W, Zhong Y, Hoffman A J and Wasserman D 2015 Photonic materials, structures and devices for Reststrahlen optics Opt. Express 23 A1418–33
- [215] Pires H, Baudisch M, Sanchez D, Hemmer M and Biegert J 2015 Ultrashort pulse generation in the mid-IR *Prog. Quantum Electron.* 43 1–30
- [216] Lin C and Stolen R H 1976 New nanosecond continuum for excited-state spectroscopy Appl. Phys. Lett. 28 216-8
- [217] Lin C, Nguyen V T and French W G 1978 Wideband near-IR continuum (0.7–2.1 μ m) generated in low-loss optical fibres Electron. Lett. 14 822–3
- [218] Ranka J K, Windeler R S and Stentz A J 2000 Visible continuum generation in air-silica microstructure optical fibers with anomalous dispersion at 800 nm Opt. Lett. 25 25–27
- [219] Xia C, Kumar M, Kulkarni O P, Islam M N, Terry J F L, Freeman M J, Poulain M and Mazé G 2006 Mid-infrared supercontinuum generation to 4.5 μm in ZBLAN fluoride fibers by nanosecond diode pumping *Opt. Lett.* 31 2553–5
- [220] Kedenburg S et al 2017 High repetition rate mid-infrared supercontinuum generation from 1.3 to 5.3 μ m in robust step-index tellurite fibers J. Opt. Soc. Am. B 34 601
- [221] Guo K et al 2018 Appl. Opt. 57 2519-32
- [222] Petersen C R et al 2014 Mid-infrared supercontinuum covering the 1.4–13.3 μ m molecular fingerprint region using ultra-high NA chalcogenide step-index fibre Nat. Photon. 8 830–4
- [223] Cheng T, Nagasaka K, Hoang Tuan T, Xue X, Matsumoto M, Tezuka H, Suzuki T and Ohishi Y 2016 Mid-infrared supercontinuum generation spanning 2.0–15.1 μm in a chalcogenide step-index fiber Opt. Lett. 41 2117–20
- [224] Lemière A et al 2021 1.7–18 μ m mid-infrared supercontinuum generation in a dispersion-engineered step-index chalcogenide fiber Results Phys. 26 104397
- [225] Serrano E *et al* 2023 Multi-octave mid-infrared supercontinuum generation in tapered chalcogenide-glass rods *Opt. Lett.* **48** 5479–82
- [226] Cui S, Chahal R, Boussard-Plédel C, Nazabal V, Doualan J-L, Troles J, Lucas J and Bureau B 2013 From selenium- to tellurium-based glass optical fibers for infrared spectroscopies J. Mol. 18 5373–88
- [227] Le Coq D, Cui S, Boussard-Plédel C, Masselin P, Bychkov E and Bureau B 2017 Telluride glasses with far-infrared transmission up to 35 μm Opt. Mater. 72 809–12
- [228] Zhao Z, Wu B, Wang X, Pan Z, Liu Z, Zhang P, Shen X, Nie Q, Dai S and Wang R 2017 Mid-infrared supercontinuum covering 2.0–16 μm in a low-loss telluride single-mode fiber *Laser Photon. Rev.* **11** 201700005
- [229] Mouawad O et al 2018 Expanding up to far-infrared filamentation-induced supercontinuum spanning in chalcogenide glasses Appl. Phys. B 124 182
- [230] Savage J A and Nielsen S 1965 Chalcogenide glasses transmitting in the infrared between 1 and 20 μ m-a state of the art review Infrared Phys. 5 195–204
- [231] Zhu X and Peyghambarian N 2010 High-power ZBLAN glass fiber lasers: review and prospect Adv. OptoElectron. 2010 501956
- [232] Zhu X, Zhu G, Wei C, Kotov L V, Wang J, Tong M, Norwood R A and Peyghambaraian N 2017 Pulsed fluoride fiber lasers at 3 μm *J. Opt. Soc. Am.* B 34 A15–A28
- [233] Li X, Xu Y, Yang L, Cui Y, Zhou Z, Wang M and Wang Z 2023 2.3-μm single-frequency Tm:ZBLAN fiber amplifier with output power of 1.41 W Opt. Express 31 40991
- [234] Jackson S D 2004 Single-transverse-mode 2.5-W holmium-doped fluoride fiber laser operating at 2.86 µm Opt. Lett. 29 334
- [235] Zhu X and Jain R 2007 10-W-level diode-pumped compact 2.78 μ m ZBLAN fiber laser Opt. Lett. 32 26
- [236] Fortin V, Bernier M, Bah S T and Vallee R 2015 30 W fluoride glass all-fiber laser at 2.94 μ m Opt. Lett. 40 2882
- [237] Aydin Y O, Fortin V, Vallee R and Bernier M 2018 Towards power scaling of 2.8 µm fiber lasers Opt. Lett. 43 4542
- [238] Newburgh G A and Dubinskii M 2021 Power and efficiency scaling of Er:ZBLAN fiber laser Laser Phys. Lett. 18 095102
- [239] Fortin V, Jobin F, Larose M, Bernier M and Vallee R 2019 10-W-level monolithic dysprosium-doped fiber laser at 3.24 μ m Opt. Lett. 44 491
- [240] Lemieux-Tanguay M, Fortin V, Boilard T, Paradis P, Maes F, Talbot L, Vallee R and Bernier M 2022 15 W monolithic fiber laser at 3.55 μ m Opt. Lett. 47 289
- [241] Maes F, Fortin V, Poulain S, Poulain M, Carree J, Bernier M and Vallee R 2018 Room-temperature fiber laser at 3.92 μm *Optica* 5.761
- [242] Nunes J J et al 2021 Room temperature mid-infrared fiber lasing beyond 5 μ m in chalcogenide glass small-core step index fiber Opt. Lett. 46 3504
- [243] Koltashev V V, Denker B I, Galagan B I, Snopatin G E, Sukhanov M V, Sverchkov S E, Velmuzhov A P and Plotnichenko V G 2023 150 mW Tb³⁺ doped chalcogenide glass fiber laser emitting at $\lambda > 5 \mu$ m *Opt. Laser Technol.* **161** 109233
- [244] Bernier M, Fortin V, Caron N, El-Amraoui M, Messaddeq Y and Vallee R 2013 Mid-infrared chalcogenide glass Raman fiber laser Opt. Lett. 38 127
- [245] Tang Y, Wright L G, Charan K, Wang T, Xu C and Wise F W 2016 Generation of intense 100 fs solitions tunable from 2 to 4.3 μ m in fluoride fiber *Optica* 3 948
- [246] Nampoothiri A V V et al 2012 Hollow-core optical fiber gas lasers (HOFGLAS): a review Opt. Mater. Express 2 948
- [247] Gladyshev A V et al 2017 4.4-µm Raman laser based on hollow-core silica fibre Quantum Electron. 47 491
- [248] Ehrenreich T, Leveille R, Majid I, Tankala K, Rines G and Moulton P F 2010 1-kW, all-glass Tm:fiber laser Proc. SPIE 7580 758016
- [249] Hemming A et al A monolithic cladding pumped holmium-doped fiber laser CLEO 2013 (Paper CW1M.1 OSA Technical Digest)
- [250] Bernier M, Faucher D, Vallee R, Saliminia A, Androz G, Sheng Y and Chin S L 2007 Bragg gratings photoinduced in ZBLAN fibers by femtosecond pulses at 800 nm Opt. Lett. 32 454

- [251] Smith P W 1971 A waveguide gas laser Appl. Phys. Lett. 19 132-4
- [252] Gonchukov S A, Kornilov S T, Petrovskii V N, Protsenko E D and Rubezhnyi Y G 1975 Helium–neon waveguide laser Sov. J. Quantum Electron. 5 232–3
- [253] Jensen R E and Tobin M S 1972 CO₂ waveguide gas laser Appl. Phys. Lett. 20 508–10
- [254] Russell P S J 2006 Photonic-crystal fibers J. Lightwave Technol. 24 4729-49
- [255] Benabid F, Knight J C, Antonopoulos G J and Russell P S 2002 Stimulated Raman scattering in hydrogen-filled hollow-core photonic crystal fiber Science 298 399–402
- [256] Shephard J D, MacPherson W N, Maier R R J, Jones J D C, Hand D P, Mohebbi M, George A K, Roberts P J and Knight J C 2005 Single-mode mid-IR guidance in a hollow-core photonic crystal fiber Opt. Express 13 7139–44
- [257] Pryamikov A D, Biriukov A S, Kosolapov A F, Plotnichenko V G, Semjonov S L and Dianov E M 2011 Demonstration of a waveguide regime for a silica hollow-core microstructured optical fiber with a negative curvature of the core boundary in the spectral region > 3.5 μm Opt. Express 19 1441–8
- [258] Wang Y Y, Wheeler N V, Couny F, Roberts P J and Benabid F 2011 Low loss broadband transmission in hypocycloid-core Kagome hollow-core photonic crystal fiber *Opt. Lett.* **36** 669–71
- [259] Yu F, Wadsworth W J and Knight J C 2012 Low loss silica hollow-core fibers for 3-4 \(\mu\) m spectral region Opt. Express 20 11153-8
- [260] Kolyadin A N, Kosolapov A F, Pryamikov A D, Biriukov A S, Plotnichenko V G and Dianov E M 2013 Light transmission in negative curvature hollow core fiber in extremely high material loss region *Opt. Express* 21 9514–9
- [261] Cui Y, Wang Z, Zhou Z, Huang W, Li H, Wang M, Gao S and Wang Y 2022 Towards high-power densely step-tunable mid-infrared fiber source from 4.27 to $4.43~\mu m$ in CO₂-filled anti-resonant hollow-core silica fibers *J. Lightwave Technol.* 40 2503–10
- [262] Zhou Z, Huang W, Cui Y, Li H, Pei W, Li X, Li Z, Wang M and Wang Z 2022 3.1 W mid-infrared fiber laser at 4.16 μ m based on HBr-filled hollow-core silica fibers Opt. Lett. 47 5785–8
- [263] Xu M, Yu F, Hassan M R A and Knight J C 2018 Continuous-wave mid-infrared gas fiber lasers *IEEE J. Sel. Top. Quantum Electron.* 24 1–8
- [264] Dadashzadeh N, Thirugnanasambandam M P, Kushan Weerasinghe H W, Debord B, Chafer M, Gerome F, Benabid F, Washburn B R and Corwin K L 2017 Near diffraction-limited performance of an OPA pumped acetylene-filled hollow-core fiber laser in the mid-IR Opt. Express 25 13351–8
- [265] Zhang X, Peng Z, Dong Z, Yao P, Hou Y and Wang P 2022 High-power mid-infrared 2.8-μm ultrafast Raman laser based on methane-filled anti-resonant fiber *IEEE Photonics Technol. Lett.* **34** 1007–10
- [266] Gladyshev A V et al 2018 2.9, 3.3, and 3.5 μ m Raman lasers based on revolver hollow-core silica fiber filled by 1 H $_2$ /D $_2$ gas mixture IEEE J. Sel. Top. Quantum Electron. 24 1–8
- [267] Astapovich M S, Gladyshev A V, Khudyakov M M, Kosolapov A F, Likhachev M E and Bufetov I A 2019 Watt-level nanosecond 4.42-μm Raman laser based on silica fiber *IEEE Photonics Technol. Lett.* 31 78–81
- [268] Kosolapov A F, Pryamikov A D, Biriukov A S, Shiryaev V S, Astapovich M S, Snopatin G E, Plotnichenko V G, Churbanov M F and Dianov E M 2011 Demonstration of CO₂-laser power delivery through chalcogenide-glass fiber with negative-curvature hollow core Opt. Express 19 25723–8
- [269] Zhang H, Chang Y, Xu Y, Liu C, Xiao X, Li J, Ma X, Wang Y and Guo H 2023 Design and fabrication of a chalcogenide hollow-core anti-resonant fiber for mid-infrared applications Opt. Express 31 7659–70
- [270] Murphy L R and Bird D 2023 Azimuthal confinement: the missing ingredient in understanding confinement loss in antiresonant, hollow-core fibers *Optica* 10 854–70
- [271] Pryamikov A 2023 Local energy velocity of the air-core modes in hollow-core fibers *Photonics* 10 1035
- [272] Flamini F, Spagnolo N and Sciarrino F 2019 Photonic quantum information processing: a review Rep. Prog. Phys. 82 016001
- [273] Senellart P, Solomon G and White A 2017 High-performance semiconductor quantum-dot single-photon sources *Nat. Nanotechnol.* 12 1026
- [274] Arakawa Y and Holmes M J 2020 Progress in quantum-dot single photon sources for quantum information technologies: a broad spectrum overview *Appl. Phys. Rev.* 7 021309
- [275] Grosjean T, Mivelle M, Burr G W and Baida F I 2013 Optical horn antennas for efficiently transferring photons from a quantum emitter to a single-mode optical fiber *Opt. Express* 21 1762
- [276] Schlehahn A, Fischbach S, Schmidt R, Kaganskiy A, Strittmatter A, Rodt S, Heindel T and Reitzenstein S 2018 A stand-alone fiber-coupled single-photon source *Sci. Rep.* 8 1340
- [277] Musiał A et al 2020 Plug&play fiber-coupled 73 kHz single-photon source operating in the telecom O-band Adv. Quantum Technol. 3 2000018
- [278] Bemer L, Rodt S and Reitzenstein S 2022 Fiber-coupled quantum light sources based on solid-state quantum emitters *Mater. Quantum. Technol.* 2 042002
- [279] Fujiwara M, Toubaru K, Noda T, Zhao H-Q and Takeuchi S 2011 Highly efficient coupling of photons from nanoemitters into single-mode optical fibers Nano Lett. 11 4362–5
- [280] Bremer L et al 2020 Quantum dot single-photon emission coupled into single-mode fibers with 3D printed micro-objectives APL Photonics 5 106101
- [281] Heindel T, Kim J-H, Gregersen N, Rastelli A and Reitzenstein S 2023 Quantum dots for photonic quantum information technology Adv. Opt. Photon. 15 613–738